



PONTIFICIA UNIVERSIDAD CATOLICA DE CHILE
SCHOOL OF ENGINEERING

**A METHODOLOGY TO OPTIMIZE THE
TECHNO-ECONOMIC DESIGN OF
SOLAR POWER PLANTS WITH
STORAGE SYSTEMS**

ADRIANA ZURITA VILLAMIZAR

Thesis submitted to the Office of Graduate Studies in partial fulfillment of
the requirements for the Degree of Doctor in Engineering Sciences

Advisor:

DR. RODRIGO ESCOBAR

Santiago de Chile, November, 2020

© 2020, Adriana Zurita Villamizar



PONTIFICIA UNIVERSIDAD CATOLICA DE CHILE
SCHOOL OF ENGINEERING

A METHODOLOGY TO OPTIMIZE THE TECHNO-ECONOMIC DESIGN OF SOLAR POWER PLANTS WITH STORAGE SYSTEMS

ADRIANA ZURITA VILLAMIZAR

Members of the Committee:

DR. RODRIGO ESCOBAR

DR. JOSÉ MIGUEL CARDEMIL

DR. ÁLVARO LORCA

DR. FERNANDO ANTOÑANZAS

DR. RAFAEL GUÉDEZ

DR. JUAN DE DIOS ORTÚZAR

Thesis submitted to the Office of Graduate Studies in partial fulfillment of
the requirements for the Degree Doctor in Engineering Sciences

Santiago de Chile, November, 2020

*To my beloved parents and my sister
Andrea for all their unconditional
support and love.*

*“To do the impossible, you need
people who believe the same as you.”*

ACKNOWLEDGEMENTS

A doctorate is often seen as a very solitary path. In my case, this dissertation is the result of four years of very hard work and effort, but truth is, this work would not had been possible without the support of many people who surrounded me throughout this journey.

To Dr. Rodrigo Escobar, my research supervisor at the Pontificia Universidad Católica of Chile, I would like to express my deep and sincere gratitude for opening me the doors to his team in Chile, giving me the opportunity to do research and providing me invaluable guidance and support throughout this research. Thank you for all the barbeques with the team, and for providing me trust, confidence and vision.

To Dr. José Miguel Cardemil, I am extremely grateful for his valuable feedback, advice and support throughout these years. Thank you for the encouragement, insightful discussions, motivation, guidance and sometimes hard questions that led me to deliver a better work.

To all the people of Grupo Solar UC, I want to thank them for all the laughs during the lunches and their support in the technical area too. Special thanks to Kerstin, Carlos F., Gonzalo, Felipe, Mauricio, Roberto, Fernando Antoñanzas, and Anita.

To the other Ph. D. students in the research team, such as Redlich, Armando, Mario, Yeliz, Josue and Andrés, I want to express my special thanks for their support, advice and empathy during the most difficult times.

To Dr. Rafael Guédez and Dr. Björn Laumert at KTH University in Stockholm, Sweden, I would like to express my deep gratitude for giving me the honor and privilege to work with them and the KTH's CSP group, which is one of the top universities in the world. Thanks for providing me the opportunity of living three months in such a rich and almost ideal culture. I also extend my sincere appreciation to Silvia Trevisan for her valuable advice, guidance and support during this research stay, and to the people who became my family in Sweden, specially to Patrick, Yeliz, Nelson and all their family, and Alfredo.

To Dra. Loreto Valenzuela, I want to thank her for giving the opportunity of working for six months in the Medium-Concentration Unit at the CIEMAT in Madrid, Spain, which is one of the most relevant solar thermal research centers in Europe and worldwide. I would like to express my deep gratitude to all the people who received me there and made me feel so welcome, such as Dra. Lourdes González, Dr. Mario Biencinto, Dr. Antonio Ávila, and Dra.

Rocio Bayon. Special thanks also to Paco, Raúl, Carlos Sanz, and Elisa for their empathy, good vibes and laughs during my research stay. During this experience, I also met amazing people and made invaluable friendships. I want to express my heartfelt and deep thanks to Belén, Álvaro, Leti and Ana for becoming my family in Madrid and giving me one of the best experiences I ever had.

To my best friends from Venezuela who are scattered over the globe, many thanks for their unconditional friendship and support along these years despite the distance, in particular Adri, Ylye, Jesús C., Jesús P., Andrea H., Anthony D., Daniel B., Manuel P. and Jaime H., thank you for always being there and believing the best of me. To my friends in Chile who have become my family in this country, Kerstin, David, Catalina, Daniela, Kenneth, Santiago, Teobaldo, Natalia, Cristian, Alan, Alicia, Joselyn and Paulo, infinite thanks for their unconditional support, fun and good times.

To my family, I am extremely grateful for their love, prayers and caring from the distance. This achievement has been a result of all the sacrifices that my parents did for educating and preparing me, which have given me the tools to build my future. To my mom, dad, and my sister Andrea, my success is only thanks to you. They are my biggest inspiration. Thanks for always loving me.

Lastly but not any least, to my loving and supportive boyfriend: Carlos. I cannot express enough thanks, because you have got me through this long path, giving me your encouragement, love, understanding and infinite patience. Thank you for being my home, helping me getting through the most difficult times during these years, for always being there and unconditionally believing in me. I also want to extend my gratitude to his family, who have supported and worried about me throughout all these years.

Finally, I acknowledge the funding from VRI's scholarship at the beginning of my studies, and the funding from ANID PFCHA/Doctorado Nacional 2019 – 21191591.

Thank you all for having been part of this journey!

CONTENTS

Pag.

ACKNOWLEDGEMENTS	iii
LIST OF TABLES	ix
LIST OF FIGURES.....	xi
NOMENCLATURE.....	xiv
RESUMEN.....	xx
ABSTRACT	xxii
LIST OF APPENDED PAPERS.....	xxiv
1. INTRODUCTION	1
1.1. Context	1
1.2. Thesis Objectives	3
1.3. Hypotheses	4
1.4. Methodology	5
1.5. Summary of Main Contributions to State-of-the-Art.....	10
1.6. Contents.....	12
1.7. Main Results.....	13
1.7.1. Techno-economic analysis of the hybrid CSP-PV- TES-BESS plant (Chapter 2)	14
1.7.2. Time resolution impact on the modeling of the hybrid CSP-PV- TES- BESS plant (Chapter 3).....	16
1.7.3. Multi-objective optimization, dispatch strategy influence, and comparison between technology combinations (Chapter 4).....	18
1.8. Research Contributions	20
1.8.1. Contributions applicable to the industry.....	21
1.9. Recommendations for future work.....	23
1.10. Study Limitations	25

2.	TECHNO-ECONOMIC EVALUATION OF A HYBRID CSP-PV PLANT INTEGRATED WITH THERMAL ENERGY STORAGE AND A LARGE-SCALE BATTERY ENERGY STORAGE SYSTEM FOR BASE GENERATION.....	27
2.1.	Introduction	27
2.2.	System description	30
2.2.1.	CSP plant with TES	33
2.2.2.	PV plant with BESS.....	34
2.3.	Methodology	36
2.3.1.	Operation Modes.....	38
2.3.2.	Economic analysis	40
2.3.3.	Parametric analysis	43
2.4.	Results	44
2.4.1.	Parametric and techno-economic analysis	44
2.4.2.	Cost distribution and sensitivity analysis.....	51
2.4.3.	Fixed-tilted mounting vs. one-axis tracking system	54
2.5.	Discussions.....	61
2.6.	Conclusions	63
3.	ASSESSMENT OF TIME RESOLUTION IMPACT ON THE MODELING OF A HYBRID CSP-PV PLANT: A CASE OF STUDY IN CHILE	65
3.1.	Introduction	65
3.2.	System Description	68
3.2.1.	CSP plant with TES and power block	68
3.2.2.	PV plant and BESS	70
3.3.	Modeling and Simulation	71
3.3.1.	Location and solar resource	71
3.3.2.	PV plant and battery bank model.....	73
3.3.3.	Power block model	73
3.3.4.	Central receiver power plant model.....	74
3.3.5.	Operating mode.....	80
3.4.	Techno-economic analysis	81
3.5.	Results	82
3.5.1.	Daily operation curves	83
3.5.2.	Annual performance prediction	90

3.5.3. Techno-economic results	92
3.6. Discussion	99
3.7. Conclusions	102
4. MULTI-OBJECTIVE OPTIMAL DESIGN OF SOLAR POWER PLANTS WITH STORAGE SYSTEMS ACCORDING TO DISPATCH STRATEGY	104
4.1. Introduction	104
4.2. System Description	106
4.2.1. Locations	108
4.2.2. Dispatch strategies	109
4.3. Cost Scenarios	110
4.3.1. CSP costs	110
4.3.2. PV and BESS costs	111
4.4. Methodology	116
4.4.1. Modeling and Simulation.....	116
4.4.2. Multi-objective optimization	118
4.4.3. Surrogate model	119
4.4.4. Optimization parameters and decision-making process	120
4.5. Results and Discussions	121
4.5.1. Pareto front results	122
4.5.2. Comparison between technology combinations	123
4.5.3. Design configurations along the Pareto curves.....	124
4.5.4. Cost reduction scenarios	127
4.5.5. Location and solar resource conditions impact.....	129
4.6. Conclusions	131
5. CONCLUSIONS	134
BIBLIOGRAPHIC REFERENCES	139
APPENDICES.....	150
APPENDIX A: APPENDIX FOR CHAPTER 2	151
APPENDIX B: APPENDIX FOR CHAPTER 3	152
Appendix B1: Supplementary Data	152
Appendix B2: Cost Data	152

Appendix B3: Cost Functions.....	154
APPENDIX C: APPENDIX FOR CHAPTER 4	156
APPENDIX D: SIMULATION MODEL IN TRNSYS	158
APPENDIX D1. PV plant model.....	161
APPENDIX D2. CSP plant based on central receiver technology	162
APPENDIX D3. BESS model	165

LIST OF TABLES

Pag.

Table 1-1: Summary of the main contributions of the papers appended in this thesis.	10
Table 2-1: Main design parameters of the CSP plant and the power block under nominal conditions.	34
Table 2-2: Main parameters of the PV plant and BESS.....	36
Table 2-3: Economic parameters considered for the CSP plant.....	41
Table 2-4: Economic parameters considered for the PV plant and BESS.	43
Table 2-5: Values considered for the parametric analysis.	44
Table 2-6: Minimum LCOE configuration for each BESS size analyzed.	47
Table 2-7: Techno-economic results of the hybrid CSP-PV plant for the minimum LCOE configurations.....	49
Table 2-8: Techno-economic indicators of the hybrid CSP-PV plant considering fixed-angle PV arrays or one-axis tracked PV arrays for the minimum LCOE configurations.....	56
Table 3-1: Main design parameters of the CSP plant and the power block under nominal conditions.	69
Table 3-2: Main parameters of the PV plant and BESS.....	70
Table 3-3: Meteorological station features.....	72
Table 3-4: Applicable range of the power block polynomial regression.	74
Table 3-5: Daily total generation using different time steps for a clear-sky day (Jan 2 nd) in Carrera Pinto and Santiago.....	85
Table 3-6: Daily total generation using different time steps for a day with high-frequency transients of DNI (July 21 st) in Carrera Pinto and a cloudy day (June 19 th) in Santiago....	85
Table 3-7: Annual total generation and percentage differences using different time steps for Carrera Pinto.	91
Table 3-8: Annual total generation and percentage differences using different time steps for Santiago.....	91
Table 3-9: Techno-economic results for the hybrid plant in Carrera Pinto for different time steps.....	93

Table 3-10: Techno-economic results for the hybrid plant in Santiago for different time steps.	93
Table 3-11: Description of cases of study.....	95
Table 3-12: Results for different case studies varying the time resolution of the simulation.	96
Table 4-1: Dispatch strategies chosen for each case of study.....	110
Table 4-2: Current and specific CSP cost scenarios data.....	111
Table 4-3: PV and BESS cost scenarios data.....	113
Table 4-4: Decision variables for every optimization problem, depending on the technology combination.....	119
Table 4-5: Variables in parametric analyses performed for every technology combination and dispatch strategy.....	120
Table 4-6: Multi-objective optimization parameters.....	121

LIST OF FIGURES

	Pag.
Figure 1-1: Methodology flow chart.	6
Figure 1-2: Scheme of a hybrid solar power plant with storage integrating a PV plant, CSP plant, TES, and BESS.	8
Figure 1-3. Graphical abstract with the main results of this research thesis.	15
Figure 2-1: Scheme of the hybrid CSP-PV plant integrated with TES and BESS.....	31
Figure 2-2: Daily total of DNI from January to December 2012 at Crucero, Chile.	32
Figure 2-3: Hourly generation of Chile's national electric system composed by the SING and the SIC transmission systems on a typical day.	32
Figure 2-4: Dispatchability of the hybrid plant during (a) summer season, (b) winter season.	40
Figure 2-5: Annual contribution of generation and capacity factor of the hybrid plant for a base case with 130 MW of PV, 14h of TES, 2.4 of SM, and 350 MWh of BESS. A parametric analysis was performed varying a) PV size, b) TES capacity, c) BESS size, and d) SM. ..	45
Figure 2-6: LCOE and capacity factor of the hybrid plant for different BESS sizes. Circle marks represent the minimum LCOE configuration for each BESS size analyzed.	46
Figure 2-7: Capacity factor and installation cost of the hybrid plant for different BESS sizes. Circle marks represent the minimum LCOE configuration for each BESS size.	50
Figure 2-8: Cost distribution of the LCOE of the hybrid plant for different BESS sizes. ..	51
Figure 2-9: Variation in the minimum LCOE configurations obtained for different percentages of reduction of the BESS storage cost and different BESS sizes in terms of the PV size, SM, TES capacity, capacity factor, and the percentage contribution of the BESS to the annual hybrid plant generation.	53
Figure 2-10: Total annual production and capacity factor of the hybrid CSP-PV plant considering fixed-angle PV arrays and one-axis tracking system.....	55
Figure 2-11: Dispatchability of the hybrid plant during summer and winter seasons, considering fixed-angle PV arrays or one-axis tracked PV arrays, for the configuration D with 170MW of PV, 300MWh of BESS, 2.2 of SM, and 14h of TES.	57

Figure 2-12: Monthly power production of each component of the hybrid plant with fixed PV arrays and with one-axis-tracking system, for the configuration D with 170MW of PV, 300MWh of BESS, 2.2 of SM, and 14h of TES.	58
Figure 2-13: Monthly distribution of dumped PV energy and PV energy excess of the hybrid CSP-PV plant with one-axis-tracking system, for a configuration with 170MW of PV, 300MWh of BESS, 2.2 of SM, and 14h of TES.	59
Figure 2-14: LCOE obtained for each minimum LCOE configuration implementing fixed PV modules or one-axis-tracking system. Percentage differences of LCOE are presented for an increase in both installation and O&M costs of the PV plant with a one-axis-tracking system.....	60
Figure 3-1: Hybrid plant model scheme.....	68
Figure 3-2: DNI profile in a) Carrera Pinto and b) Santiago.	72
Figure 3-3: Receiver operation in Carrera Pinto with 1-minute time resolution for two types of days: a) Clear-sky day, and b) Variable day.	79
Figure 3-4: Operating mode of the hybrid plant.	81
Figure 3-5: Solar irradiance in a 1-minute time scale for a) a clear-sky day in Carrera Pinto, b) a clear-sky day in Santiago, c) a variable day with high-DNI levels and high-frequency transients in Carrera Pinto and, d) a variable day with low DNI levels in Santiago.	84
Figure 3-6: Production profile of the hybrid plant at Carrera Pinto in a variable day (July 21st) for different time steps: a) 1 minute, b) 5 minutes, c) 10 minutes, d) 15 minutes, e) 30 minutes, and f) 60 minutes	86
Figure 3-7: Central receiver operation during a variable day (July 21 st) in Carrera Pinto for different time steps: a) 1 minute, b) 5 minutes, c) 10 minutes, d) 15 minutes, e) 30 minutes, and f) 60 minutes.....	87
Figure 3-8: Central receiver operation during a variable day (June 19 th) in Santiago for different time steps: a) 1 minute, b) 5 minutes, c) 10 minutes, d) 15 minutes, e) 30 minutes, and f) 60 minutes.....	89
Figure 3-9: Normalized annual generation vs. time step of the simulation for different cases.	97

Figure 3-10: Normalized CSP generation vs. time step of the simulation for different cases.	98
Figure 3-11: Normalized LCOE vs. time step of the simulation for different cases.....	99
Figure 4-1: Technology combinations of storage and solar power plants considered in this study.	108
Figure 4-2: Typical hourly blocks implemented in electric tenders of Chile.....	109
Figure 4-3: Scheme of the methodology followed for the multi-objective analysis.	116
Figure 4-4. Pareto fronts for every technology combination and the base cost scenario of 2020 to provide energy in a) baseload, b) Block B+C (daytime and evening), c) Block A+C (evening and night), d) Block B (daytime) in Carrera Pinto.....	122
Figure 4-5. Design configurations along the Pareto curve of the a) hybrid CSP-PV-TES- BESS plant and b) PV-BESS plant, for all the dispatch strategies, considering the base case cost scenario of 2020 in Carrera Pinto.	126
Figure 4-6. Pareto fronts for every technology combination and cost scenarios to provide energy in a) Baseload, b) Block B+C (daytime and evening), c) Block A+C (evening and night), d) Block B (daytime) in Carrera Pinto.....	128
Figure 4-7. Pareto curves for baseload and night dispatch (Block A+C) considering two solar resource conditions: (a)-(b) in Carrera Pinto (DNI of ~ 3400 kWh/m ² -yr), and (c)-(d) in Santiago (DNI of ~ 2100 kWh/m ² -yr) for the low-cost scenario of 2030.....	130
Figure D-1: Simplified and illustrative scheme of the hybrid plant model in TRNSYS simulation studio.	160
Figure D-2: Illustrative scheme of the PV plant model in TRNSYS.....	161
Figure D-3: Illustrative scheme of the CSP plant model in TRNSYS.....	162
Figure D-4: Layout of the power cycle.	164
Figure D-5: Illustrated scheme of the BESS model in TRNSYS simulation studio.	165

NOMENCLATURE

Abbreviations

ACC	Air-Cooled Condenser
ACSP	CSP Association of Chile
BESS	Battery Energy Storage System
BoP	Balance of Plant
BoS	Balance of System
CAPEX	Capital Expenditures
CD	Cerro Dominador
CEN	National Electric Coordinator
CF	Capacity Factor
CFWH	Closed Feed Water Heater
CPV	Concentrated Photovoltaics
CSP	Concentrated Solar Power
DHI	Diffuse Horizontal Irradiance
DNI	Direct Normal Irradiance
E/P	Energy-to-Power ratio
EES	Equation Engineering Solver
EPC	Engineering & Procurement Costs
GA	Genetic Algorithm
GHI	Global Horizontal Irradiance
HC	High-cost scenario
HTF	Heat Transfer Fluid
LC	Low-cost scenario
LCOE	Levelized Cost of Electricity
NCRE	Non-Conventional Renewable Energies
NRMSD	Normalized Root-Mean-Square Deviation
NSGA-II	Non-Dominated Sorted Genetic Algorithm
O&M	Operation & Maintenance

OPEX	O&M Expenditures
PCS	Power Conversion System
PPA	Power Purchase Agreement
PV	Photovoltaics
RE	Renewable Energy
RSBR	Rotating Shadow Band Radiometer
SAM	System Advisor Model
SIC	Sistema Interconectado Central
SING	Sistema Interconectado del Norte Grande
SM	Solar Multiple
SOC	State of Charge
STEC	Solar Thermal Electric Components
TES	Thermal Energy Storage
TMY	Typical Meteorological Year
TOPSIS	Technique for Order of Preference by Similarity to Ideal Solution
TRNSYS	Transient System Simulation
UA	Heat transfer coefficient
WACC	Weighted Average Capital Cost

Symbols

A	area	[m ²]
A_f	capital recovery factor	[-]
C	total cost or thermal capacitance	[USD] or [kJ/K]
c	specific cost	[USD/kW, USD/m ² , USD/MWh or USD/m]
$CAPEX$	capital expenditures	[USD]

CF	capacity factor	[%]
$Cont$	contingency percentage	[%]
Cp	heat capacity	[kJ/kg-K]
D	energy demand	[MWh]
DNI	direct normal irradiance	[W/m ²]
DR	annual degradation rate	[%]
E	energy	[MWh]
E/P	energy-to-power-ratio of the BESS	[MWh/MW]
EPC	engineering and procurement cost percentage	[%]
exp	reference exponent	[-]
f	variation limit or persistence	[W/m ² /min] or [-]
$\hat{f}(\vec{x})$	surrogate function	[-]
F	objective function	[-]
F_a	availability factor	[%]
F_s	sufficiency factor	[%]
h	height	[m]
k	number of replacements of the BESS	[-]
L	lifetime of the hybrid plant	[yr]
$LCOE$	levelized cost of electricity	[USD/MWh]
LR	learning rate	[%]
\dot{m}	mass flow rate	[kg/s]
n	lifecycles of the BESS	[-]
N_{sim}	number of simulations	[-]
N_{var}	length of decision variables vector	[-]
$OPEX$	operation and maintenance expenditures	[USD]
P	power or cumulative capacity	[MW]
r	discount rate	[%]
S	size of the BESS in terms of energy	[MWh]

SM	solar multiple	[-]
SOC	state of charge	[MWh]
t	replacement period of the BESS	[yr]
T	temperature	[K]
T_c	corporate tax rate	[%]
TES	thermal energy storage	[h]
W	power output	[kW]
$WACC$	weighted average capital cost	[%]
x	decision variable	[-]
\vec{x}	decision variables vector	[-]
z	number of operating hours of the BESS at maximum capacity per year	[h]

Greek symbols

η	efficiency	[%]
Δt	simulation time step	[min]
τ	reference exponent	[-]

Subscripts

amb	ambient
annual	annual value
BESS	battery energy storage system
BoP	balance of plant
BoS	balance of system
c/d	charge/discharge
cap	capacitance
cond	condenser or turbine exhaust
CSP	concentrating solar power
d	direct

debt	debt
disch	discharged
DNI	direct normal irradiance
eq	equity
f	fixed cost
gross	gross
h	hour
hel	heliostats
HF	heliostats field
HTF	heat transfer fluid
hybrid	hybrid plant
i	current time step or operational year
id	indirect
in	inlet
inst	installation labor
inv	investment
invt	inverter
lim	limit
min	minimum
mod	pv module
mode2	receiver control mode 2
net	net power
O&M	operation & maintenance
off	time delay to begin receiver start-up
other	other costs
out	outlet
overh	installer margin and overhead
pb	power block
PCS	power conversion system
PV	photovoltaic plant

rec	receiver
ref	reference
rep	replacement
si	site improvement
stor	storage section
t	time step size
TES	thermal energy storage
tow	tower
turb	turbine
v	variable cost
var	variable

Superscripts

AC	AC size
DC	DC size
e	electric
inv	inverter
L	lower boundary
n	normalized
nom	nominal
th	thermal
U	upper boundary

PONTIFICIA UNIVERSIDAD CATOLICA DE CHILE
ESCUELA DE INGENIERIA

**METODOLOGÍA PARA OPTIMIZAR EL DISEÑO TECNO-ECONÓMICO DE
PLANTAS SOLARES DE POTENCIA INTEGRADAS CON SISTEMAS DE
ALMACENAMIENTO ENERGÉTICO**

Tesis enviada a la Dirección de Postgrado en cumplimiento parcial de los requisitos para el grado de Doctor en Ciencias de la Ingeniería.

ADRIANA ZURITA VILLAMIZAR

RESUMEN

Este trabajo de investigación se centra en la optimización tecno-económica de plantas de energía solar y sistemas de almacenamiento bajo las condiciones meteorológicas y de mercado eléctrico de Chile. La investigación se presenta a lo largo de tres artículos de revistas científicas. El objetivo general es desarrollar una metodología que permita determinar el conjunto de configuraciones óptimas de plantas de generación solar y de sistemas de almacenamiento para una ubicación y una estrategia de despacho dadas en Chile. Los objetivos específicos planteados incluyen: desarrollar el modelo físico de una planta solar híbrida con almacenamiento, que presente una planta de receptor central de Concentración Solar de Potencia (CSP), una planta fotovoltaica (PV), un sistema de almacenamiento térmico (TES) y baterías (BESS) para obtener su producción anual; desarrollar un modelo tecno-económico para evaluar la factibilidad de las plantas en términos de Costo Nivelado de Electricidad (LCOE) y factor de planta; realizar una optimización multiobjetivo considerando minimizar el LCOE y maximizar el factor de suficiencia como funciones objetivos para diferentes estrategias de despacho y ubicaciones; y determinar los rangos de competitividad y viabilidad de la planta híbrida frente a otras combinaciones tecnológicas de tecnologías solares y sistemas de almacenamiento.

La metodología de esta investigación comprende tres fases principales: modelación y simulación, análisis tecno-económico, y optimización multi-objetivo. La tesis está organizada en cinco capítulos. El Capítulo 1 presenta la introducción. Los Capítulos 2, 3 y 4 corresponden al primer, segundo y tercer paper de esta tesis respondiendo a los objetivos específicos. Finalmente, el Capítulo 5 presenta las conclusiones de esta investigación.

De la etapa de modelación y simulación, se encontró que la resolución temporal tiene un impacto significativo en la simulación y estimación de producción de energía de la planta híbrida. Los resultados de esta tesis indican que utilizar una resolución temporal horaria en

la simulación puede llevar a una sobreestimación de la producción anual de la planta híbrida CSP-PV-TES-BESS (y por tanto, a una subestimación del LCOE) entre un 2-6% con respecto a los resultados obtenidos con una resolución temporal de 1 minuto. El análisis también demostró que la operación de los sistemas térmicos como el receptor central de la planta CSP fueron los más afectados por la resolución temporal. De tal manera, una sobreestimación de la producción anual de la planta de CSP entre 14-15% se obtuvo al utilizar un paso de tiempo de 1h. Estos resultados enfatizan la importancia de elegir una resolución de tiempo apropiada al modelar plantas de energía solar con almacenamiento.

Por otro lado, los resultados de la evaluación tecno-económica de la planta híbrida CSP-PV-TES-BESS para proporcionar generación base en Chile confirman que ambas tecnologías y ambos tipos de almacenamiento pueden operar de forma sinérgica para proporcionar factores de suficiencia superiores al 80%, sin embargo, la rentabilidad de las baterías depende en gran medida de los objetivos de optimización evaluados. Cuando el único objetivo es minimizar el LCOE, las configuraciones de diseño no incluyen baterías en la planta híbrida debido a que el alto costo de inversión de las baterías supera su beneficio técnico de incrementar el factor de suficiencia de la planta. Sobre este punto, se determinó que diseñar plantas de energía solar con almacenamiento para alcanzar el mínimo LCOE puede no ser el enfoque más adecuado cuando se quiere garantizar un cierto nivel de suministro. Por ejemplo, los resultados de esta tesis de investigación muestran que la combinación PV-BESS siempre ofrece los LCOE más bajos para todas las estrategias de despacho, pero estas soluciones con costo mínimo también proporcionan los factores de suficiencia más bajos entre 30 y 70%, dependiendo de la estrategia de despacho.

Los resultados de esta tesis tienen como objetivo demostrar que, para cada ubicación y estrategia de despacho, se puede utilizar una optimización tecno-económica para obtener las soluciones de diseño óptimas que satisfagan funciones objetivo-conflictivas, como minimizar el LCOE y maximizar el factor de suficiencia. De la etapa de optimización multi-objetivo, este estudio revela que las soluciones más costo-efectivas para proporcionar energía en Chile incluyen la combinación PV-BESS cuando se requieren pocas horas de almacenamiento (4-5h), y centrales híbridas CSP-PV integradas con TES (y opcionalmente BESS) cuando se requieren largas horas de almacenamiento (>12h). Esto primero demuestra el valor que la energía solar puede tener en Chile para incrementar la diversidad de recursos en su futura matriz energética, y, en segundo lugar, destaca el valor de la hibridación como solución para complementar tecnologías, brindando flexibilidad al despacho y logrando costos de electricidad más competitivos.

Miembros de la Comisión de Tesis Doctoral:

Dr. Rodrigo Escobar

Dr. José Miguel Cardemil

Dr. Álvaro Lorca

Dr. Fernando Antoñanzas

Dr. Rafael Guédez

Dr. Juan de Dios Ortúzar

Santiago, Noviembre 2020

PONTIFICIA UNIVERSIDAD CATOLICA DE CHILE
ESCUELA DE INGENIERIA

A METHODOLOGY TO OPTIMIZE THE TECHNO-ECONOMIC DESIGN OF SOLAR
POWER PLANTS WITH STORAGE SYSTEMS

Thesis submitted to the Office of Graduate Studies in partial fulfillment of the
requirements for the Degree of Doctor in Engineering Sciences by

ADRIANA ZURITA VILLAMIZAR

ABSTRACT

This dissertation focuses on the design optimization of solar power plants integrated with storage systems under Chile's meteorological and electric market conditions. The thesis is presented in three scientific journal articles. The general objective is to develop a methodology that allows determining the set of optimal configurations of solar power plants with storage systems for a given location and dispatch strategy in Chile. The specific objectives proposed include: developing the physical model of a hybrid plant with storage that is comprised of a Concentrated Solar Power (CSP) plant based on a central receiver technology, a Photovoltaic (PV) power plant, a molten salt Thermal Energy Storage (TES) system, and batteries (BESS). The aim is to obtain their annual production, create a techno-economic model to evaluate the feasibility of the plants in terms of Levelized Cost of Electricity (LCOE) and sufficiency factor, perform a multi-objective optimization to minimize the LCOE and maximize the sufficiency factor considering different dispatch strategies and locations, and determine the competitiveness and viability range of the hybrid plant in comparison to other technology combinations of solar power plants and storage systems.

The methodology of this research comprises three main phases: modeling and simulation, techno-economic analysis, and multi-objective optimization. The thesis is organized into five chapters. Chapter 1 is the Introduction. Chapters 2, 3, and 4 correspond to the first, second, and third papers of this thesis, which respond to the specific objectives presented above. Finally, Chapter 5 presents the conclusions of this research work.

From the modeling and simulation stage, it was found that time resolution has a significant impact on the hybrid plant's energy production estimation. Results of this thesis indicate that using an hourly time resolution can lead to an overestimation of the annual production of the hybrid CSP-PV-TES-BESS plant (and, therefore, to an underestimation of the LCOE) between 2-6% with respect to the results obtained with a time resolution of 1 minute. The analysis also showed that the operation of thermal systems such as the central receiver of the CSP plant were the most affected by time resolution. An overestimation of the CSP plant's

annual production between 14-15% was obtained using a time step of 1h. These results emphasize the importance of choosing an appropriate time step when modeling solar power plants with storage.

From the techno-economic evaluation stage, a hybrid CSP-PV-TES-BESS plant was analyzed to provide base generation in Chile. Results of this research work confirm that both technologies and both types of storage can operate synergistically to provide sufficiency factors higher than 80%, however, the inclusion of a BESS to the hybrid scheme is highly dependent on the objective functions considered. When the only objective is to minimize LCOE, the design configurations do not include a BESS in the hybrid plant because the batteries' high investment cost outweighs their technical benefit of increasing the plant's sufficiency factor. In this context, it was determined that designing solar power plants with storage to achieve the minimum LCOE may not be the most appropriate approach when you also want to guarantee a certain level of supply. For example, the results of this research thesis show that the PV-BESS combination always offers the lowest LCOE for all dispatch strategies. Still, these least-cost solutions also provide the lowest sufficiency factors between 30 and 70%, depending on the dispatch strategy.

The results of this thesis aim to demonstrate that, for each location and dispatch strategy, a techno-economic optimization approach can be implemented to obtain the set of optimal design solutions that satisfy objective-conflicting functions, such as minimizing the LCOE and maximizing the factor of sufficiency. From the multi-objective optimization stage, this study reveals that the most cost-effective solutions to provide energy in Chile are the PV-BESS combination when few hours of storage are required (4-5h) and the hybrid CSP-PV hybrid with TES (and optionally BESS) when long storage hours are needed (> 12h). This first shows the value that solar energy can have in Chile to increase the diversity of resources in its future energy matrix. Secondly, it highlights the value of hybridization as a solution to complement technologies, providing flexibility to the dispatch, and achieving more competitive electricity costs.

Members of the Doctoral Thesis Committee:

Dr. Rodrigo Escobar

Dr. José Miguel Cardemil

Dr. Álvaro Lorca

Dr. Fernando Antoñanzas

Dr. Rafael Guédez

Dr. Juan de Dios Ortúzar

Santiago, November 2020

LIST OF APPENDED PAPERS

The papers published, accepted, or submitted during this research project as the principal author are listed below. The author of this dissertation executed the major work in writing these papers, such as creating methodology and models, simulations, interpretation of results, and discussion.

This dissertation is based on the following journal papers, referred to in the text by their Roman numerals.

- I. **Zurita, A.**, Mata-Torres, C., Valenzuela, C., Felbol, C., Cardemil, J. M., Guzmán, A. M., & Escobar, R. A. “Techno-Economic Evaluation of a Hybrid CSP-PV Plant Integrated with Thermal Energy Storage and a Large-Scale Battery Energy Storage System for Base Generation”. *Solar Energy*, Volume 173, October 2018, Pages 1262–1277.
- II. **Zurita, A.**, Mata-Torres, C., Cardemil, J. M., & Escobar, R. A. “Assessment of Time Resolution Impact on the Modeling of a Hybrid CSP-PV Plant: A Case of Study in Chile”. *Solar Energy*, Volume 202, May 2020, Pages 553-570.
- III. **Zurita, A.**, Mata-Torres, C., Cardemil, J. M., Guédez, R., & Escobar, R. A. “Multi-Objective Optimal Design of Solar Power Plants with Storage Systems according to Dispatch Strategy”. (*Submitted to the Journal of Energy in January 2021*).

Research articles not included:

The author of this thesis was also involved in these articles during her Ph.D. studies. These papers are not appended or discussed in this thesis., and they are listed below.

- i. **Zurita, A.**, Castillejo-Cuberos, A., García, M., Mata-Torres, C., Simsek, Y., García, R., Antonanzas-Torres, F., & Escobar, R. A. “State of the art and future prospects for

solar PV development in Chile.” *Renewable & Sustainable Energy Reviews*, Volume 92, September 2018, Pages 701–727.

- ii. Mata-Torres, C., **Zurita, A.**, Cardemil, J. M., & Escobar, R. A. “Exergy cost and thermoeconomic analysis of a Rankine Cycle + Multi-Effect Distillation plant considering time-varying conditions”. *Energy Conversion and Management*, Volume 192, July 2019, Pages 114-132.
- iii. Mata-Torres, C., Palenzuela P., **Zurita, A.**, Cardemil, J. M., Alarcón-Padilla, D. C., & Escobar, R. A. “Annual thermoeconomic analysis of a Concentrating Solar Power + Photovoltaic + Multi-Effect Distillation plant in northern Chile”. *Energy Conversion and Management*, Volume 213, June 2020, 112852.
- iv. Mata-Torres, C., **Zurita, A.**, Palenzuela, P., Cardemil, J. M., Alarcón-Padilla, D.-C., & Escobar, R. A. Comparative analysis between hybrid Concentrating Solar Power + Photovoltaic plant integrated with Multi-Effect Distillation and Reverse Osmosis Desalination plants. (*Submitted to the Journal of Desalination in October 2020*).
- v. Mata-Torres, C., Palenzuela, P., Alarcón-Padilla, D.-C., **Zurita, A.**, Cardemil, J. M., & Escobar, R. A. Multi-objective optimization of a Concentrating Solar Power + Photovoltaic + Multi-Effect Distillation plant: understanding the impact of the solar irradiation and the plant location. (*Submitted to the Journal of Energy Conversion and Management in December 2020*).

Additionally, the author has published different conference papers, participating in various international conferences with oral presentations. These works are listed below:

- i. **Zurita, A.**, Mata-Torres, C., Valenzuela, C., Cardemil, J. M., & Escobar, R. A. “Techno-economic analysis of a hybrid CSP-PV plant integrated with TES and

BESS in Northern Chile”. *AIP Conference Proceedings 2033* (2018), 180013. SolarPACES 2017, Santiago de Chile, Chile.

- ii. **Zurita, A.,** Mata-Torres, C., Cardemil, J. M., & Escobar, R. A. “Evaluating different operation modes of a hybrid CSP-PV+TES+BESS plant varying the dispatch priority.” *AIP Conference Proceedings 2126* (2019), 090007. SolarPACES 2018, Casablanca, Morocco.
- iii. **Zurita, A.,** Strand, A., Guédez R., & Escobar R. A. “Identifying Optimum CSP Plant Configurations for Spot Markets Using a Dispatch Optimization Algorithm – A Case Study for Chile.” SolarPACES 2019, Daegu, South Korea. (*Accepted in Conference Proceedings*).
- iv. **Zurita, A.,** Mata-Torres, C., Cardemil, J. M., & Escobar, R. A. “Time resolution impact on the performance prediction of a hybrid plant with storage in Chile.” ISES Solar World Congress 2019, Santiago de Chile, Chile.

1. INTRODUCTION

1.1. Context

Renewable power generation can help countries meet their sustainable development goals by providing clean and affordable energy (REN21, 2020). Renewables are also the lowest-cost source of new power generation in most countries. Since 2014, the global-weighted average cost of electricity of solar Photovoltaics (PV) has dropped into the fossil-fuel cost range (IRENA, 2019c), and cost reductions for solar PV and wind technologies are set to continue. In Chile's case, the country has become a focus of interest for solar energy investors in Latin America due to the very high solar irradiation levels of its territory. According to (Escobar et al., 2015), Chile is endowed with one of the highest levels of solar irradiation in the world, especially in the northern region where hyper-arid areas predominate with a large number of days per year with clear sky. The growth of solar PV capacity has been evidenced in the last ten years in Chile (REN21, 2020). This trend has been accelerated by the global costs decline of PV module prices, and it has been encouraged by the government's objectives of diversifying the energy matrix to reduce exposure to fossil energy (Zurita et al., 2018).

By 2009, the Chilean electric demand was only supplied by conventional power plants, predominantly based on fossil fuels such as coal (28%), oil-diesel (18%), and gas (8%), followed by hydro (43%). By 2013, the Non-Conventional Renewable Energies (NCRE) law 20/25 was promoted to establish a goal of 5% of renewable electricity generation and increase this contribution by up to 20% by 2025 (Instituto de Ecología Política, 2013). This favored the introduction of renewable energies in the energy matrix of the country. In 2019, 56% of electricity generation was still produced with fossil energy, but the remaining was diversified with hydro (28%), solar PV (8%), wind (6%), biomass (2%), and geothermal (0.3%) (Comisión Nacional de Energía, 2019). By 2020, Chile became one of the 12 countries in the world with a significant role of solar PV in its energy matrix (REN21, 2020). The growth of renewable energies is expected to continue as government plans seek to diversify the energy matrix with a high penetration of renewable energies. In 2014, the 2050 Energy Plan was proposed aiming to achieve 70% of renewable energy electricity generation

by 2050, with an emphasis on solar energy and wind energy (Ministerio de Energía, 2014). In 2019, the government signed an agreement with the largest energy generation companies of the country (AES Gener, Colbún, Enel, and Engie) to stop generating electricity from coal (Ministerio de Energía, 2020). This agreement aims for Chile to become carbon neutral through a decarbonization plan of the electric sector. The plan consists of phasing out all the coal power plants by 2040, which accounts for 4774 MW of the national installed capacity (Ministerio de Energía, 2019, 2020). This strategy comprises a five-year schedule to shut down 8 of the 28 coal plants by 2025, which represents 19% of the coal-fired generation, while the ultimate goal is to shut down the remaining 20 coal-fired plants by 2040 (Center for Clean Energy Policy, 2019; Ministerio de Energía, 2020).

The feasibility of decarbonization plants will only be possible by facilitating the replacement of existing base coal generation with other production means. However, the capacity to expand the second largest mean of electricity generation in Chile, which is hydro, is strongly limited due to environmental restrictions and strong social opposition to new projects' construction. This situation leads to scenarios with a high penetration of variable renewable energies to support the exit from coal plants, which must be considered carefully due to the variable and intermittent nature of natural resources such as wind and solar and the security and reliability issues that may be caused in the grid, such as discontinuity in the electric supply, inability to balance the system demand and generation, among others.

The vast solar energy potential of Chile can be properly seized to provide part of the national demand. This evaluation makes essential to consider mitigation methods for the production variability of solar energy. These methods include storage implementation, production curtailment, geographical dispersion of plants, demand matching, and hybrid plants of different renewable energy technologies. From these options, it is known that storage, in particular batteries, it is the only solution that, by itself, could eliminate the need for back-up with conventional generation at any level of penetration (Perez et al., 2016), although the deployment of this type of systems is still limited worldwide due to the relatively high costs of batteries.

Another solution to solar production variability is the technology of Concentration Solar Power (CSP), typically coupled to a Thermal Energy Storage (TES) system. The TES integration allows improving the plant's flexibility, with the possibility of generating

electricity during non-sunlight hours with a stable output. The main drawback is that CSP electricity costs are still superior to PV costs, even though a sustained decline in its costs has been evidenced in the last ten years (IRENA, 2020).

This situation evidences a need to evaluate energy storage schemes to support the integration of solar energy technologies in the Chilean energy matrix. Storage systems can make a substantial contribution towards cleaner and more resilient power systems, but storage requirements and power plant configurations represent a location-specific problem due to the performance of the systems vary with the meteorological and geographical conditions, as well with the demand considered. In order to identify the suitability of these type of systems into the governmental goals to provide sustainable and reliable energy, this thesis research tackles the need of developing a methodology to determine the optimal design of solar power plants with storage that allow providing a reliable electrical energy supply to the grid, intending to comprehend the feasibility range of the different solar energy technologies coupled with storage mechanisms under the meteorological, geographical, economic and electric-market conditions of Chile.

1.2. Thesis Objectives

This thesis aims to support the process of establishing design decision criteria and simulation guidelines of commercially available solar technologies, in particular PV, CSP, TES systems, BESS, and hybrid CSP-PV plants. In this line, the general objective of this research is identifying the set of optimal configurations of solar generation technologies integrated with storage system, in terms of sizing and techno-economic indicators, through the development a modelling and optimization methodology that considers the influence of different location-specific conditions and dispatch strategy requirements.

To reach this goal, the following specific objectives were defined:

- i) To develop a hybrid solar power plant physical model that allows evaluating a synergic operation between its components, including a CSP plant based on a molten salt central-receiver technology, a PV plant, a TES system, and batteries.

- ii) To carry out hourly and sub-hourly simulations of the hybrid solar power plant with storage to evaluate its operational behavior and obtain the annual performance in terms of energy production.
- iii) To develop a techno-economic model that calculates the total costs throughout the project's lifetime and the key performance indicators such as the Levelized Cost of Electricity (LCOE) and capacity factor to assess the feasibility of the hybrid solar power plant with storage.
- iv) To identify the technical benefits of including batteries in the hybrid plant in terms of system performance and demand fulfillment.
- v) To perform a multi-objective optimization of the hybrid solar power plant with storage considering minimizing the LCOE and maximize the sufficiency factor as objective functions.
- vi) To determine the competitiveness ranges and viability of the hybrid plant as an electricity generation and storage solution compared to other technology combinations of solar technologies and storage systems, evaluating the effect of different locations and dispatch strategies.

1.3. Hypotheses

The hypothesis of this research is based on the possibility of determining the optimal configuration of solar power plants and storage systems for a given location and dispatch strategy.

According to this, the following hypotheses are raised:

- i) Hybrid CSP-PV plant configurations integrating both types of storage technologies (TES and BESS) can be found to fulfill a specific demand with a synergic operation.
- ii) The time resolution considered in the hybrid plant simulation has a relevant impact on the energy estimation and the operation control at a component level.
- iii) The cost reduction scenarios required for batteries to be competitive as an energy storage solution when integrated with solar power plants can be determined through sensitivity analyses.
- iv) The dispatch strategy has a significant influence on the optimum design configurations obtained for solar power plans integrated with storage.

- v) The optimum design configurations of energy projects that allow guaranteeing a certain level of supply can be identified through the obtention of trade-off curves that minimize the LCOE and maximize the sufficiency factor.

1.4. Methodology

To meet the proposed objectives, a methodology to determine the optimal plant configuration of solar power plants with storage given a location and dispatch strategy was developed.

In general, the methodology is composed of three phases:

- i) Creation of the physical model and execution of transient simulations of the systems.
- ii) Techno-economic assessment of the plant.
- iii) Multi-objective optimization and comparative analysis among the optimal solutions.

The flow chart of the methodology is illustrated in detail in Figure 1-1.

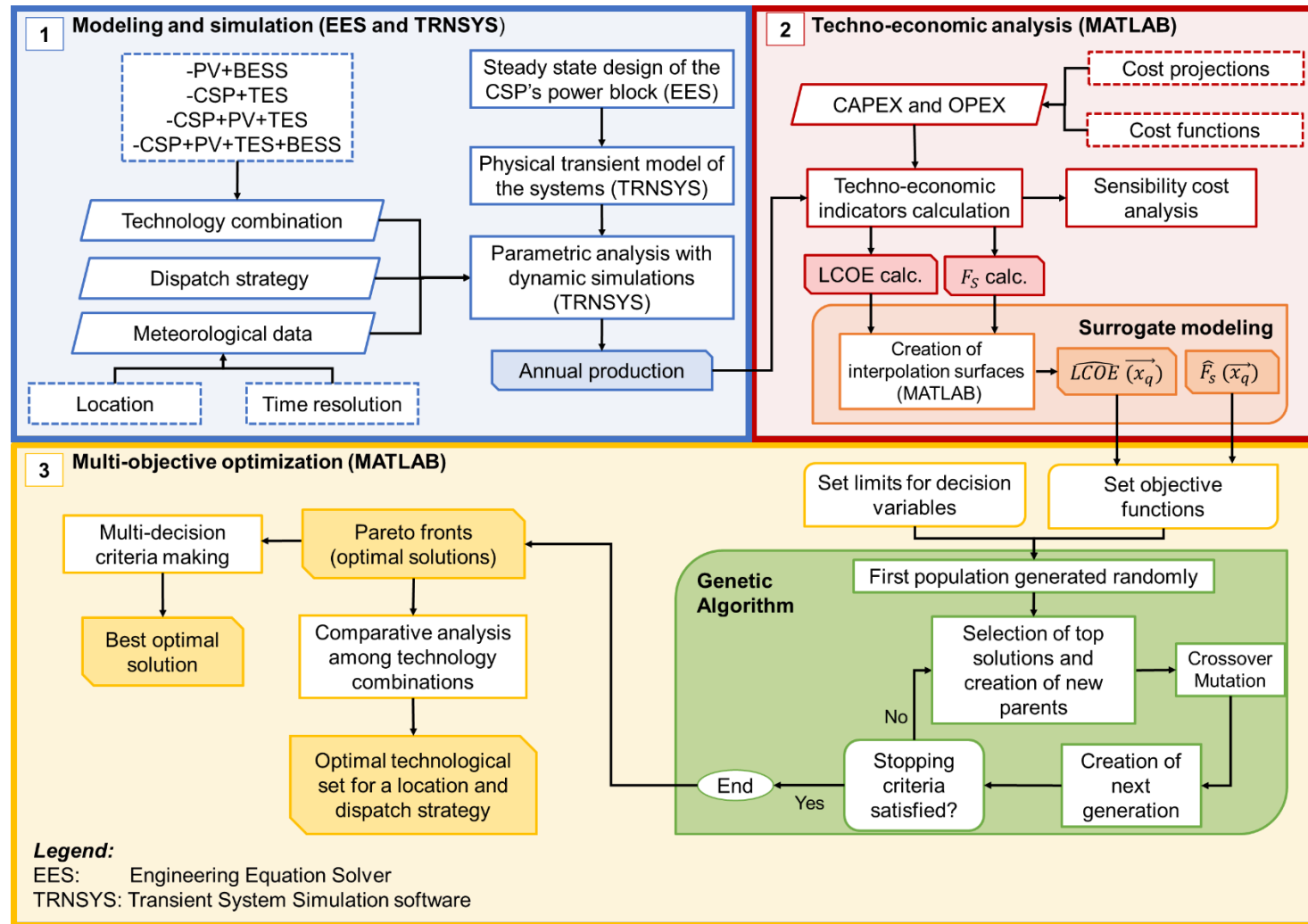


Figure 1-1: Methodology flow chart.

The first phase comprehends the creation of the physical model of the hybrid solar power plant with storage. This model was developed in the Transient System Simulation Software (TRNSYS) that simulates transient systems' behavior. TRNSYS is composed of an engine that reads and processes input files and solves the system iteratively to meet a given convergence (TRNSYS, 2020). The software also presents a library of components, which can be modified by users, and new components can be added. Each one of these components is developed in FORTRAN language and contains the performance model of one system.

The physical model of the hybrid solar power plant with storage was developed using different components of own creation and existing components of the TRNSYS libraries. The model includes five main systems: a solar PV plant, a CSP plant based on a central receiver system (including the heliostat field and the central receiver), the power block of the CSP plant, a two-tank direct TES system that operates with molten salts as Heat Transfer Fluid (HTF) and storage media, and a Battery Electrical Storage System (BESS) based on lithium-ion technology. The layout of the hybrid plant is illustrated in detail in Figure 1-2. The model of a hybrid CSP-PV plant with TES and BESS was developed in a single deck of TRNSYS to evaluate the interactions between all the plant components. Different technology combinations were also assessed (PV-BESS, CSP-tes, CSP-PV-tes, and CSP-PV-tes-BESS), and the physical model of the hybrid plant was developed to be able of simulating the rest of the technology combinations by only varying the input parameters. More details regarding the hybrid plant model developed in TRNSYS can be found in APPENDIX D: SIMULATION MODEL IN TRNSYS.

After the physical model of the hybrid plant was created, the simulations in TRNSYS were performed to obtain the annual performance and evaluate the operational curves of the thermal and electric systems under transient conditions. In first instance, the performance of the hybrid CSP-PV-tes-BESS plant was evaluated through hourly simulations.

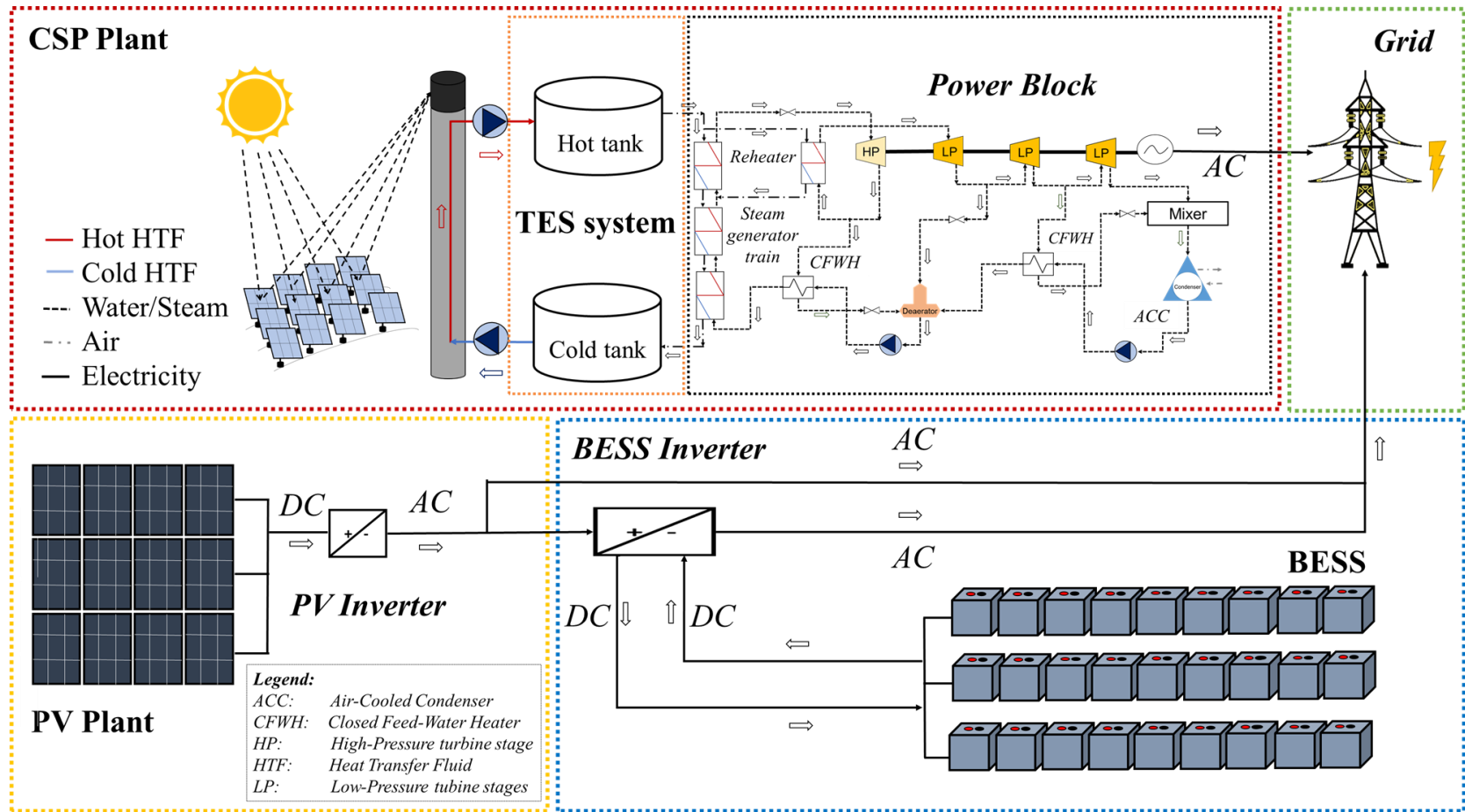


Figure 1-2: Scheme of a hybrid solar power plant with storage integrating a PV plant, CSP plant, TES, and BESS.

The second phase of the methodology comprehends creating a techno-economic model to assess the systems' performance in terms of costs and demand fulfillment. The techno-economic analysis was performed computing the Capital Expenditures (CAPEX) and the annual Operational and Maintenance costs (OPEX) to obtain the LCOE of the power plant. The research related to these two steps of the methodology, considering the hybrid plant's modeling with an hourly time resolution and the techno-economic analysis, was published as the first paper of this dissertation (Chapter 2). The assessment presented in Chapter 2 considers a parametric study of the hybrid plant's design variables for a baseload dispatch strategy.

Following this, it was identified the need to perform sub-hourly simulations that would capture the solar irradiation variability effects on the plant's performance. The main reason is that the PV plant and BESS present an instantaneous response to changes in the solar input, and the power block and the central receiver require safety control procedures to adapt their operation to high-variability irradiation episodes. Thus, an enhanced and detailed modeling of the CSP's power block and central receiver was developed. This phase comprehends the development of new components for the CSP's power block and central receiver, using TRNSYS and the Engineering Equation Solver (EES) software, including the modeling a thermal inertia, start-up, ramp, shut-down procedures, and an enhanced control logic to change operational modes. These modifications in the model would allow performing sub-hourly simulations to accurately evaluate and capture the effects of high-variability irradiation episodes on the plant's performance. Besides, a significant decrease in the computational time of the simulation was achieved. The specific methodology for this phase is explained in detail in the second paper of this dissertation (Chapter 3).

After the physical and techno-economic models were created, and the hybrid plant could be assessed through hourly and sub-hourly simulations, the third and final phase of the methodology was developed. This phase consists of executing a multi-objective optimization with a genetic algorithm to obtain the set of optimal solutions that minimize the LCOE and maximize the demand fulfillment of the hybrid solar power plant and other technology combinations. This optimization problem was established in terms of the design variables (nominal power of the PV plant, solar multiple of the CSP plant, TES capacity, BESS size, and inverter's power rate).

The multi-objective optimization was performed considering four technology combinations: a PV-BESS plant, a CSP-TES plant, a hybrid CSP-PV plant with TES, and a hybrid CSP-PV plant with TES and batteries. It was also analyzed the effect of the dispatch strategy on the technology combinations' trade-off curves, considering four dispatch profiles: baseload, night, daylight and evening, and only daylight. The last phase of the methodology comprehends a comparative analysis among the set of optimal solutions found for every technology combinations and dispatch strategy. This would allow understanding the competitiveness range of the solar power plant technologies with storage within the Chilean electric market scheme. The methodology followed to perform the multi-objective optimization, and the comparative analysis for the different technology combinations is widely described in the third paper of this dissertation, that puts together all the work done during this Doctorate (Chapter 4).

1.5. Summary of Main Contributions to State-of-the-Art

This thesis is presented in a compendium of three scientific articles format. Table 1-1 summarizes each research article's main contributions to the state-of-the-art and provides a general outlook of the publication timeline. The thesis's overall contribution to the state-of-the-art is provided in Section 1.8 and the link between the contributions and the papers is discussed in more detail in Section 0.

Table 1-1: Summary of the main contributions of the papers appended in this thesis.

Paper I:	<i>“Techno-Economic Evaluation of a Hybrid CSP-PV Plant Integrated with Thermal Energy Storage and a Large-Scale Battery Energy Storage System for Base Generation”</i>
Journal :	Solar Energy (2018) Vol. 173
Research Topic:	Techno-economic analysis of hybrid CSP-PV-TES-BESS plants
Contributions to state-of-the-art:	<ul style="list-style-type: none"> • A physical and techno-economic model to evaluate the performance of the hybrid plant is developed. • A new insight into this type of power plants' techno-economic viability is introduced and compared against state-of-art.

	<ul style="list-style-type: none"> • It provides a new outlook about the design configurations required to integrate both TES and BESS and achieve a synergetic operation. • Minimum LCOE design configurations under different cost reduction scenarios of the batteries are provided.
Paper II:	<i>“Assessment of Time Resolution Impact on the Modeling of a Hybrid CSP-PV Plant: A Case of Study in Chile”</i>
Journal:	Solar Energy (2020) Vol. 202
Research Topic	Modeling and simulation of hybrid CSP-PV-TES-BESS plants
Contributions to state-of-the-art:	<ul style="list-style-type: none"> • A new physical model of a molten salt central receiver that integrates a thermal capacitance to capture the effects of DNI variability and thermal inertia is introduced. • A new insight into the influence of the solar variability on the dispatchability of the hybrid plant at a component level (PV, CSP-TES, and BESS) and the control procedures that rule the operation of the plant is provided. • It quantifies the impact of time resolution on estimating the annual production, the LCOE, and capacity factor. • It provides a qualitative analysis to argue the use of a time resolution at the different stages in developing a hybrid solar power plant.
Paper III:	<i>“Multi-Objective Optimal Design of Solar Power Plants with Storage Systems according to Dispatch Strategy.”</i>
Journal:	Submitted to Energy (2021)
Research Topic:	Multi-objective optimization of solar power plants integrated with storage
Contributions to state-of-the-art:	<ul style="list-style-type: none"> • A multi-variable and multi-objective techno-economic approach for obtaining the optimal design of different technology combinations is introduced. • It provides relevant information concerning under which conditions a technology combination is preferable over another. • It quantifies the influence that dispatch strategy, solar resource conditions, and cost projections have on the competitiveness of storage-integrated technology options in terms of cost and demand fulfillment. • It provides a new insight concerning the need to include the sufficiency factor as an objective function in the techno-

	economic design optimization of energy projects, especially when a certain supply level needs to be guaranteed.
--	---

1.6. Contents

The present work is organized into five chapters. The first chapter is the Introduction. Chapters 2, 3, and 4 answer the specific objectives of this dissertation, while Chapter 0 presents the conclusions of this thesis. Chapters 2, 3, and 4 also constitute each of the research papers (journal papers I, II, and III). They contain the state-of-the-art literature review, methodology, results, and conclusions of this research within its scope. In this way, each chapter is an autonomous unity, and they can be read without the strict need for reading the rest of the chapters. However, some redundant contents may be found between them, especially in the introduction and system description sections.

The content of each chapter is indicated as follow:

- In Chapter 2, the techno-economic analysis of a hybrid CSP-PV plant integrated with a TES system and a large-scale BESS to provide base generation is carried out. This chapter includes the first published paper. This publication provides a preliminary insight into the techno-economic viability of this type of power plants in northern Chile and the design configurations that allow achieving the lowest LCOEs under different cost reduction scenarios of the BESS. This research brings a new outlook about integrating two types of storage that had always been analyzed competing against each other, aiming to evaluate the configurations that provide a synergetic operation. The study also presents an analysis regarding the cost distribution in the LCOE of the hybrid plant and a comparative study between implementing a fixed-tilt PV configuration or a one-axis tracking system in the hybrid plant scheme in terms of the gain on the annual production and the BESS participation to the total output.
- In Chapter 3, the time resolution impact on the modeling of the hybrid CSP-PV plant is evaluated considering two locations in Chile. This chapter includes the second published paper. This work presents a methodology to assess the impact of time resolution on the operation, performance, and dispatchability of the hybrid plant

integrated with a TES and BESS. This evaluation was considered vital to comprehend how the time resolution can affect the operation prediction and the hybrid plant's annual production estimation. The paper provides a new insight into the influence of the solar variability on the dispatchability of the hybrid plant at a component level (PV, CSP-TES, and BESS) and how the time resolution affects the control procedures that rule the operation of the plant. The study also brings some recommendations to the different actors involved in developing hybrid solar power plant projects regarding the advantages and drawbacks of implementing different time steps at every stage of the projects (preliminary feasibility evaluation, bankability assessment, real technical-operation simulation, or bid preparations).

- Chapter 4 presents the final research paper of this dissertation, unifying and applying all the research done. The research considers a comprehensive analysis evaluating the impact of the dispatch strategy on the optimal design configurations of different combinations of solar power plants with storage. This chapter includes the manuscript submitted to the Energy journal. This paper aims to determine the competitiveness ranges of each technology combination to establish which is the least-cost technological option that allows meeting a dispatch strategy with a certain level of supply guarantee, considering cost scenarios in 2020 and 2030 and two locations with different conditions of solar resource in Chile. A multi-objective optimization approach was followed to obtain the optimal solutions that minimize the LCOE and maximize the sufficiency factor. The analysis considered four technology combinations, including a solar PV plant with batteries, a CSP plant with TES, a hybrid CSP-PV plant with TES, and a hybrid CSP-PV plant with TES and batteries. This work allows determining the influence of the dispatch strategy on the competitiveness of these storage-integrated technology options in terms of cost and demand fulfillment, giving relevant information concerning under which conditions one technology combination is preferable over another.

1.7. Main Results

This section summarizes the main results from the appended papers presented in Chapters 2, 3, and 4. However, it is recommended to read it alongside the appended publications for

a better understanding. These results are summarized in a graphical abstract in Figure 1-3. Main results are presented as follows.

1.7.1. Techno-economic analysis of the hybrid CSP-PV-TES-BESS plant (Chapter 2)

Chapter II presents the first approach of the thesis towards the techno-economic modeling and analysis of a hybrid plant that integrates a PV, CSP, TES, and BESS plant. This approach considers a parametric study of the design variables (nominal PV power size, the TES size, the SM, and the BESS capacity) to evaluate their effect on the LCOE and capacity factor to obtain the minimum LCOE configurations.

The analysis was performed for a case of study in northern Chile considering a baseload profile, performing hourly simulations in TRNSYS. The hybrid plant consisted of a fixed-module PV configuration, a molten salts central receiver plant, and a BESS with a fixed power size inverter of 100 MW, while the energy capacity was varied to increase the energy-to-power (E/P) ratio of the batteries. The E/P ratio was defined as the relationship between the nominal energy capacity (MWh) and the BESS's power rate (MW).

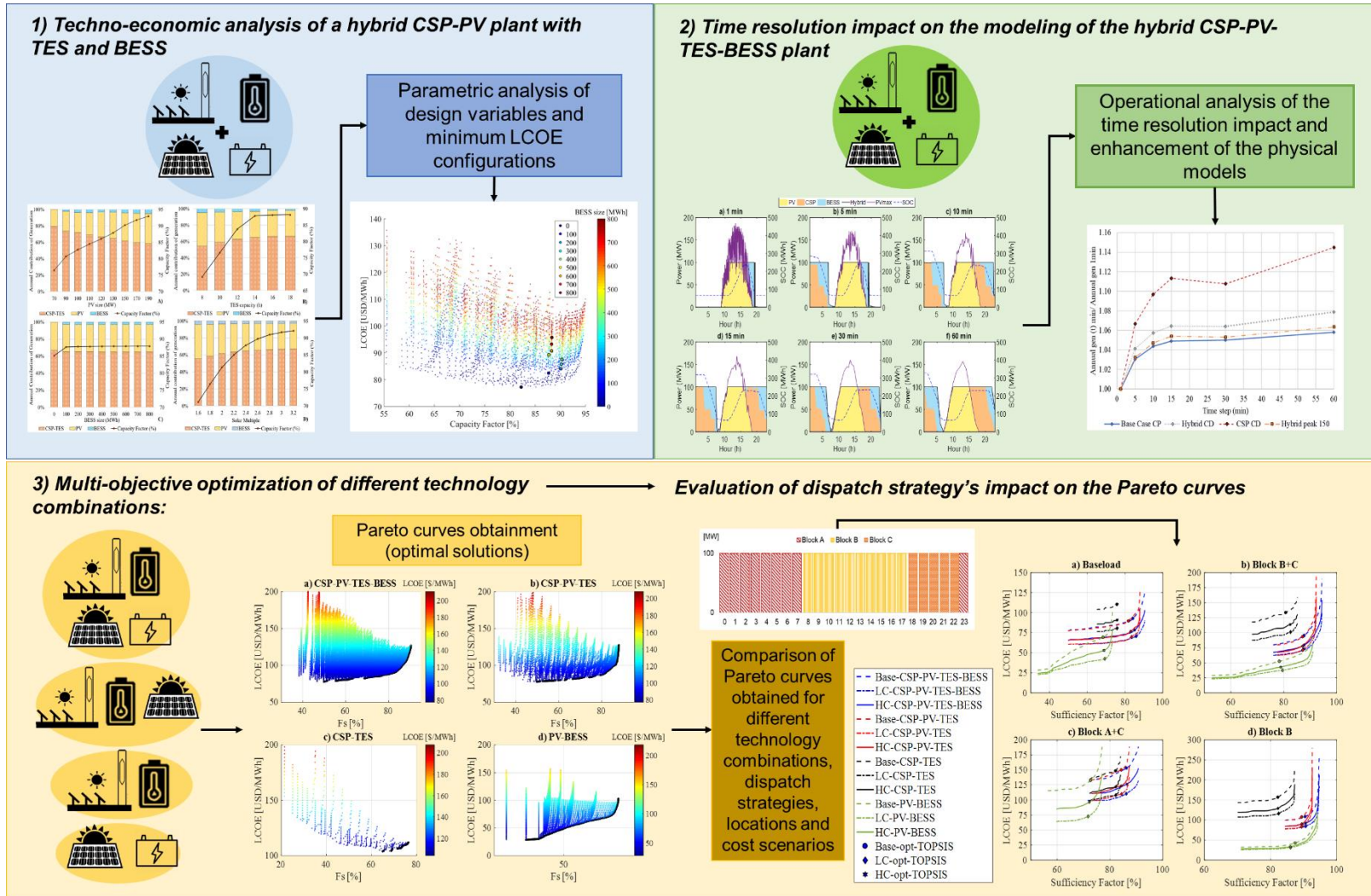


Figure 1-3. Graphical abstract with the main results of this research thesis.

The main techno-economic results found in Chapter 2 can be summarized as follows:

- Design configurations with E/P ratios between 1 and 4 have lower installation costs and capacity factors up to 90%. In comparison, higher E/P ratios present higher installation costs without benefitting the capacity factor, mainly due to a reduction of the CSP plant size and reaching the upper limit of the PV nominal size simulated.
- Current investment costs of the batteries make unprofitable its integration into the hybrid plant when the only goal is to achieve the lowest LCOE. In this concern, when the cost distribution of the LCOE was evaluated in terms of each component of the plant, it was found that the power conversion system's cost (or BESS inverter) presents the highest contribution to the total BESS cost for systems with E/P ratios between 1 and 4. In contrast, for higher E/P ratios, the storage or battery pack cost accounts for most of the BESS costs.
- It is required a reduction of approximately 60–90% of the battery pack cost (based on a reference value of 300 USD/kWh) to achieve competitive LCOEs compared to those obtained for a hybrid plant without BESS. Under this BESS cost reduction scenario, it was found a solutions domain with different hybrid plant configurations that allows integrating and complementing the production of storage types in a synergetic operation. These configurations included large PV plants (190 MW), CSP plants with 1.8 of SM and 12h of TES, and BESS with E/P ratios between 4 and 6.

1.7.2. Time resolution impact on the modeling of the hybrid CSP-PV-TES-BESS plant (Chapter 3).

In Chapter 2, the performance of the hybrid plant was analyzed on an hourly basis. This means meteorological data and a simulation time step with an hourly time resolution were implemented. Yet, the time resolution presents a significant impact on the components' modeling of a hybrid solar power plant with storage.

Chapter III presents an analysis varying the time resolution from 1, 5, 10, 15, 30 to 60 minutes in the hybrid CSP-PV-TES-BESS plant simulation. A case study for two locations in Chile was analyzed, considering a design configuration obtained in the techno-economic analysis from Chapter 2. The main results of Chapter 3 are highlighted as follows:

- The operation and performance prediction of thermal systems on a daily basis were the most affected by the time resolution variation, followed by the BESS, while in the PV it was negligible.
- It was found that the time resolution highly affects the central receiver operating controls, including start-up, shutdown, and ramp procedures. These controls were better captured with time resolutions between 1 and 5 min, while with greater time steps, DNI variability effects were not perceived. For a variable day, simulations using 10 to 60-min time resolution predicted fewer variable conditions of DNI, favoring the conditions for starting up and operating the receiver. In contrast, with a 1 to 5 min time resolution, the receiver did not start operation, mainly because the minimum conditions established by the controls to start-up were not achieved throughout the day, and the minimum energy required to begin operation was not reached.
- In terms of techno-economic results, the hybrid plant's annual production is overestimated as the time step is increased, leading to an underestimation of the LCOE. Variations in the capacity factor and LCOE with respect to the 1-min results are around $\pm 2\text{-}3\%$ using the 5-minute time step and between $\pm 4\text{-}6\%$ using 10-60 min time steps. In the CSP plant case, differences in the annual production estimation were more significant, with a maximum variation between 14 and 16% using the hourly time step. Results also indicated that the time resolution impact is lower for hybrid plants with oversized PV configurations with respect to the CSP plant and higher when the CSP plant is oversized with respect to the PV, regardless of the dispatch strategy.
- The 5-minute time resolution provides a well-balanced relationship between accuracy and computational time of the simulation; however, in the paper, it was highlighted that temporal resolution would mainly depend on the simulation's purpose, how much accuracy is expected from the results, and the computational time limitations. In this context, it was recommended to use an hourly time step to perform pre-feasibility studies since it provides the lowest computational time, while a time resolution between 1-5min was suggested in the development phase of the project,

in which a higher accuracy is needed by the EPC developers and financial entities to achieve bankability.

1.7.3. Multi-objective optimization, dispatch strategy influence, and comparison between technology combinations (Chapter 4).

In Chapters 2 and 3, the hybrid plant's techno-economic performance was assessed considering a baseload dispatch strategy. Chapter 4 evaluates the impact of the dispatch strategy on the optimal configurations. Thus, four dispatch strategies were studied: baseload, evening and night, daylight and evening, and only daylight hours. Four technology combinations were also evaluated, including a PV-BESS, a CSP-TES, a hybrid CSP-PV-TES, and a hybrid CSP-PV-TES-BESS. A case study for northern Chile was considered, and a multi-objective optimization approach was followed to obtain the Pareto curves that minimize the LCOE and maximize the sufficiency factor.

The main results of this study are:

- The optimal solutions with the lowest LCOEs were obtained in baseload for all the technology combinations, followed by the dispatch profiles that only supply energy during sunlight hours or including few hours in the evening, while the highest LCOEs were achieved with the dispatch strategy that considers only evening and night hours.
- The PV-BESS plant provides the lowest LCOE optimum solutions in all the cases analyzed in northern Chile, but its ability to guarantee the energy supply varies with the dispatch strategy considered. When covering daylight and evening dispatch, sufficiency factors above 90% can be reached with PV-BESS plants, and they represent the most cost-effective technology combination to provide energy in these dispatch strategies. When considering baseload and night dispatch, the hybrid CSP-PV plants (with or without batteries) are the most competitive option since they represent the only option that can reach sufficiency factors above 80% with moderate costs in these dispatch strategies.
- The PV-BESS plants are the most competitive technology when 4-5h of storage is required. Still, when long hours of storage are needed, i.e., during the operation at night (more than 12 hours), thermal storage is the best option in terms of cost-

competitiveness. Besides, solutions integrating both storage technologies were found for the hybrid plants, demonstrating that these technologies can work in synergy.

- When the 2030 cost projections are considered, the impact on the reduction of the LCOE is more significant in the PV-BESS plant than in the hybrid CSP-PV-TES-BESS plant, mainly because the cost scenarios implemented for the BESS are aggressive, while for the CSP plant are more conservative (based on the available literature). In this context, if current trends evidenced in the CSP industry were considered (lower installation costs of the CSP technology like those reported in China, and more favorable financial conditions for the projects), lower LCOEs could be achieved in the short-term future (even before 2030), which would enhance the competitiveness of the CSP technology, mainly in long-duration storage applications (>12h) such as baseload and night dispatch.
- In locations endowed with high solar resource ($\text{DNI} > 3000 \text{ kWh/m}^2/\text{yr}$), the optimal solutions for long-duration storage applications (>12h) consider hybrid CSP-PV plants in which the BESS primarily acts as a back-up of the CSP-PV plant, with the TES providing most of the overnight storage. In contrast, the PV-BESS plant becomes the most suitable technology combination under less favorable solar resource conditions ($\text{DNI} \sim 2000 \text{ kWh/m}^2/\text{yr}$). This occurs due to the CSP performance is strongly affected by the decrease in the DNI levels, reducing its cost-effectiveness to provide long duration storage. Because of this, large BESS capacities are preferred in the optimal solutions of the hybrid CSP-PV plants, with medium CSP sections supporting the PV-BESS plant. These results highlight the competitiveness that the BESS can provide over the TES under these conditions.
- Finally, the results of this section suggest that, even though the concept of designing solar power plants to achieve the minimum LCOE has been frequently used, this approach may not be the most appropriate when a certain level of supply wants to be guaranteed. For example, a PV-BESS plant located in Chile always offers the lowest LCOEs among the technology combinations for all the dispatch strategies (baseload, sunlight hours, sunlight and evening hours, and night), but the minimum LCOE solutions of PV-BESS plants tend to provide sufficiency factors between 30 and 70% depending on the dispatch. In these cases, results suggest that the correct approach

would be to determine which is the least-cost option that meets the demand with at least 80% of sufficiency factor for fulfilling dispatch contracts.

1.8. Research Contributions

The major contributions of this dissertation are listed below. Note that detailed contributions are explained in each chapter, including the specific contributions of published and submitted journal articles. In general, the main contributions to the state-of-the-art are:

- i) A physical model to evaluate a hybrid CSP-PV plant's performance at utility-scale integrated with TES a large-scale battery energy storage system is developed. The model integrates variables that enhance the accuracy of the performance prediction of the plant with respect to others implemented in the state-of-the-art, such as:
 - It allows performing simulations using hourly and sub-hourly time resolution, with a well-balanced relationship between precision and computational time.
 - It includes the part-load operation of the CSP's power block.
 - It includes start-up, ramp, and shut down procedures of the CSP's power block.
 - It integrates the model of a molten salts central receiver based on cylindrical tubes with a thermal capacitance to capture the effects of DNI variability.
 - It considers start-up and shut-down procedures for the central receiver.
 - It implements a control logics procedure of the central receiver to change its operational mode during DNI variability episodes.
 - It includes the operational logics control of a PV-CSP-TES-BESS integration.
- ii) A techno-economic model that allows obtaining the total expenditures and the plant's key performance indicators such as the LCOE and the capacity factor was developed. The methodology enables considering:
 - The variation in financial parameters such as the project's lifetime and the discount rate.
 - Cash flows throughout the lifetime of the project.
 - Assumptions regarding the degradation and replacement costs of the systems.

- iii) A methodology to optimize the techno-economic design of different combinations of solar power plants with storage was developed. This methodology also allows evaluating other effects, such as:
 - The variation of the solar irradiation and meteorological conditions given by a location.
 - The variation of the dispatch strategy.
 - Cost reduction scenarios of the different technologies.
 - The variation of the optimization objectives, such as the LCOE, sufficiency factor, PPA, etc.

In addition:

- iv) The impact of the design variables of the hybrid CSP-PV plant with TES and batteries on its techno-economic performance was determined. A solutions domain in which all the systems operate synergistically is presented, and the optimal solutions are provided.
- v) The time resolution impact on the modeling of the hybrid CSP-PV plant with TES and batteries is quantified in terms of variations in the annual production, LCOE, and capacity factor estimation.
- vi) Advantages and drawbacks of implementing different time steps at each stage in the development of a hybrid solar power plant are provided, including preliminary feasibility evaluation, bankability assessment, real technical-operation simulation, and bid preparations.
- vii) The competitiveness ranges of different technology combinations of solar power plants with storage systems are established, and the least-cost technological options that allow meeting a dispatch strategy with a certain level of supply guarantee under the Chilean electric market conditions are obtained.

1.8.1. Contributions applicable to the industry

Beyond the scientific contributions, the models, methodologies, and results obtained in this thesis also contribute to knowledge transferable to different industry areas.

Regarding the techno-economic modeling and simulation of hybrid CSP-PV-TES-BESS plants:

- The models, methodologies, and designing criteria established in this thesis provide valuable information to project developers and energy analysts who carry out the solar power plant simulations in the industry. The developed models allow performing hourly and sub-hourly simulations with a reasonable compromise between accuracy and computational time. The creation of the molten salt central receiver's model, including the thermal inertia effects, also represents an innovative outlook to be implemented in future simulation tools. These developments could support the process of establishing standard design criteria and guidelines for the modeling and simulation of solar power plants integrated with storage, especially in the CSP industry, in which the standardization of guidelines to simulate CSP plants is still a work in progress.

For instance, the quantification of the time resolutions' impact on energy production estimation provides valuable information for different stages in developing energy projects. In particular, the actors involved in the early phases of pre-design are benefitted from the findings of this research since they perform the simulations to select feasible and bankable design configurations to be included in their project portfolio. Actors from the Engineering and Procurement and Construction (EPC) stage are also benefitted from this thesis findings since they perform the project's detail engineering and enhancing the accuracy of their models is crucial for guaranteeing a certain level of energy production to the project owners.

Regarding the multi-objective optimization of solar power plants with storage:

- Results from the multi-objective optimization stage also provide relevant information to the field of energy policies. This research shows the importance of considering the sufficiency factor as an objective function when a certain supply level is required (sufficiency factors above 70%). These results strongly support the idea of recognizing storage as a crucial part for achieving a sustainable energy transition. In this context, energy policy creators and decision-makers such as ministries and government entities should encourage flexibility and dispatchability

as relevant features, recognizing their value in the new policies and tender processes currently being developed in different countries worldwide, such as Chile.

1.9. Recommendations for future work

The work developed in this doctoral thesis meets all the objectives previously proposed. Despite this, the research conducted in this work can be extended in several ways based on the methodologies and results obtained in this dissertation. Future work recommendations can be categorized into improvements in the modeling work and new research questions.

With regards to enhancing the models, the methodologies created in this thesis set a valid model to simulate (hourly and sub-hourly) hybrid CSP-PV plants integrated with TES and BESS with a good compromise between accuracy and computational time, but these can be improved considering some recommendations.

In first instance, the CSP plant's power block model was developed considering a fixed gross output of 100MW_e. The model comprises evaluating each power block's component under stationary and partial-load conditions in the software EES and creating the TRNSYS type through a multi-variable polynomial regression model considering the data coming parametric analyses performed in EES. This work can be further enhanced by automating these models to simulate different gross outputs of the Rankine cycle, rather than having only one model for a fixed gross output (100MW_e). This variable could also be included as a new variable decision in the optimization of the solar power plants including a CSP section, to choose the optimum net capacity of the power block in terms of the dispatch strategy. This recommendation of future work would allow evaluating a greater range of CSP technology's design configurations, and it would enhance the flexibility and application range of the current model.

Furthermore, in the CSP plant's model, the heliostat efficiency matrix is obtained simulating every solar multiple in the SolarPILOT software developed by NREL. The heliostats field component in TRNSYS uses this matrix to calculate the solar field efficiency in terms of the solar position; however, the file is read as an external input of the simulation. This methodology could be enhanced by developing a new component in TRNSYS that directly calculates the heliostat efficiency matrix during the simulation without introducing external files into the program. This improvement would improve the model's accuracy, and it would

allow simplifying the execution of parametric analyses, even though a relative increase in the simulation's computational time could be produced.

In addition, the fundamental basis of this research work was based on selecting a dispatch strategy and then optimizing the design configuration of the different solar technology combinations. This methodology can be enhanced by coupling a dispatch optimizer of the solar power plant with storage that looks ahead in the future the solar conditions and the prices in the electric grid to establish a pre-defined dispatch strategy. This optimizer would allow obtaining the dispatch profile to maximize the revenues of selling electricity to the grid and reduce the plant's start-ups. The main assumption would be that the power plant can obtain additional profit by selling a fraction of the energy to the spot market, which may be ruled by marginal costs or fixed tariffs depending on the electric market considered. This dispatch optimization routine could be coupled to the multi-objective design optimization to fully evaluate and identify the possible scenarios in which the solar plants' cost-effectiveness is higher.

In line with this last recommendation of future work, it would also be of great value to enhance the techno-economic model by including further financial evaluations, such as the effect of depreciation, taxes, the debt structure, among others, as well as having other revenue mechanisms of the energy projects, such as providing ancillary services, capacity payments, and selling a fraction of the PV energy surplus to the spot market. The financial parameters have a significant impact on the project's profitability, and the inclusion of different revenue mechanisms would allow evaluating the Internal Rates of Return (IRR) of the projects, changing the study perspective to the investor point of view, which has not been analyzed of this research work.

In terms of future research questions, the impact of evaluating different revenue mechanisms could be considered by optimizing the PPA instead of the LCOE or the project's IRR. These results can be compared with those obtained in this thesis to observe if there are changes in the design configurations chosen by the optimization algorithm. Lastly, there is also a lot of discussion regarding the storage technology that will lead the future. This includes different technologies of electric batteries, thermal storage, hydrogen (H₂) cells, and Carnot batteries. This approach indicates that other solar integrations with storage systems could be evaluated and compared to the results obtained in this dissertation, such as PV, CSP, or hybrid CSP-

PV plants integrated with H₂ cells and PV with Carnot batteries. A Carnot Battery transforms electricity into heat, stores the heat in inexpensive storage media like water or molten salt, and transforms the heat back to electricity when required. This option would be related to the integration of a PV-TES system that converts the PV electricity output into thermal energy through a direct resistance heating to heat the molten salt tanks and then transform the heat back to electricity with a power cycle when is needed.

Suggestions on future work about the evaluation of these systems could be aimed at answering how are the conversion systems' thermodynamic efficiency, if the PV technology's low costs compensate for the loss in efficiency of transforming direct electricity into heat, and what is the optimal set of storage-integrated solar power plants to provide electricity considering future developments in these technologies. Additionally, the analysis can be performed considering other CSP technologies, such as multi-tower power plants, parabolic trough collectors, linear Fresnel collectors, and other battery technologies besides lithium-ion.

1.10. Study Limitations

In line with the recommendations for future work, this section presents some limitations of the thesis, which are related to the nature of the applied research methods, time and resource constraints. These limitations could also be tackled in future works, and they are described as follows.

- The battery bank model was developed considering the lithium-ion technology in terms of a balance of state of the charge of the BESS and the charge/discharge efficiency. This approach is a simplified manner to evaluate the battery bank as a large reservoir of energy that allows varying the system's design inverter power and energy capacity. In this concern, different battery technologies as flow batteries should be evaluated through a more detailed model to assess the battery's performance in terms of other technical design parameters.
- The analysis in Chapter 2, 3, and 4 was performed using ground measurements that include meteorological and solar data for a particular year. This approach allows introducing solar data with high measurement accuracy as input to the simulation models, but it has the drawback of representing only one particular year. A common

practice is implementing a Typical Meteorological Year (TMY) that condenses multi-year long-term series into one representative year. TMYs are created from satellite-based models with a time resolution of 30min or 1h, leading to an inevitable loss of DNI variability information. For instance, a good agreement would be to employ TMYs with a higher time resolution or site adaption to enhance its parameters. TMY's implementation is relevant when financial assessments are being performed to demonstrate the solar projects' bankability.

- Due to the computational time of every simulation and the number of cases of study evaluated in this dissertation, the methodology of this thesis was only applied to three different locations in Chile, Crucero (Chapter 2), Carrera Pinto (Chapter 2 and 3), and Santiago (Chapter 2). The developed methodology should be applied to other locations in Chile to expand the analysis results and be applied in other countries.
- The CSP plant considered for all the analyses in this research is a central receiver technology integrated with a molten salt TES. Different CSP and TES technologies could also be evaluated to expand the results found in this dissertation. For instance, the Parabolic Trough Collectors (PTC) operating with synthetic oil is a mature CSP's technology that presents better performance yields than the central receiver in some world regions. The CSP's third generation is also considered for some as the future of this technology, aiming to enhance the thermodynamic conversion efficiencies through supercritical CO₂ Brayton cycles that operate with different central receiver technologies. The comparison and implementation evaluation of these technologies would give a broader outlook regarding the available solar technologies' applications.

2. TECHNO-ECONOMIC EVALUATION OF A HYBRID CSP-PV PLANT INTEGRATED WITH THERMAL ENERGY STORAGE AND A LARGE-SCALE BATTERY ENERGY STORAGE SYSTEM FOR BASE GENERATION

2.1. Introduction

Chile is endowed with a high potential of solar energy development and one of the highest levels of solar irradiation in the world, especially in northern regions where hyper-arid zones and a large amount of clear-sky days throughout the year predominate (Escobar et al., 2015). Chile also represents an emerging market taking the lead on solar energy development in Latin America. Solar Photovoltaics (PV) represents 8% of the national net installed capacity with 1852 MW operational PV power plants (CNE, 2018a). A continuous growth is expected, considering the government objectives to diversify and reduce its exposure to imported energy and international markets' volatility. However, the main problems of solar PV energy are the variability and intermittency of its electrical production related to solar resource availability. High penetration scenarios of fluctuating Renewable Energies (REs), such as solar PV, must be carefully analyzed due to the security and reliability issues that may affect the electricity supply's continuity. The integration of Electrical Energy Storage (EES) is part of the set of solutions to mitigate the variability and intermittency of the RE sources. In the case of solar energy, there is also an alternative for electricity generation through the Concentrated Solar Power (CSP) technology, which allows to integrate a Thermal Energy Storage (TES) system to guarantee a continuity of the production during hours without sunlight, increasing the dispatchability and stability of the power output of the plant.

In order to exploit the benefits of both technologies, the concept of a hybrid plant combining CSP technology with PV has been studied as a possible solution to mitigate the effects of variability and intermittency of solar energy. (Hlusiak et al., 2014) analyzed a hybrid CSP-PV plant consisted of a solar thermal collector field with TES, a PV system, and a fossil fuel burner in Morocco, evaluating the annual and daily operation and the Levelized Cost of Electricity (LCOE) of the plant. Their main results showed that CSP-PV hybrid plants are

expected to produce electricity up to 13% cheaper than a standalone CSP plant with TES. (Platzer, 2014) analyzed a solar thermal power plant based on a parabolic trough collector field with a Concentrated Photovoltaics (CPV) generator, evaluating the annual electricity production and the LCOE. Results indicated that the LCOE of the combined CSP+CPV plant was lower than the LCOE of the CSP plant, with a higher operation time. (Pan & Dinter, 2017) studied the concept of a hybrid CSP-PV plant integrated by a solar tower power plant with a molten salt TES and a fixed-angle PV system in South Africa. The power plant performance and LCOE were compared to the performance of standalone PV and CSP plants. Their results showed that a smaller CSP system is needed when it is combined with a PV system to supply a constant power generation, achieving lower LCOEs than a same-sized CSP plant and a higher annual generation.

(Zhai et al., 2017) also studied the annual thermal and economic performance of a CSP-PV system evaluating two dispatch strategies, a conventional dispatch strategy consisting of the PV and CSP sections operating independently, and a constant dispatch strategy on which the PV and CSP sections worked synergistically to provide a continuous output power. Results showed that the constant dispatch strategy presented a higher economic efficiency than the conventional dispatch strategy. More studies were performed by (Engelhard et al., 2016; Giuliano et al., 2016), which offer a techno-economical comparison of a CSP-PV plant concept with a variety of standalone PV and CSP plants integrated with batteries and fossil back-ups to follow a given load profile and decreasing the greenhouse gas emissions at the lowest cost. Their results indicate that a combination of CSP and PV plants can be the most cost-effective solution in many cases, with the PV power delivered during the day, and the CSP power preferred to be delivered at later hours.

The techno-economic potential of a hybrid CSP-PV plant has been demonstrated by different authors in recent years, showing that this concept takes advantage of the low costs of solar PV and the benefits of TES to improve the flexibility of the plant and increasing the capacity factors. Due to the high potential of solar energy development in Chile, the hybrid plant scheme has also been studied under the Atacama Desert conditions. (Green et al., 2015) analyzed the performance of a hybrid solar tower combined with a PV plant for different dispatch levels in terms of the capacity factor, with an optimal configuration for the Atacama Desert. Their results indicate that it is feasible to reach capacity factors of the hybrid plant

greater than 90%, considering appropriate its operation for a commercial structure of a Power Purchase Agreement (PPA). (Starke et al., 2016) evaluated integrating a parabolic trough collectors plant with a PV system and a solar tower-PV plant located in Crucero, Chile, to provide baseload and peak generation. This study considered a parametric analysis in terms of the PV size, TES capacity, and the Solar Multiple (SM); and an optimization problem to minimize the LCOE. The study's main results showed that the optimum LCOE of the hybrid plant was lower than the LCOE for the single CSP plant due to a reduction of the CSP solar field. (Starke et al., 2018) also performed a CSP-PV plant assessment implementing a multi-objective optimization with a genetic algorithm, considering as objective functions to minimize the LCOE and maximize the capacity factor. Results showed a clear trade-off between the LCOE and capacity factor, where the main benefits of the hybridization were related to the LCOE reduction, an increase of the capacity factor, and a substantial reduction in the solar field size.

Another concept proposes the inclusion of a Battery Energy Storage System (BESS) to the hybrid plant to cover the PV plant's production variations. This scheme has only been studied for small-scale plants (sizes less than 1MW) in Italy based on a pilot plant which implements a section of linear Fresnel collectors with thermal oil TES, coupled to an organic Rankine cycle, and a CPV plant with a bank of Sodium-Nickel batteries. (Cocco et al., 2016) analyzed and compared two dispatch strategies to deliver a constant daily power output level with this plant. They found that the strategy considering a synergic operation between both CSP+CPV plant favors the hybrid plant's operation in terms of higher annual energy production and longer load duration. Subsequently, (Petrollese & Cocco, 2016) evaluated the optimal configuration of a hybrid plant with the same characteristics to deliver a constant daily output of 1MW_e in two locations: Ottana, Italy, and Ouarzazate, Morocco. They obtained that the CSP+CPV plant is more cost-effective for load durations greater than 16h, while below 8h, the use of a PV plant with batteries represented the most cost-effective solution.

As described above, the potential of a CSP-PV plant under different configurations and technologies has been addressed by several authors. The inclusion of a BESS to the hybrid plant has also been studied but only for small-scale plants based on Linear Fresnel Collectors. However, the integration between both TES and BESS in a hybrid CSP-PV plant has not been analyzed yet in Chile in terms of sizing and techno-economic performance.

This work describes the techno-economic analysis of a utility-scale hybrid CSP-PV plant based on a central receiver system integrated with TES, a PV system, and a large BESS to provide base generation in Chile. The study aims to analyze the benefits that the electric storage can provide to a hybrid CSP-PV plant, taking advantage of the dumped energy coming from the PV surplus to increase the hybrid plant's capacity factor and dispatchability. The description of the proposed hybrid plant is presented in Section 2.2, followed by the methodology considered to perform this study in Section 2.3.

To address the usefulness of the hybrid plant scheme, a parametric analysis in terms of four design variables (PV size, SM, TES hours capacity, and BESS size) was carried out, studying the effects of these variables on the hybrid plant sizing and performance. A techno-economic evaluation was performed in terms of the LCOE and capacity factor to obtain the minimum LCOE configurations for different BESS sizes in Section 2.4.1. The cost distribution for each configuration was also obtained. A sensitivity analysis of the BESS storage section cost was carried out to obtain the required storage cost to be competitive compared to a hybrid CSP-PV without BESS in Section 2.4.2. In this concern, the present work brings a new outlook about integrating two types of storage that always have been analyzed competing against each other. It also aims to evaluate the hybrid plant configurations that complement the production of both CSP+TES and PV+BESS plants to achieve a dispatchable base solar energy. Lastly, a comparative study between considering a fixed-tilt PV field or a PV plant with a one-axis-tracking system in the hybrid plant scheme is performed in Section 2.4.3, in terms of the annual performance, seasonal dispatchability, and the LCOE. Section 2.5 presents the discussions, followed by the conclusions in Section 2.6.

2.2. System description

The proposed hybrid plant is composed of an CSP plant based on a central-receiver system and a fixed-angle PV system coupled to a battery bank. These systems are coupled in parallel in order to provide a flat power load of 100 MW_e. A simplified scheme of the hybrid plant is represented in Figure 2-1.

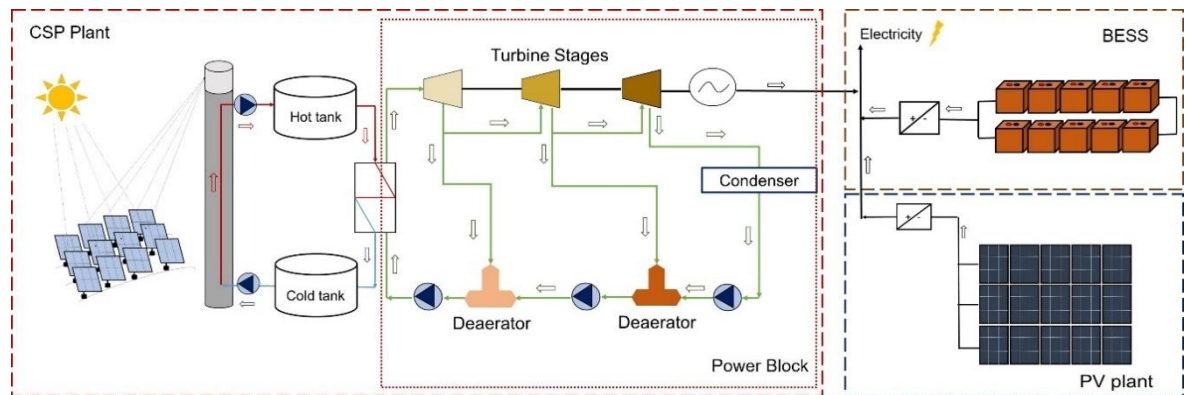


Figure 2-1: Scheme of the hybrid CSP-PV plant integrated with TES and BESS.

The model of the hybrid plant was analyzed under the solar irradiation conditions of northern Chile. Northern regions of this country present a combination of high elevation zones with extremely dry conditions resulting in one of the world's maximum solar radiation levels. These conditions are associated with hyper-aridity conditions, the reduction of the atmosphere thickness in high elevation zones, and the predominance of clear sky conditions (Antonanzas-Torres et al., 2016; Polo et al., 2014); resulting in average yearly totals between 2800 and 3800 kWh/m² of Direct Normal Irradiation (DNI) (Escobar et al., 2015; SolarGis, 2017).

The hybrid plant was simulated in Crucero, Chile (Lat. -22.24° S and Lon. -69.51° W). According to (Escobar et al., 2015), this location presents measured values of yearly totals of 3389 kWh/m² for DNI with a large number of high DNI levels during most of the day and few low-DNI days occurring during the altiplanic winter (February) and seasonal winter (Figure 2-2). The solar database source can be reviewed in detail in (Escobar et al., 2015).

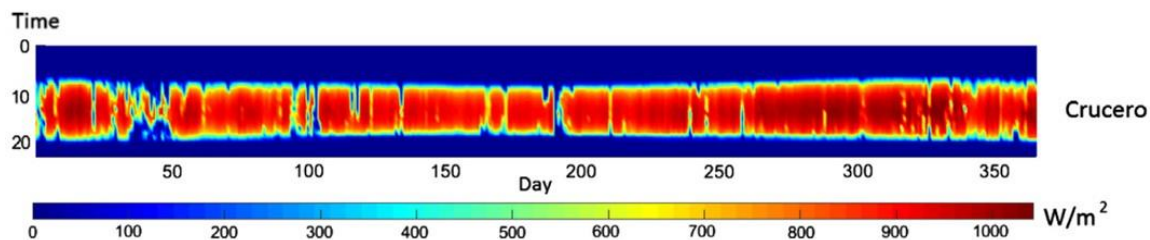


Figure 2-2: Daily total of DNI from January to December 2012 at Crucero, Chile.

A baseload profile of 100 MWe defines the power output curve. Two transmission systems mainly cover electric demand in Chile: the *Sistema Interconectado del Norte Grande* (SING), and the *Sistema Interconectado Central* (SIC), which were interconnected since November of 2017 to comprise the Electric National System with 99.3% of the total installed capacity of Chile (CNE, 2018b). The SIC covers the electricity demand of the northern regions where most of the country's mining industries are located. Simultaneously, the SIC delivers energy to the country's central zone, where most of the population is concentrated. Demand profiles of these systems are different, with a generation profile in the SING almost constant during the day due to a 24/7 demand of energy required by the mining industries, while a residential demand with a more variable profile is found in the SIC, as can be seen in Figure 2-3. This situation creates a requirement for base generation in northern regions of the country and the need to find energy generation methods that can be adapted to this demand profile.

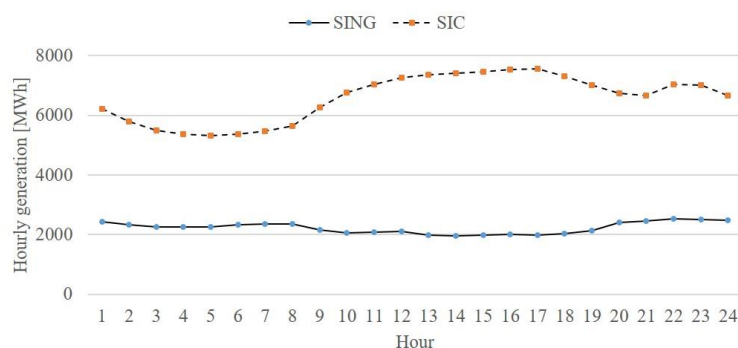


Figure 2-3: Hourly generation of Chile's national electric system composed by the SING and the SIC transmission systems on a typical day.

2.2.1. CSP plant with TES

The CSP configuration considered a central receiver system, which operates with a molten salt mixture (60% NaNO_3 and 40% KNO_3) as heat transfer fluid (HTF) and storage media. The CSP plant is based on an external receiver with a design temperature of 565°C (NREL, 2013). The TES section is based on a two-tank direct system, where the HTF is stored at 290°C in the cold tank and at 565°C in the hot tank. The molten salt flow was controlled in terms of the hybrid plant operation modes defined in the following section. Regarding the solar field, the heliostat area was defined as 144 m^2 with a reflectivity of 95%. The solar field configuration, receiver geometry, and tower height were defined as a function of the SM, representing the ratio between the thermal power output produced by the solar field at design conditions and the heat required by the power cycle at the nominal point. The CSP plant's design DNI was defined as 950 W/m^2 , which is the irradiance equivalent to 85% of the cumulative distribution function of the daily DNI of Crucero (Starke et al., 2016).

The power block coupled to the CSP plant consists of a Rankine cycle with a rated 40% efficiency and a gross power output of 110MW_e . The design inlet pressure of the turbine is 100 bar, and the condenser pressure is 0.096 bar. The latter is the saturation pressure of 45°C , which is 25°C higher than the ambient temperature that is assumed to be 20°C for the design point. It is considered an air-cooled condenser; therefore, the condensing pressure changes in terms of the ambient temperature keeping a difference of 25°C with the ambient temperature (Patnode, 2006). The turbine model considered two mass flow extractions which operate two regeneration open feed-water heaters or deaerators (Wagner, 2008). The maximum power cycle temperature is limited to 550°C and represents the temperature achieved at the super-heater output. The minimum turbine load is set at 30% of the gross power. Table 2-1 summarizes the main design parameters of the CSP and power block sections.

Table 2-1: Main design parameters of the CSP plant and the power block under nominal conditions.

Description	Unit	Value
<i>CSP plant</i>		
CSP technology	-	Central receiver system
Design DNI	W/m ²	950
Design receiver temperature	°C	565
Heliostat area	m ²	144
Reflectivity of the heliostat field	%	95
TES system	-	Two tanks direct
HTF and storage media	-	Molten salts mixture
<i>Power block</i>		
Gross power output	MW	110
Net output of electricity	MW	100
Minimum operation condition	%	30
Thermal efficiency	%	40
High-pressure turbine inlet pressure	bar	100
Medium pressure turbine inlet pressure	bar	23.8
Low-pressure turbine inlet pressure	bar	2.87
Condensing pressure	bar	0.096
Steam flow rate	kg/s	91.7

2.2.2. PV plant with BESS

The PV plant consisted of a fixed-angle module configuration. Regarding this selection, it is well known that implementing a one-axis tracking system in a PV power plant allows increasing the annual energy production, achieving higher capacity factors, and a lower LCOE in comparison to a fixed-tilt configuration. However, there is no consensus in the PV market trend in Chile about which is the most suitable tracking system for PV plants. According to (Zurita et al., 2018), total PV capacity, including operational and under-testing PV power plants of Chile for January of 2018, was about 2244MW of which 45.7% has a fixed-tilt configuration, followed by 44.4% with a one-axis-tracking system, and 3.1% with two-axis tracking. This distribution indicates that the PV market trend in Chile has not defined a clear preference or tendency to whether install fixed arrays or one-axis tracked arrays, mostly because more than 74% of the PV plants are located in northern regions of

the country, where even fixed-tilt configurations produce high energy yields in comparison to other locations in the world. In contrast, in central regions, the largest PV power plants implement tracking systems in one-axis, which may lead to the conclusion that the implementation of tracking systems in Chile is more common at higher latitudes and locations further south.

The hybrid CSP-PV plant concept has been considered by the industry in Chile under different configurations. The Abengoa Cerro Dominador project (currently under construction) includes a 110 MW molten salt tower with a 100MW PV power plant. The PV section of this project has recently started operation and implements a one-axis tracking system (Cerro Dominador project, 2018). In contrast, the Solar Reserve's project called Copiapó Solar (currently under development) includes two 130MW molten salt towers with a 150 MW PV plant, without specifying the type of tracking system (SEA, 2014). In this concern, the proposed hybrid plant considered in this study includes a fixed-tilt PV power plant. A comparative analysis considering a single-axis PV power plant is also presented in Section 2.4.3 to evaluate the techno-economic impact of implementing weather fixed or tracked-PV arrays in a hybrid plant scheme.

Studies conducted in northern Chile have shown that when a fixed-tilt PV configuration is chosen, the optimum design is given for the combination of sub-optimum configurations of both the CSP and PV plants. In that sense, (Green et al., 2015) and (Starke et al., 2016) found that the optimum configuration of a hybrid plant results in smaller CSP solar fields and a PV power plant with a tilt angle optimized for winter production. This angle is considerably higher than the optimum tilt angle of a single PV power plant to compensate the decrease of the CSP production in winter and maximize the combined output of the hybrid plant. (Starke et al., 2016) also found that the optimum tilt angle varies with the PV power size, as well as the optimum inclination tends toward the optimum angle of a PV-only plant when the PV power size increases. Therefore, in this study, the tilt angle was defined equal to the latitude to maximize the yearly production of the PV plant. The solar cell technology considered was silicon mono-crystalline (m-cSi) with the MEMC-330 Sun Edison modules (SunEdison, 2015). The inverter used was an ULTRA-TL-1100 of ABB with a maximum AC power of 1 MW (ABB, 2017). The PV plant has a scalable size in terms of the inverters number to

reach a nominal PV capacity of 100 MW_{dc}. A fixed soiling rate of 0.5% per day was also included.

The CSP-PV plant was integrated with a BESS based on a battery bank operating as a storage section, which considers a discharge depth of 84%. The BESS includes a Power Conversion System (PCS) or inverter with a charge/discharge efficiency. The PCS's power rating was fixed at 100 MW, which is the maximum power that the BESS should deliver. Table 2-2 presents the main design parameters of the PV plant and BESS system. Values of the depth of discharge, overall efficiency, and lifecycles are within the range reported by (IRENA, 2017) for lithium-ion batteries.

Table 2-2: Main parameters of the PV plant and BESS.

Description	Unit	Value
<i>PV plant</i>		
Solar cells technology	-	m-cSi
Inverter power	kW _{dc}	1000
Inverter efficiency	%	98.4
Module area	m ²	1.956
Module power	W	330
Module efficiency	%	16.9
<i>BESS</i>		
Depth of discharge	%	84
Overall efficiency	%	94
Lifecycles	cycles	5000

2.3. Methodology

The hybrid plant was modeled with the Transient System Simulation Program (TRNSYS) to obtain the annual performance of the thermal and electric systems of the plant under transient conditions. Simulations were performed throughout a year with meteorological and irradiation data with a time step of 1h as inputs in a unique TRNSYS deck.

The CSP plant was modeled considering components of the STEC library (Schwarzbözl et al., 2006), the electric library (University of Wisconsin-Madison, 2005), and types developed by authors. Particularly, it was developed a new heliostat type based on Type 394

of STEC library, including a daily soiling rate that is discretized on every simulation time step, which allows increasing the soiling losses for every time step; and a cleaning period time. The optimization of the number of heliostats, heliostat field configuration, receiver geometry, and tower height was performed using the SolarPILOT algorithm in the System Advisor Model (SAM) software (NREL, 2014). The obtained data was integrated into the TRNSYS model to perform the simulations. The PV plant was simulated as an array with a scalable size in terms of the number of inverters. As it was mentioned before, the maximum power output of the inverter was 1 MW_{dc}. This way, the PV plant coupled to the inverter was made using the Type 190 of TRNSYS based on the calculation presented by (De Soto et al., 2006), which allows to upload an inverter efficiency curve. These models are based on previous works and validations performed by the authors (Mata-Torres et al., 2017; Valenzuela et al., 2017).

The BESS section was modeled as a storage battery bank that considered only the State of Charge (SOC) variation of the battery given a charge or discharge rate. The BESS was modeled with a new type developed by the authors based on Type 47, which considers a balance of the SOC of the battery from the previous time step ($i-1$) to the next (i), with charge/discharge power efficiency, as the following equation describes:

$$SOC_{(i)} = SOC_{(i-1)} + \eta_{c/d} \cdot P_{BESS} \cdot \frac{\Delta t}{60} \quad (2.1)$$

where $SOC_{(i)}$ is the state of charge at the simulation time step i in MWh, $SOC_{(i-1)}$ is the state of charge from the previous simulation time step in MWh, P_{BESS} is the charge or discharge power of the battery in MW, $\eta_{c/d}$ is the charge or discharge efficiency, where the charge efficiency is used when the power is positive, and the discharge efficiency is used when the power is negative, and Δt is the simulation time step in minutes. The model's simplicity allows analyzing in a first approximation the value that has the BESS section in this hybrid plant concept.

To evaluate the replacement period of the battery bank, it was defined as the number of operating hours at maximum capacity per year (z). This metric was calculated as the ratio between the annual discharged energy by the BESS ($E_{disch,BESS}$) and the BESS capacity in energy terms (S_{BESS}) (Eq. 2.2). This value is associated with the discharge depth of the battery, and it was set at 5000 cycles. z was used to measure the charge/discharge cycles of

the battery bank throughout a year of the BESS. The replacement period of the BESS was defined in years (t), as a function of the life cycles of the system (n) and z (Eq. 2.3).

$$z = E_{disch,BESS}/S_{BESS} \quad (2.2)$$

$$t = n/z \quad (2.3)$$

The energy-to-power ratio (E/P ratio) is also defined as the relationship between the BESS's nominal energy capacity and the power capacity for a given application. The nominal energy capacity is the total amount of energy that the system can deliver over time in MWh. The power capacity measures the instantaneous demand requirement that the BESS can supply in MW.

2.3.1. Operation Modes

The hybrid plant's dispatch strategy is to deliver a net output of 100 MW_e to the electric grid. The operation mode prioritizes the PV output to cover the demand, while the CSP plant works as a back-up of the PV plant. Thus, three operation modes were defined:

- 1) When the PV production is below 65 MW, the CSP operates to cover the energy deficit and fulfill the demand.
- 2) When the PV production is above 65MW, but it is still not enough to meet the grid demand, the CSP plant operates at minimum power block condition (30%), and the PV energy surplus is stored in the BESS or dumped if the BESS is wholly charged.
- 3) When the PV plant produces more than the base-load capacity, the CSP power block is turned off, and the PV energy surplus is stored in the BESS or dumped if the BESS is wholly charged.

Several controllers of TRNSYS were applied to the TES system, the power block, and the BESS to implement the hybrid plant's operation modes. For both TES and power block control, a controller was inserted in terms of the available hot tank volume. It was defined three up/down limits for start-up and shut-down procedures. For the start-up, it was defined that the TES system needs 0.3h of storage capacity to start-up and increase the Rankine cycle capacity from 0 to 30%; 0.7 hours for 50% of capacity and finally 2h to reach 100% of the capacity. For the shut-down procedure, it was defined that when TES capacity decreases below 1.5h, the power block capacity drops to 50%; at 0.4h, the power block is limited to

30%, and at 0.05h, the power block is turned off. This procedure permits to decrease the number of start-ups of the power block, allowing it to operate for more than two hours.

The CSP plant was controlled to complement the PV output and fulfill the baseload capacity of 100 MW_e. A co-relation to obtain the HTF mass flow rate as a function of the required power by the Rankine cycle was implemented. Two TRNSYS controllers were applied to set the power block's minimum operating point when the PV plant output exceeds 65 MW and to turn-off the power block when the PV plant output surpasses 95 MW. Conversely, when the PV plant production goes down and reaches values below 90 MW, the power block is turned-on at the minimum operating point. Below 60 MW, the CSP plant's power block operates to complement the PV production and fulfill the demand. Thus, the steam turbine is only turned-off when the PV plant output exceeds the baseload capacity or when the TES is empty. If the TES is at full capacity, but there is thermal energy available on the receiver, the heliostats are defocused only to provide the required energy by the power cycle.

The BESS section is integrated to complement the hybrid CSP-PV plant to fulfill the demand when the TES runs out of energy. The BESS is charged when there is a surplus of PV production, which can occur when the power block is limited to operate at minimum capacity, and the PV output is greater than 65 MW, or when the PV plant output exceeds the baseload capacity. Finally, the BESS is discharged when the CSP-PV plant's net output is less than 90 MW.

Figure 2-4 shows the hybrid CSP-PV plant's operation modes described above during two different seasons for a configuration with 130 MW of PV, 2.4 of SM, 14 h of TES, and 350 MWh of BESS. Figure 2-4a illustrates the hybrid plant's operation during the summer season, which in Chile goes from December to March. During summer days, it can be observed that the baseload capacity is achieved mostly using the PV and CSP generation, with a small contribution of the BESS. In this case, the BESS is fully charged when PV net output exceeds 100 MW_e; however, during the night, the TES system's energy is almost enough to cover the demand, and the BESS is partially discharged. In contrast, Figure 2-4b shows the operation during the winter season (from June to September). The selected winter days show that when the PV plant production is not enough to cover the baseload, the CSP operates at the minimum condition of the power block, and the surplus of PV energy is stored in the BESS. However, this energy cannot fully charge the BESS, so the battery bank

remains partially charged until the night when all the energy stored in the TES and BESS are discharged to fulfill the demand. Despite this, the demand cannot be achieved entirely throughout all day, and the hybrid plant must be turned-off for some hours.

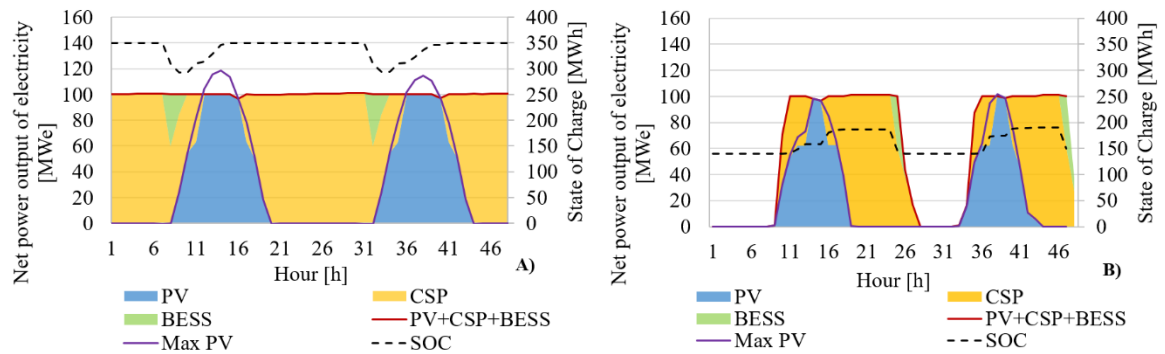


Figure 2-4: Dispatchability of the hybrid plant during (a) summer season, (b) winter season.

2.3.2. Economic analysis

To perform the economic analysis, the LCOE was considered as an economic indicator of the hybrid plant. The LCOE is a metric used to compare various power-generating technologies. The main parameters considered are the installation cost of the hybrid plant and the operation and maintenance costs. The calculation of the LCOE is based on the definition of (IRENA, 2012), and it is presented by the following equations:

$$LCOE = \frac{A_f \cdot (CAPEX + C_{rep}) + OPEX}{E_{annual} \cdot F_a} \quad (2.4)$$

$$A_f = \frac{r}{1 - \frac{1}{(1+r)^L}} \quad (2.5)$$

$$CAPEX = CAPEX_{PV} + CAPEX_{CSP} + CAPEX_{BESS} \quad (2.6)$$

$$OPEX = OPEX_{PV} + OPEX_{CSP} + OPEX_{BESS} \quad (2.7)$$

where the LCOE is in USD/MWh ; A_f is the capital recovery factor, $CAPEX$ is the total investment cost of the hybrid plant in USD and considers the investment cost of the PV plant ($CAPEX_{PV}$), the CSP and TES ($CAPEX_{CSP}$), and the BESS ($CAPEX_{BESS}$); C_{rep} is the replacement

cost of the battery bank in USD throughout the lifetime of the hybrid plant; $OPEX$ is the total operation and maintenance (O&M) cost of the hybrid plant in USD and includes the O&M costs of the PV plant ($OPEX_{PV}$), the CSP and TES ($OPEX_{CSP}$) and the BESS ($OPEX_{BESS}$); E_{annual} is the annual electricity generation of the hybrid plant, F_a is the availability factor defined in 95%, r is the discount rate of the project, and L is the lifetime of the hybrid plant. The main economic parameters of the CSP plant are listed in Table 2-3.

Table 2-3: Economic parameters considered for the CSP plant.

Description	Unit	Value
<i>Direct capital cost</i>		
Site improvements	USD/m ²	5
Heliostat field	USD/m ²	145
Balance of plant	USD/kW _e	200
Power block	USD/kW _e	800
Storage	USD/kWh _t	24
Fixed tower cost	USD	3,000,000
Tower cost scaling exponent	-	0.0113
Receiver reference cost	USD	103,000,000
Receiver reference area	m ²	1,571
Receiver cost scaling exponent	-	0.7
Contingency	-	5%
<i>Indirect capital cost</i>		
EPC and owner costs	% of direct cost	13%
Sale tax	%	0
<i>Operation and Maintenance</i>		
Fixed cost by capacity	USD/kW-yr	66
Variable cost by generation	USD/MWh	3.5

Detailed calculation of the CSP costs is presented in APPENDIX A: APPENDIX FOR CHAPTER 2. Tower and receiver costs, Engineering and Procurement costs (EPC) and the O&M costs are based on the information reported by (Turchi & Heath, 2013); while the other direct capital costs were adapted to the data obtained by the Solar Energy Program of Chile. The discount rate is defined as 5% in concordance with the CSP projects' prices in Chile. The project lifetime was established at 30 years without incentives, which do not exist in Chile for energy systems.

The economical parameters of the PV plant and the BESS are listed in Table 2-4. The PV plant costs are based on NREL values for utility-scale PV plants in 2017 (NREL, 2017). To perform the calculation of the BESS costs, it was considered the lifecycle method implemented by (Zakeri & Syri, 2015). This method considers the total capital cost of an EES unit and the lifecycle costs related to the O&M and replacement. The total capital costs include costs related to the PCS as the inverter and power interconnections, the balance of system (BoS) costs, and the storage section cost that represents the costs associated with build an energy storage bank or reservoir (for example, the energy cost of a battery bank or the cost of constructing a reservoir for a system of pumped hydro storage). Costs calculation related to the BESS are presented in the following equations:

$$CAPEX_{BESS} = (c_{PCS,BESS} + c_{BoS,BESS})P_{BESS}^{inv} + c_{stor} \cdot S_{BESS} \quad (2.8)$$

$$OPEX_{BESS} = c_{f,O\&M,BESS} \cdot P_{BESS}^{inv} + c_{v,O\&M,BESS} \cdot E_{annual,BESS} \quad (2.9)$$

$$C_{rep} = \sum_{j=1}^k \frac{1}{(1+r)^{jt}} c_{rep} \cdot S_{BESS} \quad (2.10)$$

where $c_{PCS,BESS}$ is the PCS cost in USD/kW; $c_{BoS,BESS}$ is the BoS cost in USD/kW; c_{stor} is the storage section cost in USD/kWh; $c_{f,O\&M,BESS}$ are the fixed O&M costs of the BESS in USD/kW-yr; $c_{v,O\&M,BESS}$ are the variable O&M costs of the BESS in USD/MWh; C_{rep} is the future replacement cost in USD/kWh; P_{BESS}^{inv} is the design power of the storage, which in this case is to deliver 100MWe; S_{BESS} is the BESS size in energy terms; $E_{annual,BESS}$ is the annual total energy discharged or delivered by the BESS to the grid; k is the number of replacements throughout the lifetime of the project, and t is the period of replacement in years. The BESS's economic parameters listed in Table 2-4 are based on the values reported by (Zakeri & Syri, 2015) and (Jorgenson et al., 2016).

Table 2-4: Economic parameters considered for the PV plant and BESS.

Description	Unit	Value
<i>PV plant</i>		
Investment cost for fixed-tilt	USD/W _{dc}	1.0
Investment cost for one-axis-tracking system	USD/W _{dc}	1.11
O&M cost for fixed-tilt	USD/kW-yr	15
O&M cost for one-axis tracking system	USD/kW-yr	18.5
<i>BESS</i>		
<i>Capital cost</i>		
Power conversion system cost	USD/kW	300
Balance of plant cost	USD/kW	87
Cost of storage section	USD/kWh	300
<i>Operation and Maintenance</i>		
Fixed O&M cost	USD/kW-yr	6.9
Variable O&M cost	USD/MWh	2.1
<i>Replacement</i>		
Replacement cost	USD/kWh	2/3 of the cost of storage section

2.3.3. Parametric analysis

A parametric analysis was performed in terms of four design parameters of the hybrid plant:

- Nominal PV size, related to the rated power output of the PV plant. As mentioned before, the nominal PV size is in terms of the number of inverters implemented.
- TES capacity, which relates the desired storage capacity in terms of operating hours with the volume of the molten salt tanks.
- SM, which represents the ratio between the thermal power output produced by the solar field at design conditions and the heat required by the power cycle at the nominal point.
- Nominal BESS size, related to the capacity of the battery bank in energy terms without considering the depth of discharge.

The evaluation range for each parameter in the parametric analysis is presented in Table 2-5. A total population of 4374 simulations was executed in TRNSYS to obtain the annual performance for each configuration. The techno-economic evaluation was performed in a script of Matlab developed by the authors.

Table 2-5: Values considered for the parametric analysis.

Parameter	Range	Step	Number of simulations
PV size (MW)	70-190	20	9
TES capacity (h)	8-18	2	6
SM	1.6-3.2	0.2	9
BESS size (MWh)	0-800	100	9

2.4. Results

The performance evaluation of a hybrid CSP-PV plant integrated with TES and BESS was carried out in northern Chile to analyze the effects of integrating a large-scale BESS. Results presented in the following section describe the influence of various design parameters on the configuration of the hybrid plant, implementing techno-economic indicators as the LCOE and capacity factor.

2.4.1. Parametric and techno-economic analysis

Figure 2-5 illustrates the parametric analysis results in terms of the capacity factor of the hybrid plant and the percentage contribution to the annual generation of each section of the plant (CSP+TES, PV, and BESS). The base case scenario is for a hybrid plant configuration with 130 MW of PV, 14h of TES, 2.4 of SM, and 350 MWh of BESS. In general, it was obtained that more than 60% of the hybrid plant generation comes from the CSP plant, followed by the PV plant. When the PV size is increased (Figure 2-5a), a reduction of the CSP generation is observed due to the rise of the PV contribution (up to approximately 40%), and the percentage contribution of the BESS increases as the PV size plant is larger.

It is also worth mentioning that for the case with 190 MW of PV, the largest BESS share was around 5% of the total generation. At larger TES capacities (Figure 2-5b), the capacity factor tends to increase significantly, from 69.1% at 8h to 88.2% at 18h of TES, the percentage contribution of the CSP plant rises, and both PV and BESS contributions decrease. When the BESS size is increased (Figure 2-5c) for a fixed configuration of PV size, it is noticed that the capacity factor of the plant remains stable as the contribution of the BESS does not significantly increase. This is because the surplus of PV energy that can be stored remains equal, which causes a limitation in the available energy to charge the

BESS. When this limit is reached, the percentage of PV and CSP generation remains almost stable.

Finally, Figure 2-5d shows that as the SM is lower, the contribution of both PV and BESS sections rise, which indicates that for small CSP plant configurations, BESS's contribution could increase if there is enough surplus of PV power. The SM has a significant impact on the capacity factor as the solar field's size is bigger and more energy is received and transformed.

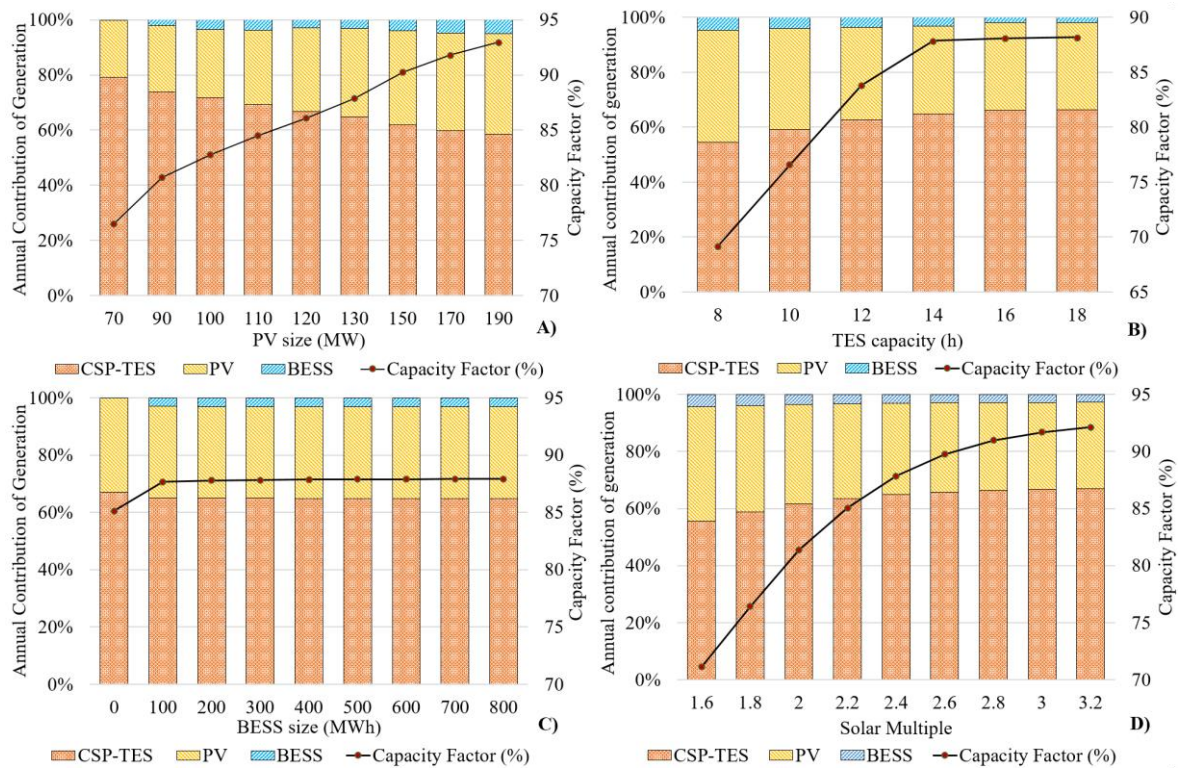


Figure 2-5: Annual contribution of generation and capacity factor of the hybrid plant for a base case with 130 MW of PV, 14h of TES, 2.4 of SM, and 350 MWh of BESS. A parametric analysis was performed varying a) PV size, b) TES capacity, c) BESS size, and d) SM.

Besides evaluating the hybrid plant performance under different configurations, a techno-economic analysis was carried out in terms of the LCOE and the capacity factor. Figure 2-6 shows the tendency found for the LCOE of the hybrid plant as a function of the capacity factor, varying the design parameters from Table 2-5. In general, the LCOE is higher as the BESS size increases. The minimum LCOE configuration was obtained for a hybrid plant

with 130 MW of PV, 2.2 of SM, 14 h of TES, and 0 MWh of BESS (point "A" in Figure 2-6), with an LCOE of 77.22 USD/MWh. In this manner, the lowest cost solution is given for a configuration without a battery bank, which indicates that the current BESS costs are still very high to achieve a competitive price generation for applications with a large-scale EES. Table 2-6 lists the minimum LCOE configurations of the hybrid plant achieved for each BESS size analyzed. These points are also represented in Figure 2-6 as colored circle marks.

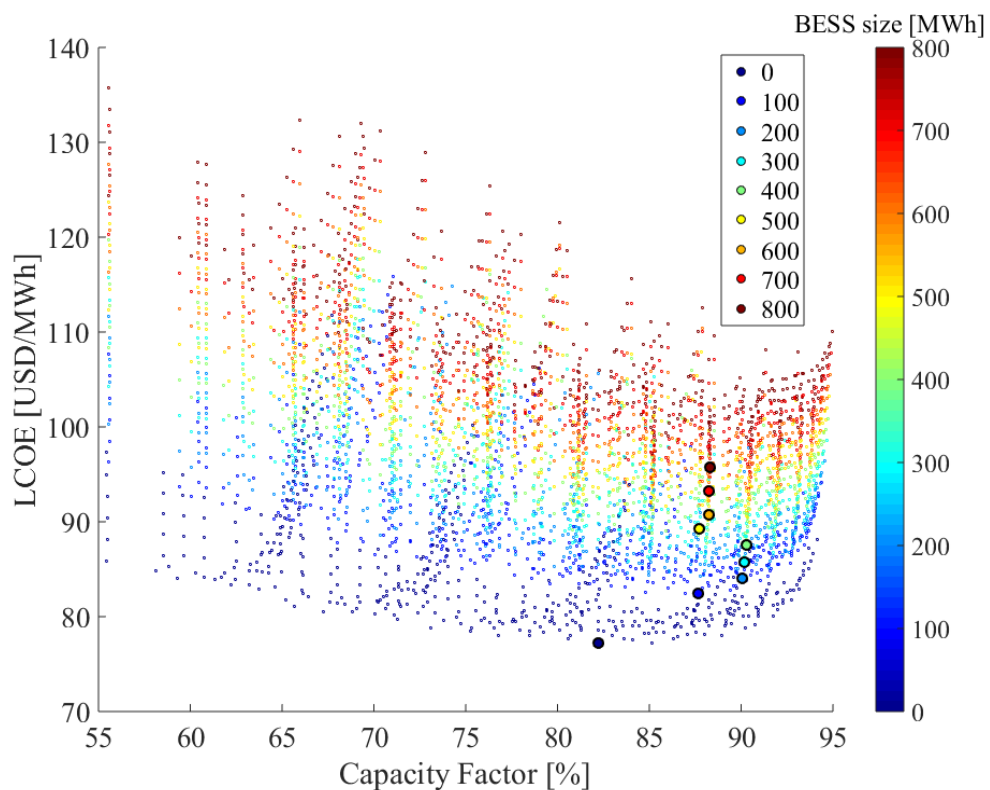


Figure 2-6: LCOE and capacity factor of the hybrid plant for different BESS sizes. Circle marks represent the minimum LCOE configuration for each BESS size analyzed.

Table 2-6: Minimum LCOE configuration for each BESS size analyzed.

Minimum LCOE configuration	BESS size [MWh]	E/P _{ratio} [-]	Nominal PV size [MW]	SM [-]	TES capacity [h]
A	0	0	130	2.2	14
B	100	1	130	2.4	14
C	200	2	150	2.4	14
D	300	3	170	2.2	14
E	400	4	190	2	14
F	500	5	170	2	12
G	600	6	190	1.8	12
H	700	7	190	1.8	12
I	800	8	190	1.8	12

It can be observed that excluding point A, these configurations are within a zone of high capacity factors above 80% and LCOE values between 82.44 USD/MWh and 95.73 USD/MWh. Figure 6 shows some vertical tendencies given for the smallest PV sizes (70 and 90MW). These configurations indicate that the system's capability to charge the battery bank fully is limited with smaller PV plants. As the BESS size increases, the electricity generation of the PV plant remains the same. Still, the battery bank capacity cannot be fully exploited, resulting only in a cost addition. As the PV size increases, this tendency becomes more linear, and the BESS capacity can be more exploited, increasing the capacity factors. The BESS costs introduction creates the gap between the point A and the zone of minimum LCOE points for each BESS sizes.

Table 2-6 also shows that the minimum LCOE configurations are given for large PV sizes between 130MW and 190MW. E/P ratios from Table 2-6 are represented by the ratio between the BESS's energy capacity and the fixed power rating of 100MW, resulting in values between 1 and 8. Above E/P ratios of 3, the minimum cost configuration of the hybrid plant results in PV sizes from 170 MW to 190 MW, which means that to exploit the BESS's capacity, large PV plants are required. In contrast, the TES size decreases from 14h to 12h of capacity, and the SM of the CSP plant slowly decreases from 2.4 to 1.8 as the E/P ratio is higher.

Table 2-7 includes the techno-economic results of the minimum LCOE configurations for each BESS size. For E/P ratios from 1 to 4, the percentage generation of the PV plant and

BESS section tends to increase, while the CSP plant's contribution decreases. The same situation occurs for E/P ratios from 6 to 8, but the increase or decrease rates of generation contribution barely vary as the BESS size increases. In this concern, capacity factors for E/P ratios between 6 and 8 are lower than the capacity factors obtained for E/P ratios between 1 and 4, remaining stable at 88.28%. This situation is due to the PV size remains at 190MW for these configurations, therefore, an increase in the BESS size does not represent a significant rise in the annual production since the available PV energy to be exploited is the same. The highest annual production was also obtained with the configuration E, while the configuration F achieved the lowest amount of dumped PV energy.

It is worth mentioning that the total PV energy excess from Table 2-7 represents the sum of the dumped PV energy that cannot be exploited by the hybrid plant and the surplus of PV energy utilized to charge the BESS when it is allowed. Results indicate that for E/P ratios between 1 and 4, the excess of solar PV energy increases due to larger PV plant sizes. In the case of an E/P equal to 5, the minimum LCOE configuration is given for a 170MW PV plant, which causes a decrease in the total of PV excess, but for E/P ratios from 6 to 8, the amount of PV excess remains stable due to the PV size of the minimum LCOE configuration remains in 190MW. Table 2-7 also shows that between 57.4% and 95.7% of the total PV energy excess is stored by the BESS to supply energy. The amount of PV energy excess utilized by the BESS is related to the PV plant capacity, the CSP configuration, and the operation mode. Similarly, as more PV excess is exploited to charge the BESS, less dumped PV energy is produced. The maximum percentage of PV surplus utilized by the BESS was obtained for the configuration F, with an LCOE of 89.19 USD/MWh. This configuration presents an LCOE 15% higher than the hybrid plant without BESS, but it increases the capacity factor from 82.20% to 87.73%.

Table 2-7: Techno-economic results of the hybrid CSP-PV plant for the minimum LCOE configurations.

	E/P ratio [-]	CF [%]	LCOE [USD/ MWh]	Gen. PV [%]	Gen. CSP+TES [%]	Gen. BESS [%]	Annual production [MWh]	Dumped PV [MWh-yr]	Total PV excess [MWh-yr]	PV excess to BESS [%]
A	0	82.20	77.22	34.27	65.73	0.00	758,298	29,234	29,234	0.00
B	1	87.63	82.44	32.06	65.03	2.91	808,434	4,192	29,011	85.6
C	2	90.01	84.04	34.10	62.03	3.86	830,439	17,720	51,669	65.7
D	3	90.23	85.70	36.15	58.48	5.36	831,685	34,291	81,506	57.9
E	4	90.34	87.53	37.55	54.83	7.62	832,572	49,788	116,893	57.4
F	5	87.73	89.19	37.25	53.51	9.24	808,748	3,577	82,443	95.7
G	6	88.28	90.68	38.48	49.94	11.58	813,562	18,367	117,824	84.4
H	7	88.28	93.20	38.47	49.92	11.61	813,922	17,988	117,824	84.7
I	8	88.28	95.73	38.45	49.90	11.65	814,258	17,635	117,824	85.0

The parametric analysis shown in Figure 2-7 indicates that higher capacity factors are related to higher installation costs of the hybrid plant. Installation cost represents the ratio between the net investment costs of the hybrid plant and the nameplate capacity. This way, the variation of LCOE values can be observed, with the lowest values located in the left zone associated with lower installation costs. It is also noticed a trade-off between the capacity factor and the installation costs. The increase of the LCOE is related to the addition of higher capacities of BESS, as shown in Figure 2-6. For the minimum LCOE configurations, it is observed that the inclusion of the BESS represents a significant increase in the installation cost that leads to a moderate rise in the capacity factor. This evidences that the BESS installation cost has a significant impact on the economics of the hybrid plant.

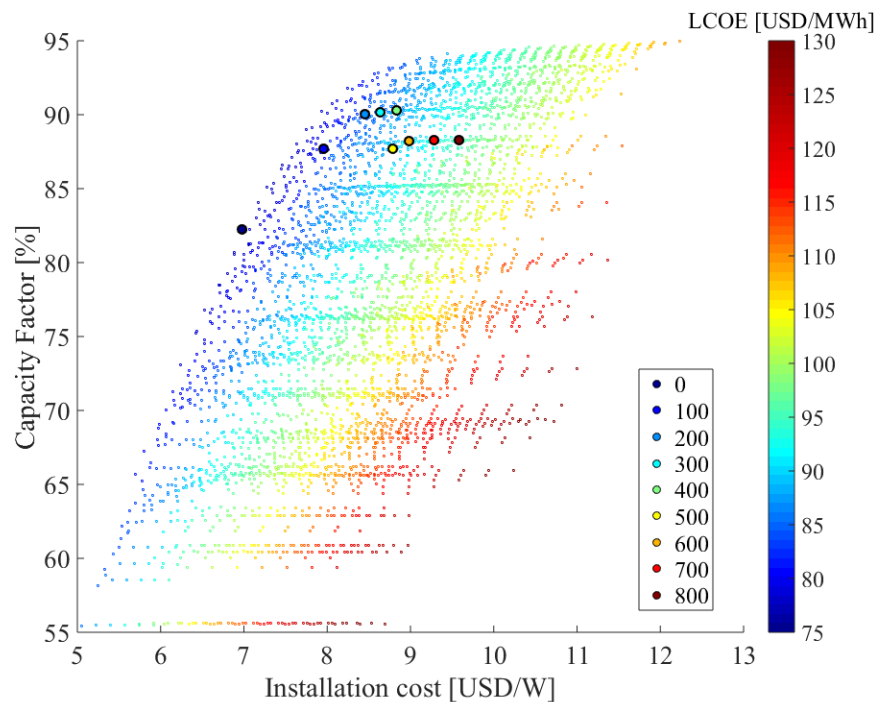


Figure 2-7: Capacity factor and installation cost of the hybrid plant for different BESS sizes. Circle marks represent the minimum LCOE configuration for each BESS size.

It is also noticed a difference in the capacity factors for configurations with more than 500 MWh (E/P ratios from 5 to 8), produced by smaller TES capacities and SMs (Table 2-6 and Table 2-7). These results indicate that configurations with E/P ratios from 1 to 4 have lower

installation costs and higher capacity factors, mainly due to a higher contribution of the CSP plant to the total generation of the hybrid plant; while E/P ratios above 5 present higher installation costs and lower capacity factors due to the reduction of the CSP plant size, which increases the PV+BESS contribution to the total generation.

2.4.2. Cost distribution and sensitivity analysis

The introduction of BESS costs represents a significant percentage of the hybrid plant costs distribution. Figure 2-8 illustrates the cost distribution of the LCOE in terms of investment and O&M costs for each hybrid plant component. It is observed that the investment cost of the CSP plant has the most significant influence on the LCOE, followed by the investment cost of the PV plant and the storage section cost of the BESS. As mentioned in Section 2.3.2, the BESS's investment cost is integrated by the PCS cost per unit of power, and the storage section cost per unit of energy. In this case, the PCS cost represents a fixed cost of the BESS associated with the inverter's cost needed to charge or discharge the battery bank at a rated power of 100MW, independently of the BESS size analyzed.

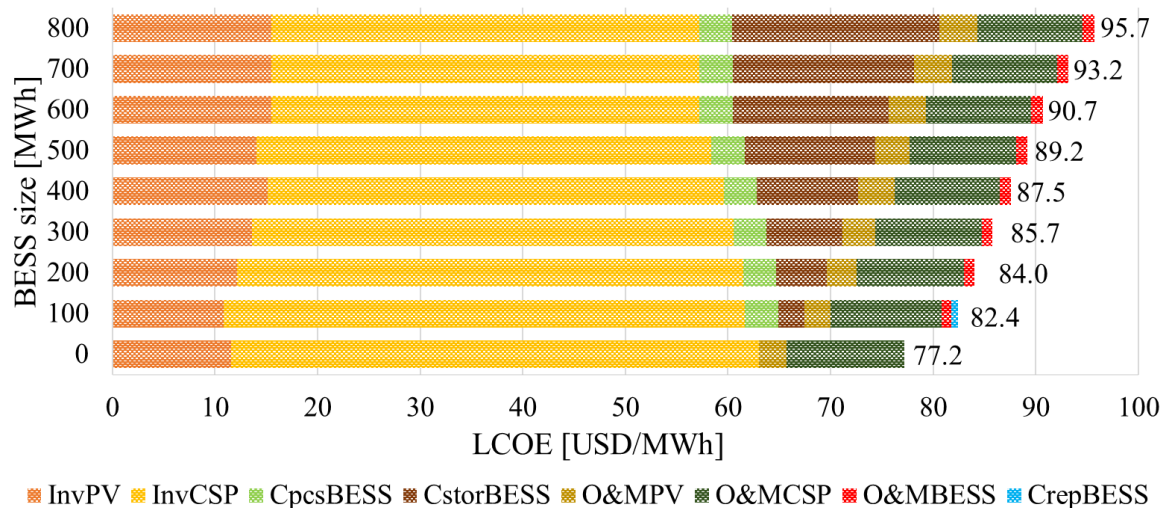


Figure 2-8: Cost distribution of the LCOE of the hybrid plant for different BESS sizes.

As the E/P ratios are higher (above 300 MWh of BESS), the storage section accounts for most of the BESS costs, with values comparable to the contribution of the investment cost of a large-size PV plant. Still, for E/P ratios of 1, the PCS cost represents the total BESS

cost's highest contribution. The replacement period of the BESS was defined in terms of the number of charges and discharge cycles throughout the hybrid plant's lifetime. Regarding replacement costs, it was found that for smaller BESS sizes, it was required at least one replacement of the battery bank, however, for E/P ratios above 2, the lifetime of the BESS was lengthened, possibly due to a minor number of hours where the BESS operated at full capacity (charged or discharged). Finally, adding a large-scale BESS to the hybrid plant could represent an increase of up to 18.51 USD/MWh in the LCOE in comparison to the value obtained without BESS.

A sensitivity analysis to evaluate the effect of reducing the BESS's storage cost on the LCOE of the hybrid plant was also performed. Figure 2-9 shows the variation on the minimum LCOE configurations obtained for each BESS size, in terms of different percentages of reduction of the BESS storage cost. Regarding the minimum LCOE configurations, the tendency was to increase the PV plant size as the BESS size was bigger (Figure 2-9a). The minimum cost solutions consider configurations with large PV plants, from 130 MW to 190 MW. For 200 MWh of BESS, the PV plant size increased from 150 MW to 170 MW after 50% of cost reduction, while the PV size for the other BESS capacities remained stable.

It is also observed that for BESS sizes above 600 MWh, the hybrid plant's configuration is the same for every percentage of cost reduction. This is because the minimum LCOE configuration is associated with the largest PV plant size possible (190 MW) and the design variables of the CSP plant remain the same.

Figure 2-9b presents the LCOE obtained for the solution of minimum cost for each BESS size. It was obtained that it is necessary to apply a cost reduction of at least 90% to reach the LCOE of the hybrid CSP-PV plant without BESS. The constant line represents this configuration for 0 MWh with an LCOE of 77.22 USD/MWh. LCOE values below 80 USD/MWh and capacity factors above 86% can already be achieved with cost reductions of 60%. Smaller BESS sizes as 100 MWh and 200 MWh presented a cost reduction curve of the LCOE with a lower slope than larger BESS sizes above 400 MWh. This means that the lowest cost configurations are associated with large BESS capacities, based on a cost reduction from 60% to 90% of the base case storage cost previously defined as 300 USD/kWh (Table 2-4).

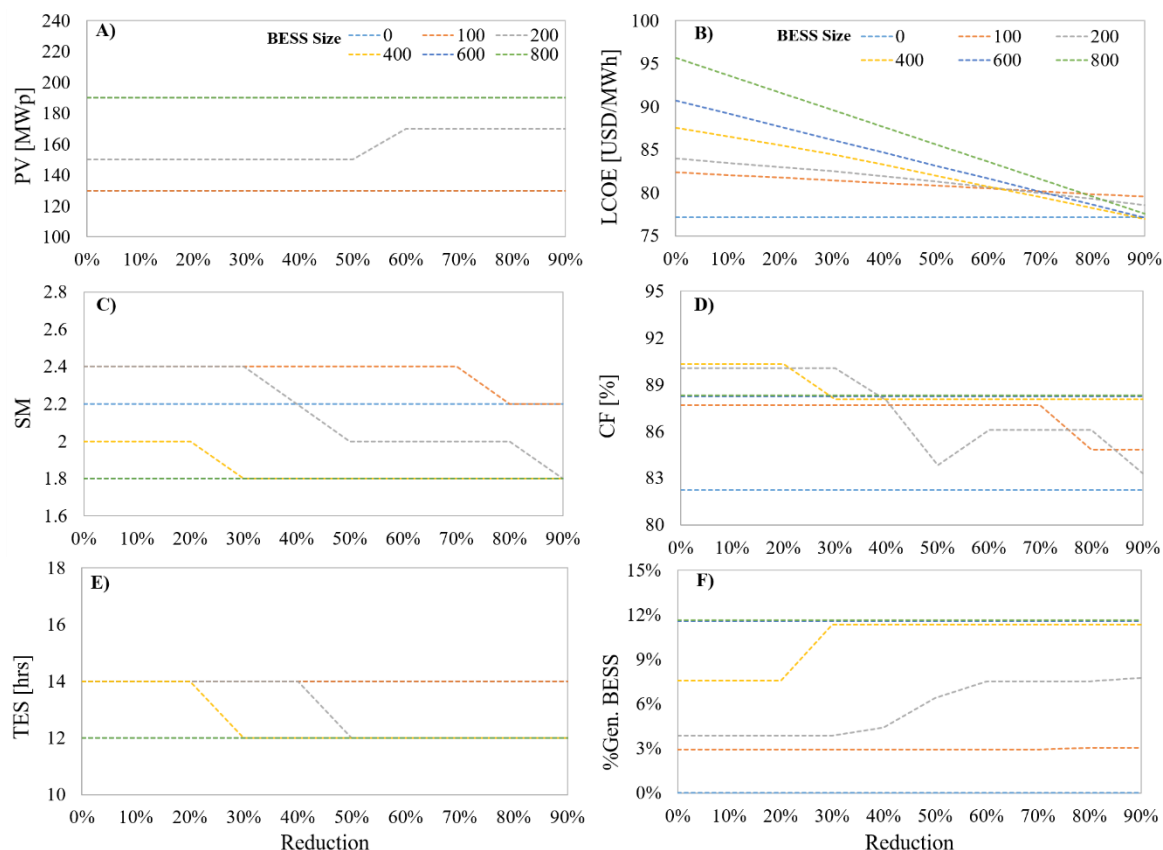


Figure 2-9: Variation in the minimum LCOE configurations obtained for different percentages of reduction of the BESS storage cost and different BESS sizes in terms of the PV size, SM, TES capacity, capacity factor, and the percentage contribution of the BESS to the annual hybrid plant generation.

Figure 2-9c shows that the SM diminishes significantly as the percentage cost reduction is higher. For 200 MWh of BESS, the SM suffers the highest reduction rate, with a gradual decrease from 2.4 to 1.8. For BESS sizes between 100 MWh and 200 MWh, the capacity factor decreases as the cost reduction is higher, but for bigger BESS sizes, the capacity factor tends to remain stable (Figure 2-9d). This situation is due to the SM and TES capacity variations, which drops from 14h to 12h in all cases after a 30-50% cost reduction, excluding 100 MWh, in which TES capacity remains stable in 14h (Figure 2-9e).

These results show that for E/P ratios between 4 and 6, the minimum LCOE configurations tend to have CSP plants with SMs of 1.8 and a TES capacity of 12h. This indicates that the

most suitable CSP configuration coupled in a hybrid CSP-PV+TES+BESS scheme presents smaller CSP solar fields and TES sizes than a hybrid CSP-PV plant without BESS.

Finally, Figure 2-9f illustrates that BESS's maximum contribution is 12% of the hybrid plant generation, which is achieved for large BESS capacities as 400 MWh and 800 MWh for 90% of storage cost reduction. In contrast, the other BESS sizes' percentage contribution was between 3 and 7.8% of the annual generation. Figure 2-9f also shows that the BESS share tends to rise with BESS sizes up to 400 MWh as the cost reduction increases. Still, with large capacities above 600 MWh, this contribution remains stable due to the plant's minimum cost configuration (for these BESS sizes) do not vary with the cost reduction.

2.4.3. Fixed-tilted mounting vs. one-axis tracking system

The present section aims to assess the differences between considering a fixed-tilt PV field or a PV plant with a one-axis-tracking system in the scheme of a hybrid CSP-PV plant with TES and BESS. The literature review about hybrid CSP-PV plants shows that the difference between considering a fixed-tilt PV field or a tracking system has not been widely studied since most of the analyses have considered fixed PV arrays (Green et al., 2015; Pan & Dinter, 2017; Petrollese & Cocco, 2016; Starke et al., 2016; Starke et al., 2018) (Giuliano et al., 2016) analyzed the performance of different configurations of hybrid CSP-PV plants considering targets to minimize CO₂ emissions and the LCOE. They found that combining a CSP-PV power plant with tracked PV arrays on one-axis represents a competitive solution to cover baseload, showing a performance slightly better than a configuration with fixed-tilt PV arrays.

This section presents a comparative study of the techno-economic indicators obtained for the minimum LCOE configurations, considering a fixed-tilt PV plant and one-axis tracked PV arrays. These configurations were previously presented in Table 2-6 for the fixed-tilt PV configuration, and Table 2-8 includes results obtained implementing a one-axis PV tracking system in an equivalent hybrid scheme.

An increase in the total annual production; therefore, on the hybrid plant's capacity factor is observed when tracked PV arrays are considered (Table 2-8). Figure 2-10 shows the increase of annual output is up to 4.21% for configuration A, which is the hybrid plant scenario without batteries, and between 1%-3.5% for the rest of the configurations that include a

BESS section. In contrast, the range of capacity factors obtained with the PV tracking system is between 85% and 92.40%, showing a tendency to achieve slightly higher values than those obtained with a fixed-angle PV configuration. These results also indicate that the percentage of total energy increase of the hybrid plant implementing tracked PV arrays does not exceed 5%; while the energy production of a PV-only plant implementing a tracking system (in comparison to a fixed configuration) can be about 30% higher for the same location.

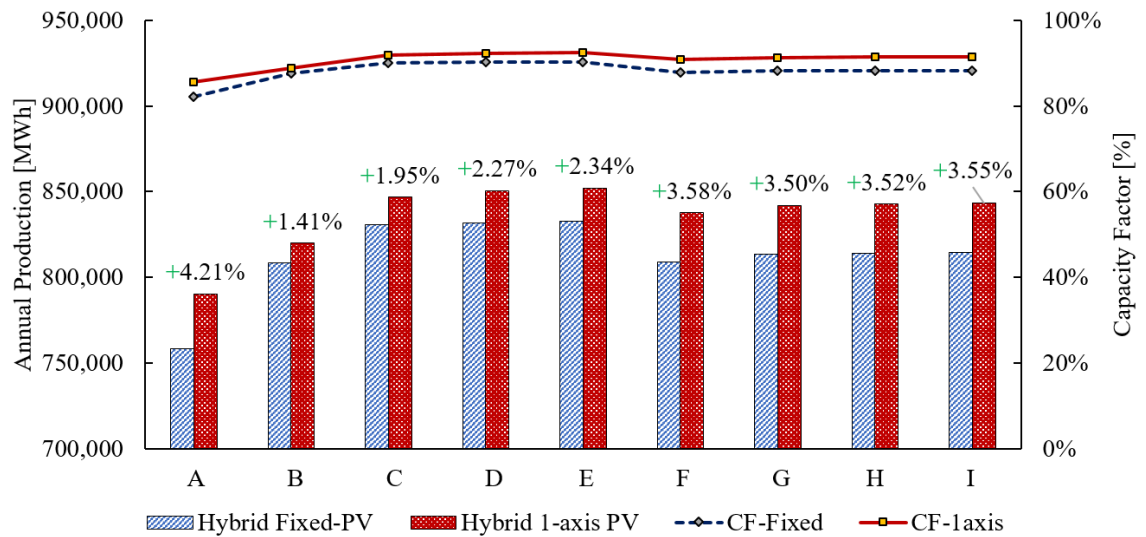


Figure 2-10: Total annual production and capacity factor of the hybrid CSP-PV plant considering fixed-angle PV arrays and one-axis tracking system.

Table 2-8: Techno-economic indicators of the hybrid CSP-PV plant considering fixed-angle PV arrays or one-axis tracked PV arrays for the minimum LCOE configurations

	CF [%]		LCOE [USD/MWh]		Annual Production [MWh]		Dumped PV [MWh]		Total PV excess [MWh]		% of PV excess to BESS	
	Fixed	1-axis	Fixed	1-axis	Fixed	1-axis	Fixed	1-axis	Fixed	1-axis	Fixed	1-axis
A	82.20	85.67	77.22	75.08	758,298	790,253	29,234	50,825	29,234	50,825	0.0	0.0
B	87.63	88.93	82.44	81.51	808,434	819,829	4,192	35,210	29,011	50,733	85.6	30.6
C	90.01	91.86	84.04	83.35	830,439	846,673	17,720	63,589	51,669	78,579	65.7	19.1
D	90.23	92.29	85.70	85.00	831,685	850,592	34,291	106,872	81,506	128,480	57.9	16.8
E	90.34	92.40	87.53	86.98	832,572	852,095	49,788	147,475	116,893	183,897	57.4	19.8
F	87.73	90.88	89.19	87.36	808,748	837,737	3,577	72,602	82,443	128,269	95.7	43.4
G	88.28	91.31	90.68	89.11	813,562	842,013	18,367	114,023	117,824	183,963	84.4	38.0
H	88.28	91.42	93.20	91.44	813,922	842,602	17,988	113,315	117,824	183,963	84.7	38.4
I	88.28	91.42	95.73	93.88	814,258	843,190	17,635	112,608	117,824	183,963	85.0	38.8

Figure 2-11 shows the dispatchability of the hybrid plant considering the configuration D (170 MW of PV, 2.2 of SM, 14h of TES, and 300 MWh of BESS), with both types of PV mounting systems during summer and winter seasons. With fixed PV arrays, the PV plant only maintains the maximum power for a few hours, close to midday in summer, and the CSP plant complements the production during the afternoon until early in the morning when the TES is completely discharged, and the BESS fulfills the baseload. During the winter season, the TES is not entirely charged during the day, requiring an earlier BESS discharge, which results in few hours with unfulfilled demand before sunrise.

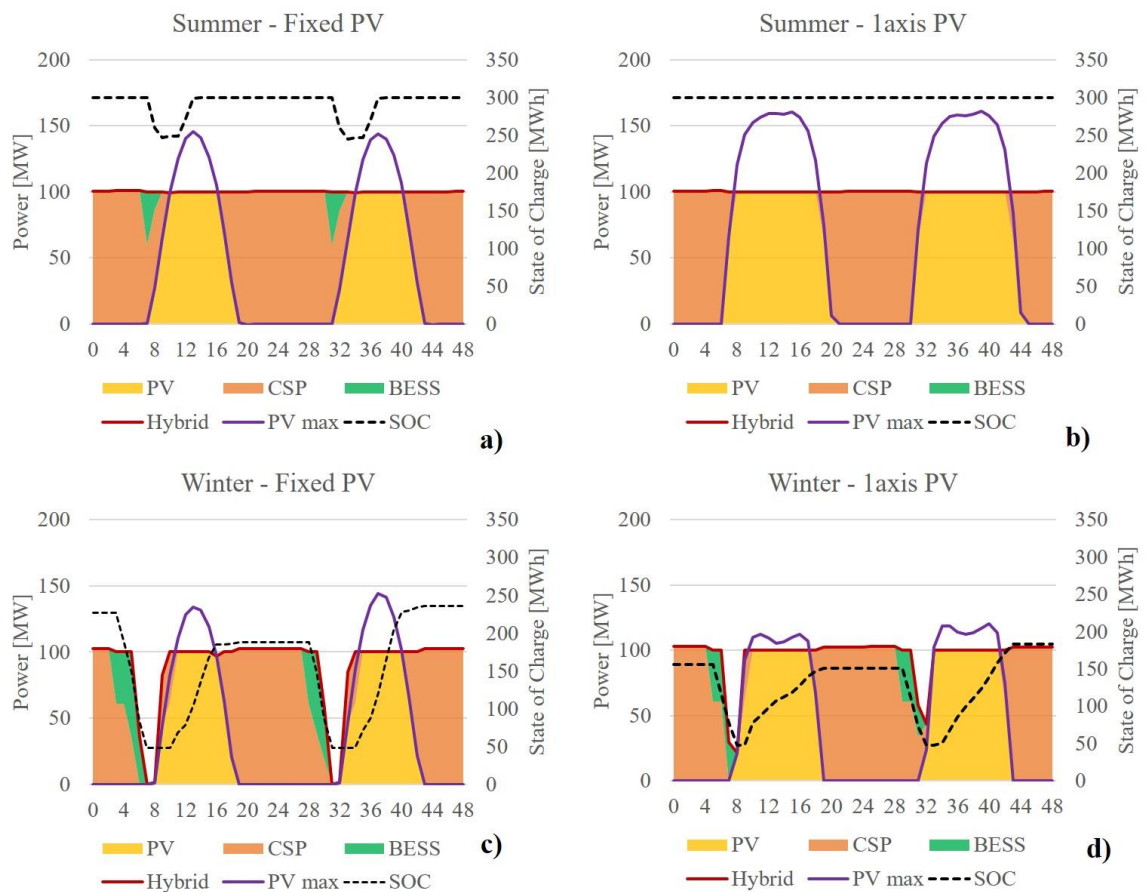


Figure 2-11: Dispatchability of the hybrid plant during summer and winter seasons, considering fixed-angle PV arrays or one-axis tracked PV arrays, for the configuration D with 170MW of PV, 300MWh of BESS, 2.2 of SM, and 14h of TES.

In contrast, as this location presents high clear sky indexes, the PV production profile with tracked arrays causes a more intensive use of the PV energy throughout sunlight hours, resulting in lower use of the BESS compared to when fixed PV arrays are considered. The main differences lie in the need to discharge the BESS to complement the generation. This difference is more relevant during summer, due to the increase of PV production delays the energy delivery of the CSP plant to later hours, making unnecessary the use of batteries in early morning hours. Figure 2-12 also shows that the PV output with the tracking system is increased both in winter and summer months. In general, the CSP output decreases, and the BESS's participation in the annual production is reduced, mostly during the summer season. Therefore, the BESS's participation in the hybrid plant's yearly production becomes more relevant in the winter months.

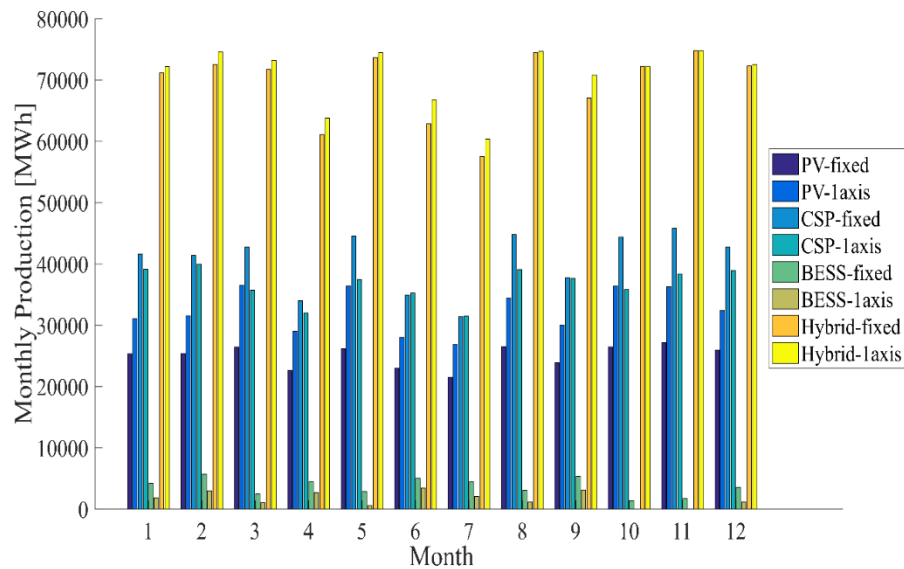


Figure 2-12: Monthly power production of each component of the hybrid plant with fixed PV arrays and with one-axis-tracking system, for the configuration D with 170MW of PV, 300MWh of BESS, 2.2 of SM, and 14h of TES.

Table 2-8 shows that the total of PV energy excess is increased with the PV tracking system, assigning lower percentages of this PV excess to charge the BESS, and the need to use the energy stored in the BESS decreases, mostly in summer months. As mentioned before, the total PV excess represents the sum of the dumped PV energy that cannot be exploited and the surplus of PV energy utilized to charge the BESS. The increase of the total PV energy

excess with the tracking system is expected, and the PV production is higher; however, the percentage of the PV surplus going to the BESS is dramatically reduced, resulting in a relevant increase of the dumped PV energy. Figure 2-13 shows that the only months in which all the PV energy excess is exploited to store energy in the BESS are June and July. In contrast, all the PV surplus is converted into dumped energy in October and November, using just a small percentage of the PV excess in other months. It is also noticed a lower total of PV excess during February, mainly due to the altiplanic winter, causing persistent cloud covers this month.

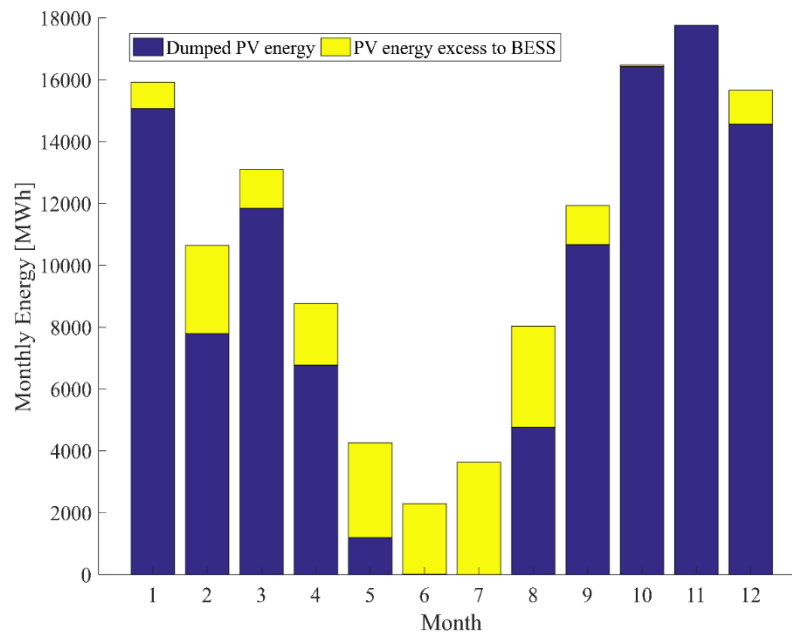


Figure 2-13: Monthly distribution of dumped PV energy and PV energy excess of the hybrid CSP-PV plant with one-axis-tracking system, for a configuration with 170MW of PV, 300MWh of BESS, 2.2 of SM, and 14h of TES.

The effect of implementing a PV tracking system on the LCOE is shown in Figure 2-14 for the sake of comparison. In this case, it was considered an installation cost for the one-axis PV tracking system of 1.11 USD/W_{dc} and an O&M cost of 18.5 USD/kW-yr. These values are based on NREL's last cost report from 2017 (Table 2-4) (NREL, 2017). In general, results show that producing a base generation with tracked PV arrays in the scheme of a hybrid

CSP-PV plant achieves lower LCOEs than with fixed PV arrays due to an increase of the hybrid plant energy production. However, the peak cost reduction was -1.98% with configuration A, which has no batteries, while when the BESS was included, the largest decrease of LCOE was up to -1.21% with configuration F. Both configurations D and E obtained an increase in the LCOE below 1%, which is almost negligible. This indicates that the single-axis tracking system brings techno-economic benefits to the performance of the hybrid plant. Still, its techno-economic impact is not as severe as it occurs for a PV plant-only.

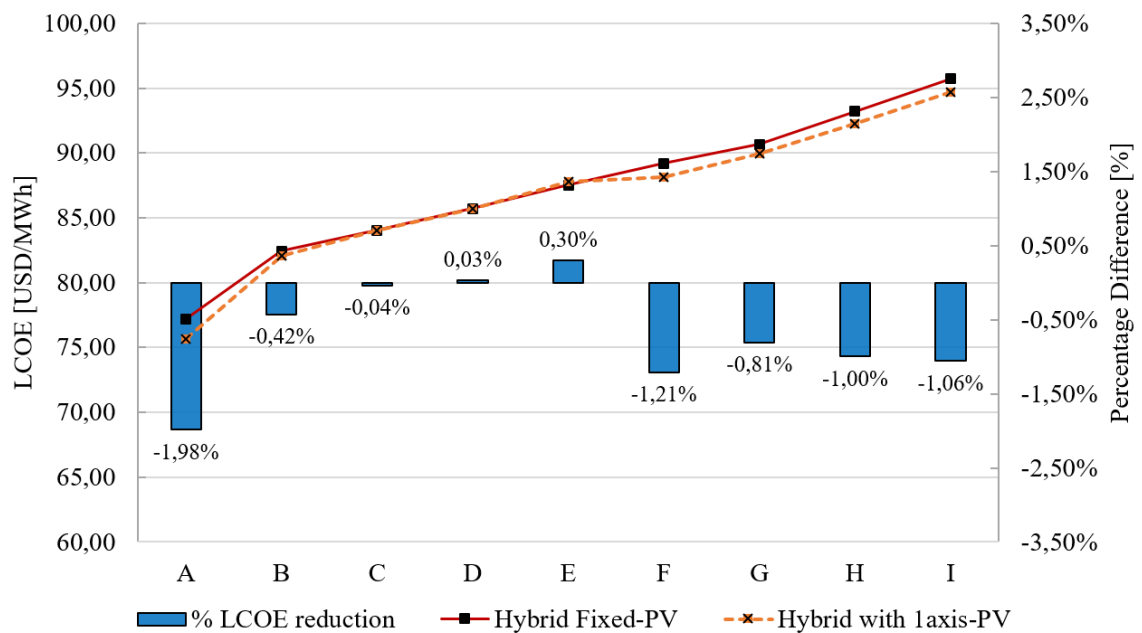


Figure 2-14: LCOE obtained for each minimum LCOE configuration implementing fixed PV modules or one-axis-tracking system. Percentage differences of LCOE are presented for an increase in both installation and O&M costs of the PV plant with a one-axis-tracking system.

In this concern, the one-axis PV tracking system brings techno-economic benefits to the hybrid CSP-PV plant's performance with TES and BESS. These benefits include achieving slightly higher capacity factors and lower LCOEs. Still, the techno-economic impact of implementing the tracking system in the hybrid plant scheme is not as severe as it occurs for a PV plant-only. The reduction of the LCOE is mainly a consequence of the increase of the

PV plant energy production, resulting in lower use of the BESS, which presents a higher cost.

The minimum LCOE configurations of the hybrid plant with one-axis PV tracked arrays given a BESS size could result in smaller PV plants since the PV production increases compared to that with a fixed-tilt PV plant. The amount of total dumped PV energy in a year is also significantly higher and much more relevant with tracked PV arrays than with a fixed-angle PV configuration. This result reinforces the idea that an optimization process of the hybrid plant design should also consider this situation, as larger PV plant sizes are considered.

2.5. Discussions

Favorable conditions of solar irradiation of Chile have favored solar energy development in the country. Large penetration of fluctuating RE sources has caused a rising interest in studying different mitigation methods of the variability production. In the case of solar generation power plants, the integration of BESS and TES systems have been previously studied separately, comparing the performance of PV+BESS systems with CSP+TES solutions. This work proposes the integration between a hybrid CSP-PV plant with TES and BESS for a base generation. Results have shown that the main limitations of implementing a large-scale battery bank for utility-scale electricity generation applications are related to the storage section's high investment costs. Under the current market conditions, these costs make unprofitable integration to the hybrid plant. The study showed that under a BESS cost reduction scenario of the storage section, hybrid plant configurations tend to PV plants of 190 MW and CSP plants with 1.8 of SM and 12h of TES, which allow to integrate their production and improving the capacity factors of the hybrid plant. Main considerations implemented to perform this work are explained below:

- The analysis of the hybrid plant was performed in Crucero, Chile. This location presents a large number of days with high DNI levels and high clear sky indexes. However, northern regions of Chile have a limited transmission capacity, and building new transmission lines introduces higher costs to an electricity generation project. This situation could lead to deploying this type of plants closer to the demand centers, where solar resource conditions are not equal to the best places identified in

northern Chile. Therefore, a techno-economic analysis performed on different locations could give another insight into the hybrid plant's operation and performance.

- A base generation profile was considered to cover a typical load profile of Chile's northern regions. This is because most of the country's mining industries are located in this part of the country, producing a nearly constant demand profile for almost the entire day. However, a different operating strategy could lead to different results in terms of the hybrid plant configuration (for example, a peak hour strategy). Results found with this analysis can be applied to other regions in the world where providing base generation can be economically attractive as well as to satisfy the minimum level of demand on an electrical grid. Nevertheless, if a different operating strategy is studied, it should be considered different operation modes and economic indicators, for example, in terms of financial profit, to find the optimal design of the plant.
- The BESS was considered as a large energy reservoir with an associated charge/discharge efficiency. Therefore, it is recommended to evaluate different battery technologies' performance as lead-acid, lithium-ion, or vanadium flow batteries, with their respective operation limitations.
- Performance of the large-scale BESS was analyzed on an hourly basis; however, it is recommendable to study the integration of the BESS considering a time step in minutes to cover the sub-hourly variations of the PV production, which by the response time of the CSP plant cannot be fulfilled.
- The power rating of the BESS was fixed at 100MW. It was observed that for E/P ratios lower than 2, the PCS cost was significantly high compared to the storage section cost. In contrast, for E/P ratios above 2, the storage section cost had the largest contribution to the BESS cost. This situation evidences that it could be considered another analysis to obtain the optimum power rating for each BESS size.
- The hybrid plant's dispatch strategy prioritizes the PV output and operates the CSP+TES plant to complement the PV production, while the BESS is utilized as a back-up of the CSP plant. This operation mode results in a low number of BESS operating hours at full capacity and low cycles of charge and discharge. A change in

the dispatch strategy, for example, if the PV-BESS output is prioritized over the CSP- TES production, could lead to different hybrid plant configurations and financial results. The control and ramp rates of the CSP plant's power block would also become more relevant to limit the turbine's starts and turn-off.

- The economic analysis was performed to obtain the required cost reduction of a battery bank in a hybrid plant scheme to be competitive with a hybrid CSP-PV plant without BESS. Results are based only on cost reductions of the BESS without considering future cost projections of the PV plant, the TES, or the CSP plant.
- The analysis performed in this work was based on a hybrid plant with a fixed-tilt PV power plant, since the PV market trend of Chile does not show any consensus on which is the most suitable tracking assembly system for PV plants (45.7% of the Chilean PV capacity has a fixed-tilt configuration, followed by 44.4% with one-axis-tracking system). The comparative analysis implementing fixed arrays or tracked PV arrays in a hybrid scheme was based on the minimum LCOE configurations found first for the fixed-tilt configuration. These results will be highly influenced by the dispatch strategy and operation modes chosen for the hybrid plant, as well as by the cost reference considered for the economic evaluation, which may differ from country to country.

2.6. Conclusions

A techno-economic analysis of a hybrid solar plant located in northern Chile was carried out, considering a CSP plant of 100MW_e coupled with TES and a PV plant integrated with a large-scale BESS. The performance and operation modes of the hybrid plant were analyzed throughout a year on an hourly basis. High clear sky indexes and a low number of cloudy days on this location allows achieving capacity factors above 85% with the hybrid plant.

The plant's performance showed that the CSP- TES plant produces more than 60% of the annual generation. The BESS achieves the highest percentage contribution to the yearly generation when large PV plant sizes are implemented, and more surplus of PV energy can be utilized; however, this share does not achieve higher values than 12% in the most favorable cases. Results of the parametric analysis indicate that E/P ratios from 1 to 4 have lower installation costs and capacity factors up to 90%, while E/P ratios above 5 present

higher installation costs but lower capacity factors (up to 88%) due to the reduction of the CSP plant size. When BESS cost distribution is analyzed, it was found that the storage cost of the battery bank accounts for most of the BESS costs, which make unprofitable the investment on a large-scale BESS for applications of utility-scale electricity generation under the current costs.

Therefore, it was shown that it is required a reduction of approximately 60-90% of the storage cost to achieve similar LCOE values than a hybrid CSP-PV plant without BESS, increasing the capacity factor between 5-6%. Under this cost reduction scenario, results favor hybrid plant configurations with E/P ratios between 4 and 6 with large PV plants of 190 MW and CSP plants with SMs of 1.8 and 12h of TES. The study shows that under a BESS cost reduction scenario of the storage section, there is a solution domain with hybrid plant configurations that allow integrating and complementing the production of both CSP and PV plants with both storage types in a synergetic operation. This opens the possibility into the future of achieving dispatchable base energy combining the benefits of both solar technologies and energy storage systems, with capacity factors above 90%.

Finally, the comparative study between considering a fixed-tilt PV configuration or a one-axis PV tracking system in a hybrid plant scheme showed that the tracking system's implementation results in the hybrid plant's higher energy production. However, this rise does not exceed 5% compared to the output obtained with the fixed PV plant, which is considerably lower than the output rise obtained with a PV-only plant. In the same way, it was found that when tracked PV arrays are considered, the participation of the BESS becomes only relevant during winter months, while in summer is almost negligible since the PV and CSP outputs are enough to cover the baseload. This situation leads to a relevant increase of the annual dumped of PV energy, especially during summer, but, in the same way, it leads to lower LCOEs of the hybrid plant, with a cost reduction of no more than -1.98%. These results also indicate that the minimum LCOE configurations of a hybrid CSP-PV plant with tracked PV arrays for a given BESS size could result in smaller PV plants compared to the nominal sizes obtained with fixed-PV arrays.

3. ASSESSMENT OF TIME RESOLUTION IMPACT ON THE MODELING OF A HYBRID CSP-PV PLANT: A CASE OF STUDY IN CHILE

3.1. Introduction

Concentrated Solar Power (CSP) technology is proposed as an alternative to producing stable and continuous solar electricity with the integration of Thermal Energy Storage (TES), but CSP technology has been less widely deployed than other renewable energy technologies such as solar Photovoltaics (PV) and wind, with only 5.5 GW of cumulative installed capacity worldwide by the end of 2018 (REN21, 2019). CSP electricity costs are still superior to fossil fuel alternatives, even though its costs have been continuing to fall in the last years (IRENA, 2018). PV costs have experienced substantial cost reductions driven by both declines in solar PV modules and balance of system costs, which have fallen solar PV costs to the fossil fuel costs range (IRENA, 2018). Still, solar PV is a variable generation mean that needs to be integrated with storage and flexibility options to guarantee the security of electric supply.

The concept of a hybrid CSP-PV plant has been widely studied by different authors in the last years to exploit both CSP and PV technologies' benefits. The hybrid scheme takes advantage of the low PV costs to achieve a lower Levelized Cost of Electricity (LCOE) and higher capacity factors than a same-sized CSP plant (Pan and Dinter, 2017). This concept was evaluated under the Atacama Desert conditions of Chile, obtaining that is possible to achieve capacity factors higher than 85% with a hybrid CSP-PV plant and lower LCOEs than those of standalone CSP plants (Bravo & Friedrich, 2018; Green et al., 2015; Starke et al., 2016; Starke et al., 2018).

A hybrid CSP-PV plant, including a Battery Energy Storage System (BESS) at a small scale, was studied by (Cocco et al., 2016; Petrollese & Cocco, 2016) analyzing different dispatch strategies of the hybrid system and evaluating the optimal configuration for two different locations in Morocco and Italy. (Zurita et al., 2018) conducted a parametric study of a hybrid plant CSP-PV plant with a large-scale BESS obtaining a domain of solutions where the production of both CSP and PV plants with both types of storage can be integrated into a synergetic operation. Zhai et al. (2018) also optimized a hybrid CSP-PV plant to achieve the

lowest LCOE, obtaining that a small battery improves the PV plant's utilization time, while the CSP brings stability to the power output.

More recently, Hamilton et al., (2019) developed a mixed-integer linear program to optimize the dispatch schedule of a CSP-PV plant with TES and a lithium-ion battery bank on a sub-hourly resolution to maximize the profits coming from electricity sales of the plant. The study considered the spot market in Chile and the utility market servicing northern and central California. They compared both hybrid systems and a CSP-only system based on a capacity factor, LCOE, and Power Purchase Agreement (PPA). They also obtained that the hybrid plant radically outperforms the CSP-only plant from a techno-economic perspective. In this way, literature has proven that the potential of a hybrid CSP-PV plant integrated with thermal and electric systems remains on the interaction between its components to supply a specific demand which would impact its dispatchability. In this regard, the PV system presents a more sensible response to the short-time variations of solar irradiance than a CSP- TES plant because the solar thermal power plants provide thermal inertia that allows smoothing transitory fluctuations. Except for the research done by (Cocco et al., 2016), most of the studies regarding the modeling of hybrid CSP-PV plants with storage have been performed using hourly time data.

This situation raises a question about the real impact that the time has on the production estimation of a hybrid power plant. Literature regarding the modeling of CSP plants suggests that a 10-minute time resolution would avoid overestimating the yield assessment of solar thermal power plants to achieve bankability, which could occur if only hourly time series are used (Hirsch et al., 2017). Still, different temporal resolution has been used in the literature to analyze solar thermal power plants. For instance, (Guédez et al., 2014) used a 10-minute time resolution to optimize a central-receiver system for peak power production. In a following study, (Guédez et al., 2014) considered an hourly time step to optimize a hybrid PV, wind, and CSP system with a gas burner as a back-up. (Guédez et al., 2016) also used a 20-minutes time step to maximize the profit of a central receiver plant considering different operating strategies.

Meybodi and Beath (2016) conducted a systematic analysis with a multi-year solar database from Australia. The simulation's time step varied from 5 to 60 minutes, and the molten salt storage capacity from 4 to 12h. Their results showed that smaller time steps such as 5 minutes

could be used to obtain a realistic prediction of the CSP performance for optimizing purposes, while with the 60-minute data, it was obtained the lowest performance prediction and the least realistic. They also recommended time steps between 15-30 minutes to get an average representation of the plant's actual operation if computational time was a concern. Regarding the time resolution of PV power plants, different authors have analyzed the effect of averaging the time-step. Ayala-Gilardón et al. (2018) studied the impact of time resolution on the self-consumption and self-sufficiency of different grid-connected PV systems using time steps ranging from 10 seconds to 1 year. They obtained that these values were overestimated with time steps larger than 1 hour, concluding that using a low time resolution could cause the loss of relevant system information. Paravalos et al. (2014) also mentioned that the use of meteorological data with a 1-hour time step could significantly reduce accuracy on the estimation of energy production of a PV plant.

This paper presents a methodology to assess the impact of time resolution on modeling a hybrid CSP-PV plant with thermal and electric storage. The study considers a case study in Chile with two different locations that present different meteorological conditions. The hybrid plant's performance was analyzed, varying both the time resolution of the solar data and the time step of the simulation from 1, 5, 10, 15, 30 to 60 minutes. This work allows understanding how the time resolution can affect a hybrid plant's operation prediction and the annual energy estimation. The study also brings a new outlook about the influence of the solar variability on the dispatchability of the hybrid plant at a component level (PV, CSP-TES, and BESS) and how the temporal resolution influences the control procedures ruling the operation of the plant. This work provides some recommendations to the different actors and phases involved in the development of a hybrid solar power plant, analyzing the advantages and drawbacks of implementing different time steps at every stage of the project. Section 3.2 presents a description of the hybrid plant scheme; Section 3.3 describes the methodology to perform the modeling and simulations, and Section 3.4 explains the details of the techno-economic analysis. Results of this work are presented in three subsections: the daily plant performance for different day types was evaluated for both locations in Section 3.5.1, the annual performance analysis in terms of the total generation of each component of the plant is described in Section 3.5.2, and the influence of time resolution on the techno-

economic evaluation for different cases of study is presented in Section 3.5.3. Finally, Section 3.6 presents the discussions, followed by the conclusions in Section 3.7.

3.2. System Description

The hybrid plant model consists of a central receiver system and a PV power plant coupled to a direct molten salts TES and a lithium-ion battery bank. Figure 3-1 presents the complete scheme of the proposed hybrid plant. Each one of the plant components is described in this section.

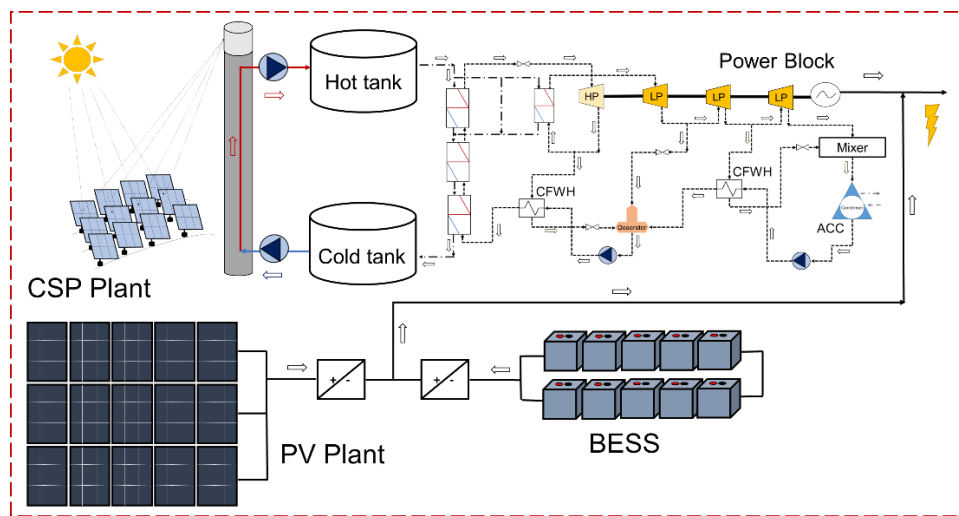


Figure 3-1: Hybrid plant model scheme.

3.2.1. CSP plant with TES and power block

The CSP plant is based on a molten salt central-receiver system technology that operates with a mixture of 60% NaNO_3 and 40% KNO_3 . The TES section is a two-tank direct system where the molten salts work as Heat Transfer Fluid (HTF) and storage media. The cold and hot tank temperatures are set at 295°C and 565°C . The heliostats field configuration and efficiency, the receiver height, receiver diameter, and tower height are optimized in terms of the Solar Multiple (SM), which represents the ratio between the thermal power output produced by the solar field at design conditions and the heat required by power cycle at the nominal point. Table 3-1 presents the main design parameters of the CSP plant and power block.

Table 3-1: Main design parameters of the CSP plant and the power block under nominal conditions.

Description	Unit	Value
<i>CSP plant</i>		
CSP technology	-	Central receiver
Design receiver temperature	°C	565
Heliostat area	m ²	144
Reflectivity of the heliostat field	%	95
TES system	-	Two-tanks direct
HTF and storage media	-	Molten salts mixture
<i>Power block</i>		
Gross power output	MW	110
Net output of electricity	MW	100
Minimum operation condition	%	30
Nominal thermal efficiency	%	39.12
Design ambient temperature	°C	30
Design steam mass flow rate	kg/s	630
Design HTF fluid inlet temperature	°C	565
Design HTF fluid outlet temperature	°C	295
Inlet of the high-pressure turbine	bar	100
Inlet of the medium-pressure turbine	bar	22
Inlet of the low-pressure turbine	bar	10
Condensing pressure	bar	0.012
Superheater pinch point	°C	15
Evaporator pinch point	°C	30
Reheater pinch point	°C	20
CFWH terminal temperature difference	°C	5
High-pressure turbine efficiency	%	90
Medium and low-pressure turbine efficiency	%	86
Condensate pumps efficiency	%	80
Generator efficiency	%	96

The CSP plant's power block consists of a Rankine cycle with a nominal efficiency of 39.12% and a gross power output of 110 MW_e. The power block is composed of a steam train generator which includes a reheating stage, two Closed Feed-Water Heaters (CFWH), a deaerator, two feed-water pumps, an Air-Cooled Condenser (ACC), and a turbine with a

high-pressure stage and three mass flow rate extractions in the low-pressure stages. The maximum power cycle temperature is limited to 550°C, and the minimum turbine load is 30% of the gross power.

3.2.2. PV plant and BESS

The PV plant consists of a fixed-angle module configuration. The solar cell technology considered was silicon mono-crystalline based on the MEMC-330 Sun Edison modules (SunEdison, 2015) with a nominal power of 330 W_{dc}. The inverter is an ULTRA-TL-1100 of ABB with a maximum AC power of 1 MW_{ac} (ABB, 2017). The PV plant has a scalable size in terms of the number of inverters to reach the nominal PV capacity. A fixed soiling rate of 0.5% per day was also considered (Zurita et al., 2018). Table 2-2 presents the main design parameters of the PV plant and BESS.

Table 3-2: Main parameters of the PV plant and BESS.

Description	Unit	Value
<i>PV Plant</i>		
Solar Cells Technology	-	m-cSi
Inverter Power	kW _{ac}	1000
Inverter Efficiency	%	98.4
Module Area	m ²	1.956
Module Power	W	330
Module Efficiency	%	16.9
<i>BESS</i>		
Depth of Discharge	%	84
Overall Efficiency	%	94
Life Cycles	cycles	5000
Calendar Life	yr	20

The BESS section is a lithium-ion battery bank with a maximum discharge depth of 84%. The BESS couples to a Power Conversion System (PCS) with a power rating of 100 MW.

3.3. Modeling and Simulation

The hybrid plant was modeled with the Transient System Simulation Program (TRNSYS) to obtain the annual performance and operation curves of the thermal and electric systems of the plant under transient conditions. Simulations were performed throughout a year, varying the time step from 1, 5, 10, 15, 30 to 60 minutes. The model was developed in a single TRNSYS deck to evaluate the interactions between all the plant components. Ground-measurements of solar irradiation with a 1-minute time resolution were implemented to create a new set of data files, averaging the 1-minute gross data for each time step. The following subsections will explain the solar database features, the simulation models, and the plant operating modes.

3.3.1. Location and solar resource

The study considered two different locations in Chile: Carrera Pinto and Santiago of Chile. Figure 3-2 shows the Direct Normal Irradiance (DNI) measured during 2015 and 2013 for Carrera Pinto and Santiago. Both locations were chosen since they present different weather features. Carrera Pinto is in a vast desert plain where extremely arid conditions are predominant throughout the year. This location shares the high radiation levels and features typical in northern Chile, with low aerosol content, a minimum cloud cover, and high clear-sky indexes throughout the year.

In contrast, Santiago is Chile's capital city located next to the Andes high range in the central region with a relatively dry climate, heavy aerosols, and pollution episodes during winter. Santiago's solar resource presents a high variability throughout the year with a strong seasonality due to a typical presence of persistent cloud covers during winter (Escobar et al., 2015). This location represents a place of relevance in terms of energy demand for the country, as it represents the meteorological conditions in the central region of Chile.

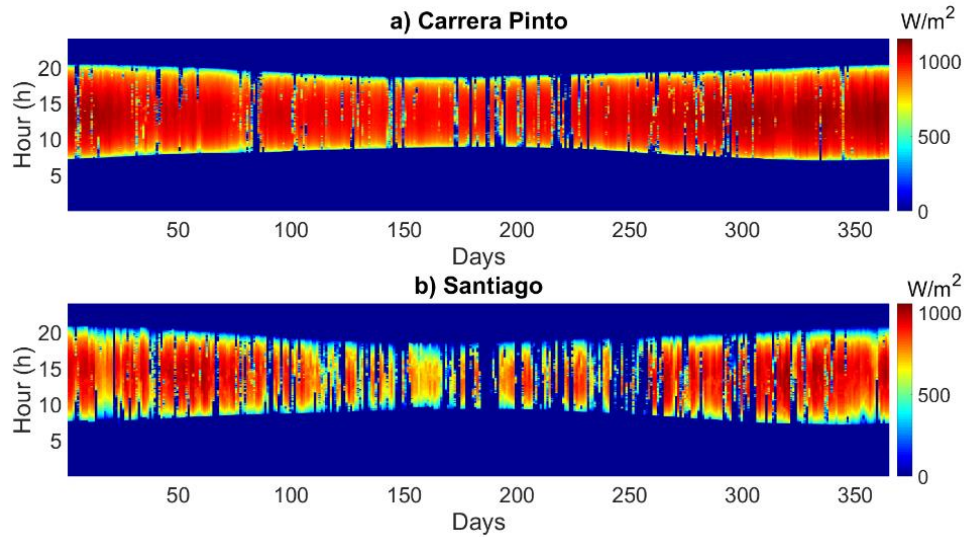


Figure 3-2: DNI profile in a) Carrera Pinto and b) Santiago.

Meteorological and solar data comes from ground station measurements situated in Carrera Pinto and Santiago. Table 3-3 presents the main features of both ground stations. Carrera Pinto's station is in the site where it is planned to be deployed the Copiapó project in the Atacama Region of Chile, while Santiago's station is at Pontificia Universidad Católica de Chile. Both stations operate under the Baseline Surface Radiation Network standards and guidelines, and their main features and instruments are accurately described by Escobar et al. (2015) and Rojas et al. (2019).

Table 3-3: Meteorological station features.

Description	Carrera Pinto	Santiago
Latitude (°)	27.083 S	33.497 S
Longitude (°)	69.93 W	70.61 W
Altitude (m)	1640	580
Ground station type	RSBR	Sun tracker
Yearly total of DNI (kWh/m ² -yr)	3462.58	2153.78
Yearly total of GHI (kWh/m ² -yr)	2519,47	1941.07

The gross data coming from both ground stations was obtained with a 1-minute time resolution. Quality criteria used to evaluate the data are described by (Rojas et al., 2019). Only valid data was considered to create a new set of data files averaging the 1-minute data

for each time step (5, 10, 15, 30, and 60 minutes).

3.3.2. PV plant and battery bank model

The PV plant was simulated as an array with a scalable size in terms of the number of inverters, considering a maximum inverter power output of 1 MW_{ac}. The model was implemented using the Type 190 of TRNSYS, which allows to include the inverter efficiency curve as an input. The validation of the PV plant model has been presented in previous studies (Valenzuela et al., 2017; Zurita et al., 2018). The BESS model is based on Eq. 3.1 that describes the variation of State of Charge (SOC) on the battery bank given a charge or discharge rate ($\eta_{c/d}$) from a previous time step ($i-1$) to the next (i),

$$SOC_{(i)} = SOC_{(i-1)} + \eta_{c/d} \cdot P_{BESS} \cdot \frac{1}{60} \cdot \Delta t \quad (3.1)$$

where P_{BESS} is the charge or discharge power of the battery, and Δt is the simulation time step in minutes. The type developed for the battery is also described in detail by (Zurita et al., 2018).

3.3.3. Power block model

The power block model was developed in the Equation Engineering Solver (EES) based on previous works (Mata-Torres et al., 2019) to obtain the performance under nominal and off-design conditions. The model is comprised of mass, energy, and heat transfer balances at every component of the Rankine Cycle illustrated in Figure 3-1. The design conditions consider the parameters presented in Table 3-1 to calculate the design overall heat transfer coefficients (UA) of heat exchangers, the design HTF mass flow rate, and the cycle's thermal design efficiency. The off-design model considers a constant pressure control for the part-load operation, and it calculates the heat-exchangers effective UA under variations of the steam mass flow rate based on the equations described by (Patnode, 2006). Variations in the steam turbine's efficiency and pressures were also considered according to Stodola's ellipse law.

The EES model was used to create a performance map of the power block through a parametric analysis varying three operational conditions: the inlet hot HTF temperature (T_{inHTF}), the HTF mass flow rate (\dot{m}_{inHTF}), and the ambient temperature (T_{amb}), considering 6048 points for a valid range described in Table 3-4.

Table 3-4: Applicable range of the power block polynomial regression.

Variable	Units	Applicable range
T_{inHTF}	°C	[500:565]
m_{inHTF}	kg/s	[160:630]
T_{amb}	°C	[0:40]

Then, a polynomial multi-variable regression model was developed, employing the data coming from the parametric analysis. Output variables of the regression model were: the net power output from the turbine-generator (W_{net}), the exhaust mass flow rate of the turbine (m_{cond}) and temperature of the HTF returning to the solar field (T_{outHTF}). The equations and coefficients of the multi-variable polynomial regression model are provided in detail in APPENDIX B: APPENDIX FOR CHAPTER 3.

The polynomial regressions were used to create a new component in TRNSYS that allows evaluating the power block operation in a significantly lower computational time. The Normalized Root-Mean-Square Deviation (NRMSD) was utilized to assess the errors associated with the regressions, achieving NRMSDs of 0.13%, 0.01%, and 0.80%, corresponding to the W_{net} , m_{cond} , and T_{outHTF} , respectively.

3.3.4. Central receiver power plant model

The central-receiver plant model was developed using different components developed by authors and existing components of TRNSYS libraries. The heliostats field was modeled using a component based on Type 394 of the Solar Thermal Electric Components (STEC) library (Schwarzbözl et al., 2006), which provides the incident power on the receiver surface, including a daily soling rate and cleaning period (Zurita et al., 2018). This type uses as input a matrix indicating the field efficiency at different solar azimuth and zenith angles, which interpolates during the simulation to obtain the heliostats field efficiency in terms of solar position. The TES system was modeled considering two tanks (hot and cold tank) with variable volume, using the Type 39 from TRNSYS library, in which the HTF pump consumption by the power block was also considered.

Regarding the central receiver, a new component was also developed by authors that include the modeling of a cylindrical tubular central receiver. The developed model calculates in a

simplified manner the thermal power absorbed by the HTF in the receiver based on the work developed by (Wagner, 2008), introducing as inputs the receiver and tower dimensions, which are optimized in terms of the SM using SolarPILOT from the (National Renewable Energy Laboratory (NREL), 2018). The model formulation considers an equations system of energy balances on a receiver tube element, including the incident radiation and thermal losses, constituted by radiation, natural and forced convection losses. The outlet HTF mass flow rate and temperature are calculated in terms of the absorbed thermal power. The receiver surface temperature is calculated considering the heat transfer across the receiver tube wall from the HTF fluid running through the tube to the receiver surface. Since there are many relationships in the equation system, the receiver model comprises an iterative process computed until the receiver surface temperature, the HTF outlet temperature, and the HTF mass flow rate in the receiver converge. The electric power consumption of the HTF tower pumps is also considered.

Besides, the receiver includes the simple modeling of a thermal capacitance to represent the receiver's thermal inertia. With this purpose, an adiabatic capacitance was added after the receiver calculation, in which the inlet stream is the HTF outlet mass flow rate of the receiver, and the outlet stream is the HTF mass flow rate that goes to the hot TES tank with the capacitance temperature. The performance of the thermal capacitance is assessed by following the next differential equation:

$$C^{th} \frac{dT_{cap}}{dt} = \dot{m}_{HTF} C_p T_{rec,out} - \dot{m}_{HTF} C_p T_{cap} \quad (3.2)$$

where C^{th} is the thermal capacitance in kJ/K, $T_{rec,out}$ is the HTF outlet temperature of the receiver in K, T_{cap} is the capacitance temperature in K, \dot{m}_{HTF} is the HTF mass flow rate in kg/s, and C_p is the heat capacity of the HTF in kJ/kg-K. This approach allows adding the thermal inertia to the receiver performance without penalizing the computational time. A more detailed approach could be considered if the thermal inertial term is introduced in the receiver tube's energy balance and the HTF fluid. However, the iterative process would be more complex, and it would require a significantly higher computational time to converge. Moreover, the thermal inertia was considered only for the time steps under 30 minutes, due to its effect is not representative for low time resolution.

3.3.4.1. Control modes of the central receiver operation

The central receiver's operation is one of the most critical points at the time of simulating a solar tower power plant. Due to the fluctuating nature of solar radiation, solar tower power plants are exposed to transient effects. However, the thermal power generation does not follow the fluctuating irradiance instantaneously since large amounts of molten salts and pipes provide thermal inertia to the system. Despite this, information regarding operation controls of molten salts central receiver systems is difficult to obtain since very few of them are successfully operating worldwide, and access to this information is limited.

This study evaluates the central receiver's performance with sub-hourly simulations, making it necessary to implement control procedures that capture the effects of DNI variability. A set of control parameters were applied to simulate the most similar performance observed in CSP operating facilities. In this way, assumptions made in this study are based on the experience provided by some experts in CSP plants; and the Engineering, Procurement, and Control (EPC) of current CSP projects.

In first instance, the operation considers the limitations of starting up the receiver through three control parameters:

1. A minimum energy level required to start-up, set at 25% of the receiver's energy at the design point for one hour.
2. A minimum thermal power is required to begin the start-up procedure, set at 20% of the receiver design thermal power.
3. A minimum thermal power to start the receiver's effective operation, set at 25% of the receiver design thermal power.

Two control modes to operate the receiver were established to regulate the mass flow rate and the outlet HTF temperature in the receiver:

1. A perfect mass flow rate control (mode 1): in this control mode, the receiver's HTF mass flow rate is calculated to maintain constant the HTF design outlet temperature at the receiver. This mode is commonly activated in stable periods of DNI, such as during clear-sky days or periods with low variability.
2. A fixed mass flow rate control (mode 2): in this control mode, the HTF outlet temperature is calculated to maintain a constant HTF mass flow rate in the receiver,

allowing the HTF outlet temperature to vary within a safety limit during variable conditions of DNI. This mode is activated during intermittent cloudy days or periods with a high DNI variability, ensuring the receiver integrity. In this case, if the receiver outlet temperature falls below 470°C, the HTF flow is diverted to the cold tank to avoid excessive cooling in the hot tank. Moreover, the fixed mass flow rate is computed as 105% of the maximum flow calculated by mode 1 in the last 30 minutes.

A maximum DNI variation limit (f_{DNI}) was defined that must be surpassed to change from mode 1 to mode 2. This limit was set at 10 W/m²/min, and it was chosen to evaluate the natural variability of the DNI during a clear-sky day to ensure not obtaining misleading results. The DNI variability ($f_{DNI(i)}$) was calculated with the persistence of the DNI, as the following equation indicates:

$$f_{DNI(i)} = \frac{|DNI_{(i)} - DNI_{(i-1)}|}{\Delta t} \left[\frac{\text{W}}{\text{m}^2} \right] \left[\frac{\text{min}}{\text{min}} \right] \quad (3.3)$$

where $DNI_{(i)}$ is the DNI at the current time step, $DNI_{(i-1)}$ is the DNI at the previous time step, and Δt is the time step in minutes. Besides, it was implemented four time-delay parameters in terms of the variability to control how much time every mode would be activated and to establish start-up delays:

1. $t_{min\ mode2}$: it is the minimum amount of time in which the receiver must operate at mode 2 when it changes from mode 1. It was set at 60 minutes.
2. $t_{var\ mode2}$: it is the minimum amount of time in which the DNI variability must not exceed the f_{DNI} for the receiver to be able to change from mode 2 to mode 1. If the DNI variability exceeds the f_{DNI} the time delay is reset, and the receiver continues operating at mode 2. It was set at 15 minutes. This parameter ensures that DNI's variability conditions must be under a limit to return to mode 1.
3. t_{off_1} : it is the time delay to begin the start-up procedure of the receiver. This time delay is only activated if the receiver was previously turned-off and it is reset if DNI variability exceeds 100 W/m²/min (10 times f_{DNI}) within this time. It was set to 120

minutes. This parameter ensures that the receiver will not begin the start-up procedure during highly variable days.

4. t_{off_2} : it is a second-time delay to begin the startup procedure, in which the DNI variability must not exceed $20 \text{ W/m}^2/\text{min}$ (2 times f_{DNI}). If the DNI variability exceeds this threshold while the receiver is off, the time delay is reset, and the receiver will not initiate the startup. It was set at 15 minutes. This parameter ensures that DNI's variability conditions must be under a limit to begin the start-up procedure. In this way, both t_{off_1} and t_{off_2} must have been fulfilled to begin the start-up.

For a better understanding of these parameters, Figure 3-3 illustrates the central receiver's operation for two days with a clear-sky and a variable DNI profile in Carrera Pinto using a 1-minute time resolution. In this case, the central receiver has a design thermal power of 512 MWt corresponding to a 100 MW CSP plant with a SM of 2 and 14h of TES. Figure 3-3 shows the incident power coming on the receiver, the start-up power, and the effective receiver for a clear-sky and a variable day. The control mode leading the receiver operation is also shown down in the graphs.

At the beginning of the clear-sky day (Figure 3-3a), the receiver takes between 30-40 minutes in the start-up process before initiating its effective operation. It is observed that the receiver starts operation at mode 2, but it changes to mode 1 in a few minutes, maintaining this mode for the rest of the day. At 15:00h, the hot tank reaches its maximum level of molten salts, which causes a defocusing of the heliostats to remain stable the hot tank volume. Three hours later, the CSP plant starts to operate since the PV output starts decreasing. It is observed that the receiver does not require a start-up procedure to begin operation again since it is supposed that a small part of the heliostats remain focused to keep warm the receiver while the hot tank is full. Finally, Figure 3-3a also shows that the HTF outlet temperature in the receiver remains stable in the design point throughout the day due to control mode 1.

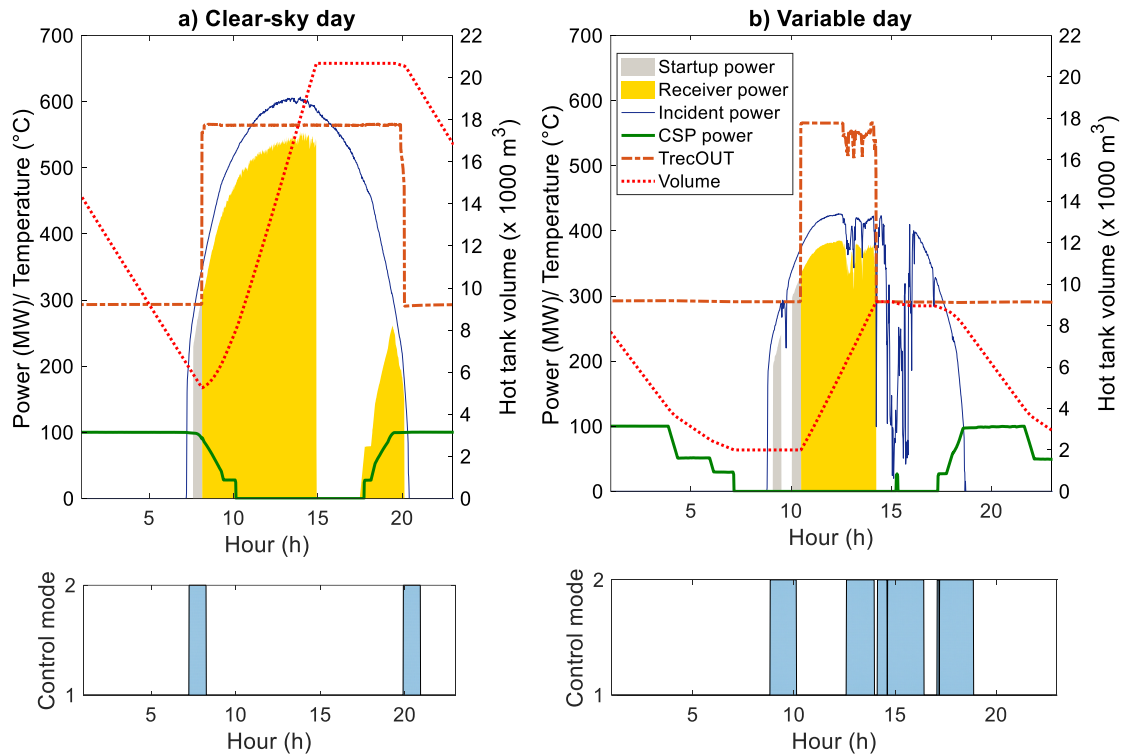


Figure 3-3: Receiver operation in Carrera Pinto with 1-minute time resolution for two types of days: a) Clear-sky day, and b) Variable day.

In contrast, Figure 3-3b shows a day with a variable DNI profile presenting values close to 100 W/m^2 in some moments of the day. During the first hours of the day, the receiver delays the start-up procedure due to DNI variability, but it starts regular operation after reaching the minimum energy required. The receiver operates in mode 1 approximately until 13:00 h, when it switches to mode 2 due to a DNI variability event. During this period, a variation in the HTF outlet temperature between 510 and 565°C leads to a temperature decrease in the hot TES tank. After the 14:30 h, the receiver is turned off because the incident power is lower than the minimum thermal power to operate. The receiver is not restarted for the rest of the day due to the startup delay times are activated. It is also worth mentioning that before the receiver is shut down, the thermal inertia keeps working the receiver for around five more minutes.

3.3.5. Operating mode

The operating mode of the hybrid plant considers delivering a base demand (P_{lim}), which was defined at 100 MW_e for the base case of this study. In this way, the PV output has priority to cover the demand, while the CSP plant operates as a back-up of the PV output, and the BESS is activated when the CSP-PV production is not enough to cover the demand. Figure 3-4 shows a flow chart describing the operation mode of the hybrid plant, where P_{pb} is the power block nominal output, $P_{PV(i)}$ is the PV net output (subtracting the parasitic consumption of the heliostats and the tower), $P_{CSP(i)}$ is the CSP power output, $P_{PV,exc(i)}$ is the PV surplus that charges the batteries or that becomes in dumped energy, $P_{BESS(i)}$ is the battery output power, $SOC_{(i)}$ is the batteries' SOC and Cap_{min} is the minimum capacity of the batteries.

When the PV output is $0.4 P_{pb}$ below P_{lim} the CSP-PV plant operates together to cover the demand. When the PV production is $0.4 P_{pb}$ above P_{lim} , but it is not enough to fulfill the demand, the CSP plant operates at minimum power block condition ($0.3 P_{pb}$) while the PV surplus is stored in the BESS or dumped if the BESS is completely charged. If the PV output is at least $0.1 P_{pb}$ below P_{lim} or higher than the baseload capacity, the power block of the CSP plant is turned off, and the PV surplus is used to charge the BESS, or it is dumped if the BESS is completely charged. In this case, if the receiver is also operating because there is enough incident power coming from the solar field, then the TES is charged, but if the TES reaches its maximum level, the heliostats are defocused, and there is a solar field dumped energy.

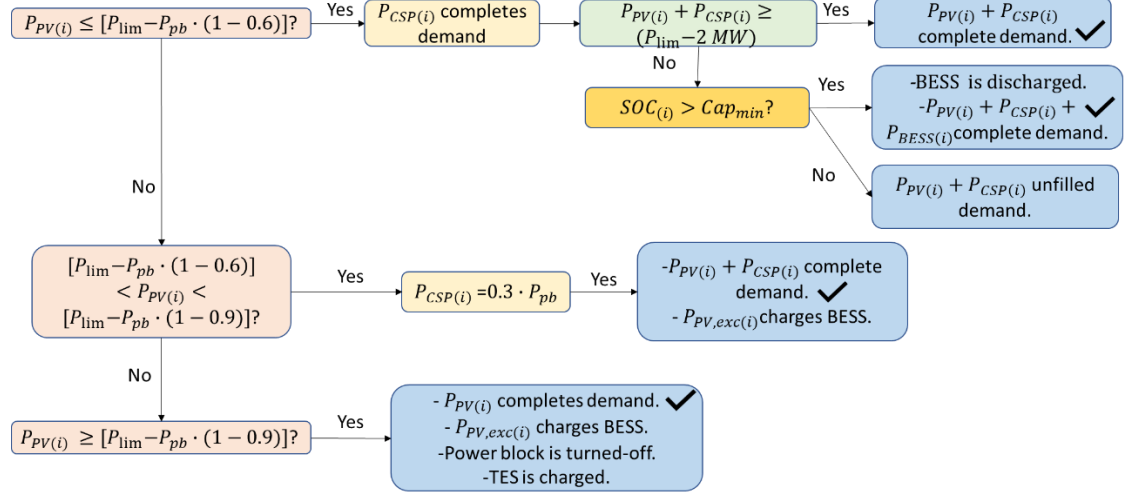


Figure 3-4: Operating mode of the hybrid plant.

In contrast, the BESS discharge is only activated when the PV-CSP output is below 2MW of the P_{lim} . This can occur during high-frequency DNI transients that cannot be fulfilled by the CSP plant during the start-up and shutdown procedures of the CSP plant (limited by the power block's ramps load), and when the TES is running out of energy.

Controllers of the TES system and power block were applied in TRNSYS, monitoring the volume charged and discharged in the hot tank. Different procedures to operate the start-up and shutdown of the plant were also implemented to increase or decrease the Rankine cycle's power output. Hot and cold start-up and shut down procedures of the power block are explained in detail in a previous work performed by the authors (Zurita et al., 2018).

3.4. Techno-economic analysis

The economic analysis was based on the computation of the LCOE for the hybrid plant based on the definition of (IRENA, 2012) and represented by Eq. 3.4:

$$LCOE = \frac{Af \cdot (CAPEX + C_{rep}) + OPEX}{E_{annual} \cdot Fa} \quad (3.4)$$

where Af is the capital recovery factor; $CAPEX$ is the total investment cost of the hybrid plant including the PV ($CAPEX_{PV}$), CSP ($CAPEX_{CSP}$), and BESS investment costs ($CAPEX_{BESS}$); C_{rep} is the replacement cost of the battery bank throughout the lifetime of the hybrid plant; $OPEX$ is the total operation and maintenance (O&M) cost of the hybrid plant; E_{annual} is the

annual electricity generation of the hybrid plant and F_a is the availability factor defined in 95%. The project lifetime considered was 35 years with a discount rate of 5%, which is in concordance with the prices offered by the CSP projects in Chile. The capacity factor (CF) was also computed as a technical indicator of the hybrid plant, and it is calculated as Eq. 3.5 indicates:

$$CF = \frac{E_{annual}}{P_{lim} * 8760h} \cdot F_a \quad (3.5)$$

CSP investment costs comprise direct and indirect capital costs representing those expenses applied in the year zero of the project, while the O&M costs represent the annual expenditures that occurred after the system is installed. The CSP cost database implemented for this study is in concordance with the values reported by the CSP Association of Chile (ACSP) in 2019, which represent costs reported in the literature for central-receiver plants (Jorgenson et al., 2016; Dieckmann et al., 2017; Kassem et al., 2017; Sharma et al., 2017; Boretti, 2018; Aly et al., 2019) validated by the industry in Chile. This economic data is presented in detail in APPENDIX B: APPENDIX FOR CHAPTER 3.

In the case of the PV plant, the module cost is based on the spot prices reported by PV Info Link (2018), while the inverter, balance of system (BoS), and the rest of the costs are based on the values reported by NREL for utility-scale PV plants in 2018 (Fu, Feldman, et al., 2018). BESS costs are based on the values reported by NREL (Fu, Remo, et al., 2018) for PV-BESS plants with a lithium-ion battery bank of a 2-hour duration. It was also considered the lifecycle method implemented by (Zakeri & Syri, 2015), which examines the total capital cost of an electric energy storage unit and the lifecycle costs related to the O&M and replacement. In this way, equations and cost data implemented to perform the economic analysis are presented in detail in APPENDIX B: APPENDIX FOR CHAPTER 3.

3.5. Results

This study considered different time steps ranging from 1, 5, 10, 15, 30 to 60 minutes to evaluate the DNI variability effects on the dispatchability of the hybrid plant and the receiver operation. In the analysis, the simulation time step was equaled to the solar data time resolution. Therefore, the input of total solar irradiation was the same for each time step evaluated.

3.5.1. Daily operation curves

A base case scenario with a hybrid plant configuration of 190 MW of nominal PV size, a SM of 2, 14h of TES, and 400 MWh was chosen to analyze its performance under different operational conditions. This configuration was based on the results obtained by (Zurita et al., 2018) for a hybrid plant with 400 MWh of BESS. Simulations were conducted in both Carrera Pinto and Santiago.

Three types of day were chosen to compare the operation of the hybrid plant. Figure 3-5 shows the three components of the solar irradiance for a clear-sky day (January 2nd) in both locations, a variable day with high levels of DNI and high-frequency transients (July 21st) in Carrera Pinto, and a variable low-level DNI day (June 19th) in Santiago, showing the Global Horizontal Irradiance (GHI) and the Diffuse Horizontal Irradiance (DHI). Figure 3-5a and Figure 3-5b illustrate a clear-sky day with a typical solar irradiation profile and high levels of DNI, with a maximum DNI of 1127 W/m² and 972 W/m² in Carrera Pinto and Santiago, respectively. In contrast, Figure 3-5c shows the solar irradiance in Carrera Pinto for a day with high-frequency transients and DNI values between 400 and 1000 W/m². A variable day with lower DNI levels and less variability are also presented in Figure 3-5d showing a more consistent cloudy condition throughout the day, reaching a maximum DNI of 688 W/m² and values below 100 W/m² during some hours in the mid-afternoon.

Daily total generation of the hybrid plant for the clear-sky day (January 2nd) in both Carrera Pinto and Santiago is presented in Table 3-5 using different time steps. This table shows the daily total maximum PV energy (without considering the curtailment of the baseload demand and the parasitic consumptions of the hybrid plant), the CSP and BESS plant total generation, and the total daily energy generated by the receiver.

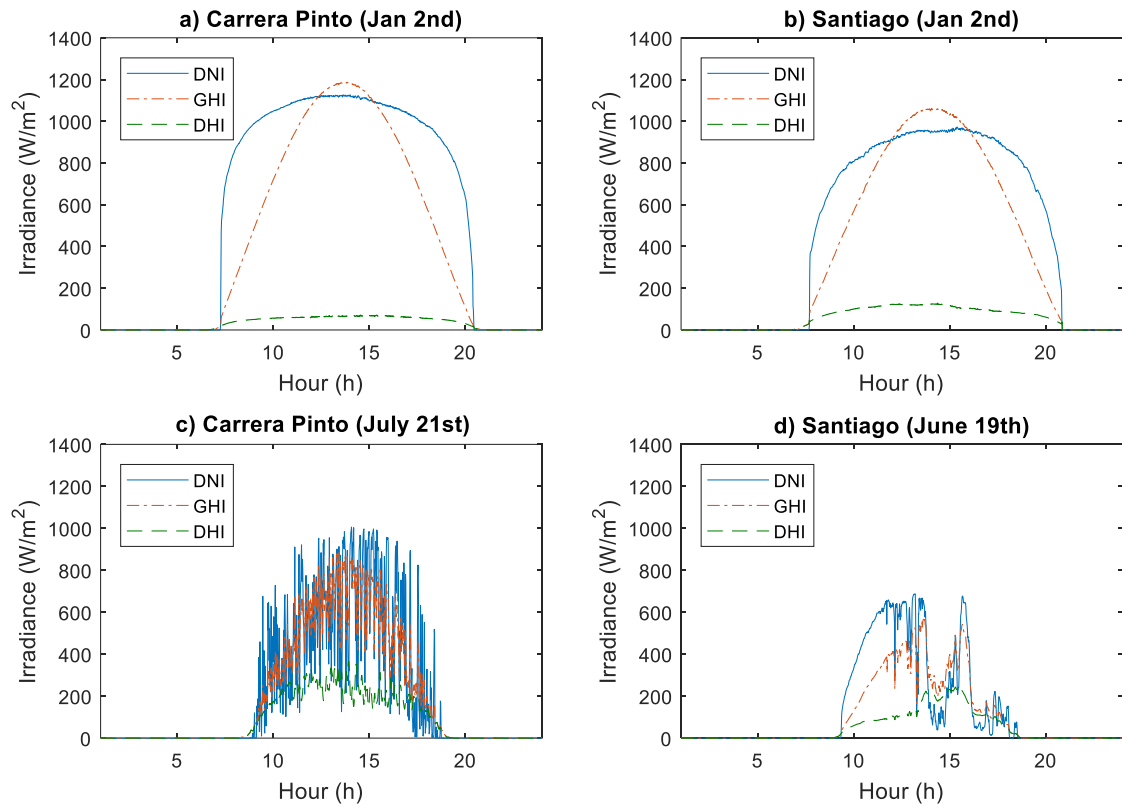


Figure 3-5: Solar irradiance in a 1-minute time scale for a) a clear-sky day in Carrerra Pinto, b) a clear-sky day in Santiago, c) a variable day with high-DNI levels and high-frequency transients in Carrerra Pinto and, d) a variable day with low DNI levels in Santiago.

In both locations, it is observed that the prediction of the daily production of all the components barely present variations as the time step is increased (below 1%) since the irradiance profile is quite stable throughout this day. Differences in the daily hybrid total generation were below $\pm 0.03\%$ as the time step was increased in both locations with respect to the 1-minute results, indicating that the influence of time resolution on the operation prediction is negligible during a clear-sky day.

Table 3-6 shows the daily total generation results for two different types of variable day, one with a highly variable irradiance profile on July 21st in Carrerra Pinto and another more consistent cloudy condition with a lower degree of variability on June 19th in Santiago.

Table 3-5: Daily total generation using different time steps for a clear-sky day (Jan 2nd) in Carrera Pinto and Santiago.

Time step (min)	January 2nd in Carrera Pinto (MWh/day)					January 2nd in Santiago (MWh/day)				
	PVmax	CSP	BESS	Hybrid	Receiver	PVmax	CSP	BESS	Hybrid	Receiver
1	1,291.97	1,472.05	9.00	2,400.59	3,749.24	1,151.65	1,459.06	33.63	2,399.78	3,848.46
5	1,292.77	1,471.75	7.66	2,400.69	3,757.80	1,154.23	1,458.69	32.59	2,399.87	3,841.26
10	1,292.58	1,476.90	5.58	2,401.17	3,735.13	1,155.64	1,461.87	30.01	2,399.40	3,832.00
15	1,292.23	1,478.29	4.56	2,400.83	3,771.05	1,156.14	1,461.94	30.75	2,400.00	3,860.59
30	1,290.30	1,489.23	3.24	2,401.25	3,795.42	1,157.17	1,475.90	25.68	2,400.00	3,815.11
60	1,285.04	1,489.78	8.35	2,401.22	3,805.43	1,157.56	1,457.98	32.18	2,400.00	3,852.39

Table 3-6: Daily total generation using different time steps for a day with high-frequency transients of DNI (July 21st) in Carrera Pinto and a cloudy day (June 19th) in Santiago.

Time step (min)	July 21th in Carrera Pinto (MWh/day)					June 19th in Santiago (MWh/day)				
	PVmax	CSP	BESS	Hybrid	Receiver	PVmax	CSP	BESS	Hybrid	Receiver
1	954.34	0.00	190.62	944.64	0.00	625.33	9.40	39.44	630.95	182.27
5	960.61	456.60	409.94	1,634.58	0.00	625.44	43.43	38.33	664.43	399.60
10	962.80	839.48	428.09	2,031.55	941.87	625.87	88.42	35.25	708.74	586.60
15	963.44	936.08	425.45	2,130.32	1,162.04	624.92	133.35	35.45	751.16	471.86
30	964.13	849.72	429.66	2,050.85	1,087.16	622.60	120.45	32.16	737.41	300.66
60	957.48	864.32	430.40	2,063.17	1,359.26	602.52	174.70	22.69	770.39	581.45

In Carrera Pinto, differences in the daily net PV output are still below 1% as the time step is increased (with respect to the results obtained with the 1-minute data); nevertheless, the most remarkable variations were obtained in the CSP plant operation. Results show that the receiver does not start operation when the simulation is performed with the 1-minute time resolution, and the CSP plant does not provide energy during this day. The same situation occurs when a 5-minute time resolution is considered, with the only difference of some hours in which the hot tank is discharged in the early morning, which accounts for the 456 MWh of CSP production. In contrast, from 10 to 60 minutes of time step, the production prediction significantly changes since the receiver does operate. These results are illustrated in Figure 3-6, which shows that the PV output variability is reduced dramatically as the time step increases, leading to discharge the BESS at later hours.

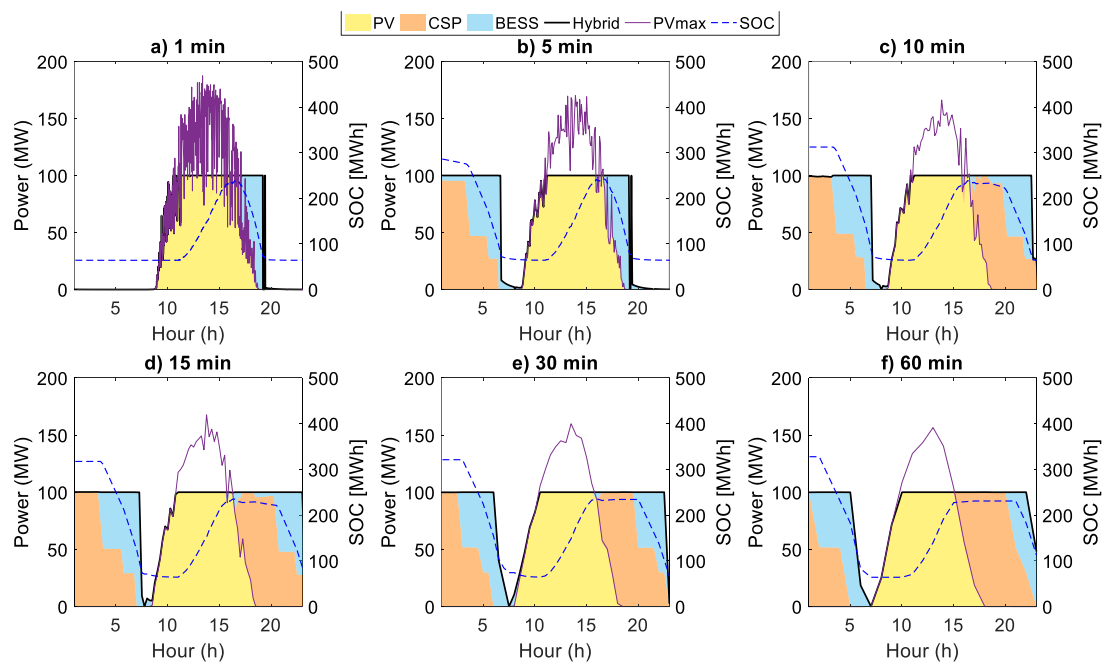


Figure 3-6: Production profile of the hybrid plant at Carrera Pinto in a variable day (July 21st) for different time steps: a) 1 minute, b) 5 minutes, c) 10 minutes, d) 15 minutes, e) 30 minutes, and f) 60 minutes

The cause behind the CSP plant variation can be elucidated in Figure 3-7, which illustrates the receiver and TES operation for July 21st in Carrera Pinto. This figure shows that in the

1-minute simulation, the receiver does not start operation due to minimum conditions established by controls to start-up are not achieved throughout the whole day. This is mainly due to the DNI profile's continuous intermittency and because the minimum energy required to begin operation is not reached. The hot tank is not charged or discharged since it is at its minimum level at the beginning of the day, and the receiver does not operate to heat the molten salts during the day.

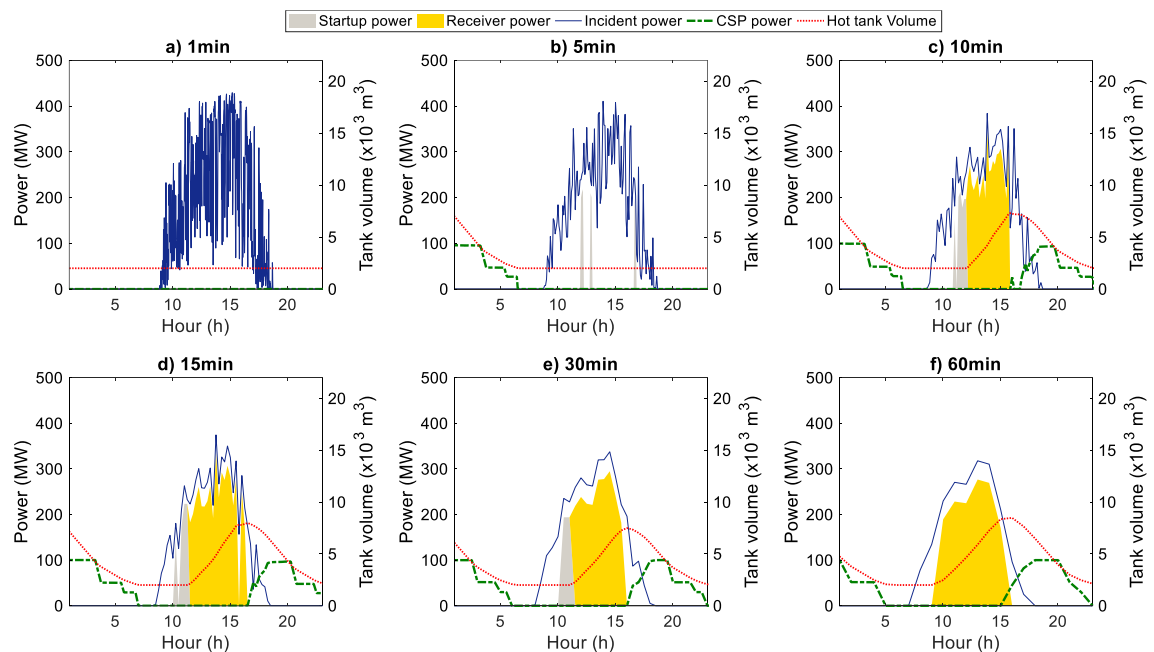


Figure 3-7: Central receiver operation during a variable day (July 21st) in Carrera Pinto for different time steps: a) 1 minute, b) 5 minutes, c) 10 minutes, d) 15 minutes, e) 30 minutes, and f) 60 minutes.

As the time step increases, the DNI variability is significantly reduced since the solar irradiance is averaged at every time step. Simulations using 10 to 60-minutes time resolution predict less variable conditions of DNI, which favor the conditions to starting up the receiver approximately before mid-day. Under these conditions, the receiver operates for most of the day, charging the hot tank and fulfilling the night's demand. These differences in the operation have a high impact on the hybrid plant generation's daily prediction due to the CSP performance variations. In this way, it was obtained that the production of the hybrid plant

with the time step of 10 minutes is more than double the predicted energy using the 1-minute time resolution. When time steps between 15 and 60 minutes are implemented, differences in the hybrid generation prediction are within a range between 1 and 5% with respect to the 10-minute time resolution results.

In the case of Santiago, results for a variable day with lower values of DNI indicate that differences in the PV generation as the time step increase are marginal, while the most significant variations occurred in the receiver and CSP plant production. As Figure 3-8 shows, the receiver presents a different performance as the time step is varied. As it happened with the intermittent day in Carrera Pinto, the DNI variability is significantly reduced as the time resolution is decreased; however, since there are periods with very low irradiance values in the afternoon, the receiver effectively operates less time in comparison to the other day. It is observed that with the 1-minute time resolution, the conditions to start the receiver's operation are initially reached in the morning. Since it is followed by a period of low DNI, the receiver only operates for a few hours. This operation tendency remains as the time step increases, varying only the number of hours that the receiver operates. Therefore, the daily prediction of CSP production tends to grow with the time step. It is also worth to mention that if perfect forecasting of the DNI was integrated into the simulation, the receiver might not operate at least under the conditions of the 1-minute time resolution since the receiver operation time is very small.

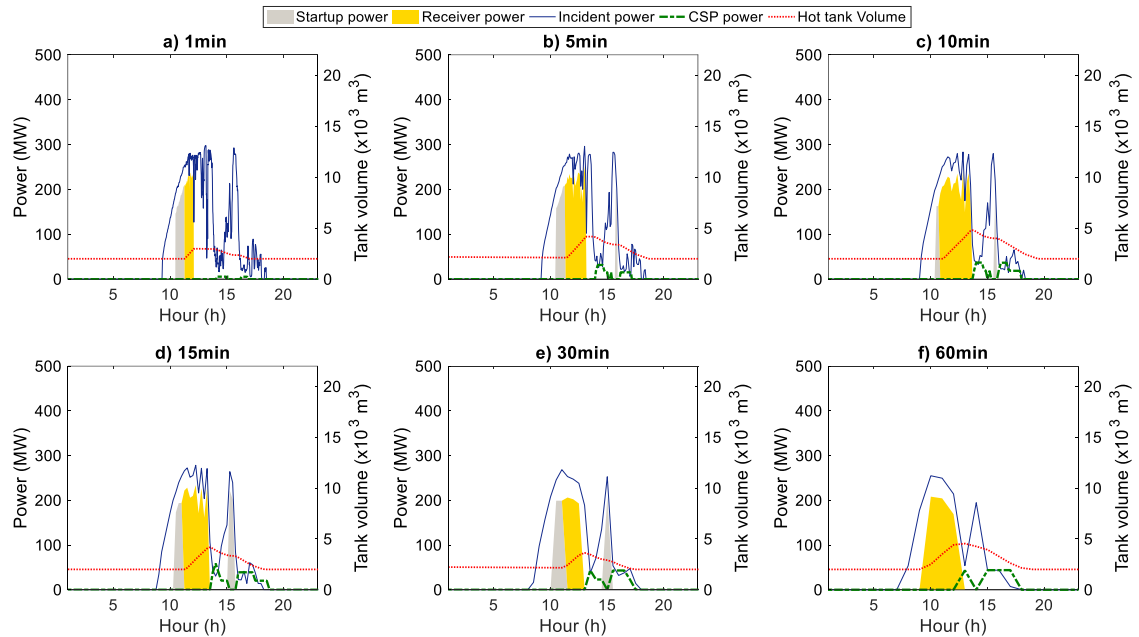


Figure 3-8: Central receiver operation during a variable day (June 19th) in Santiago for different time steps: a) 1 minute, b) 5 minutes, c) 10 minutes, d) 15 minutes, e) 30 minutes, and f) 60 minutes.

Overall results regarding the hybrid plant's daily performance indicate that the performance of thermal systems such as the receiver and the CSP plant's power block was the most affected by the time resolution. These variations in the time step of the simulation impacted the operation controls of these systems, such as the start-up, ramp-up, ramp-down, and shut-down procedures, which led to affecting the operation time and the energy produced by the receiver. This situation directly impacts the volume of molten salts charged to the hot tank, and therefore, the operation time of the CSP plant. Control procedures represent a restriction to satisfy minimum operational requirements implemented in solar thermal power plants to guarantee safe operating conditions and avoid damages in the receiver and the power block components. Still, results indicate that control operation parameters were more realistically captured with time resolutions of 1 minute and 5 minutes. With higher time steps, information regarding the DNI variability is so reduced that the hybrid plant's operational curves changed dramatically.

3.5.2. Annual performance prediction

The yearly performance of the hybrid plant for different time resolution is evaluated in this section. Table 3-7 presents the total annual generation of each component of the hybrid plant for both locations using different time steps and the percentage differences with respect to the 1-minute results. The PV column represents the net energy produced by the PV power plant applying the curtailment of the baseload demand (100MW_e). It is observed that the PV generation presents minimal variations as the time resolution is lower, with a maximum decrease of -1.70% and -0.68% with the 60-minute data in Carrera Pinto and Santiago; and the percentage differences were below $\pm 0.50\%$ with the rest of the time steps.

The most significant differences occurred in the CSP and BESS generation in both locations. First, it was obtained that the CSP total generation tends to increase as the time step is larger, which is caused by a higher prediction of the energy delivered by the receiver that presented variations up to 14.27% and 15.88% with the 60-minute data in Carrera Pinto and Santiago, respectively. As mentioned before, these differences are related to the receiver's operation time prediction that changes as the time resolution is varied. Notably, the DNI profile changes as the time resolution is lower, which impacts the start-up procedures and operation time of the receiver during the day. This also affects the volume and temperature of the molten salts tanks used to operate the CSP plant during the non-sunlight hours.

Furthermore, the BESS contribution to the annual hybrid plant generation decreased in both locations as the time step increases due to the solar irradiance variability is highly reduced. This causes a rise in the CSP generation and a reduction in the battery bank's energy to complement the PV production during the day. In the case of Carrera Pinto, a maximum percentage difference on the BESS generation of -15.17% was found with the 60-minute data, while in Santiago was about -16.22%.

Regarding the total annual generation of the hybrid plant, the maximum percentage difference found in Carrera Pinto was 5.82% with the 60-minute data. In contrast, a maximum difference of 5.95% was obtained in Santiago. These results indicate a similar tendency of overestimating the annual generation of the hybrid plant as the time resolution is decreased in both locations with approximately the same percentage differences, even though Santiago is a location that presents a more unfavorable solar resource than Carrera Pinto.

Table 3-7: Annual total generation and percentage differences using different time steps for Carrera Pinto.

Time step (min)	Annual generation (MWh)					Percentage Difference with respect to 1min results (%)				
	PV	CSP	BESS	Hybrid	Receiver	PV	CSP	BESS	Hybrid	Receiver
1	314,937	392,856	49,053	756,846	1,006,437	-	-	-	-	-
5	315,528	418,052	46,342	779,923	1,070,744	0.19%	6.41%	-5.53%	3.05%	6.39%
10	315,354	430,588	43,916	789,857	1,100,696	0.13%	9.60%	-10.47%	4.36%	9.37%
15	315,169	435,367	43,479	794,015	1,114,718	0.07%	10.82%	-11.36%	4.91%	10.76%
30	313,525	437,433	43,663	794,621	1,117,010	-0.45%	11.35%	-10.99%	4.99%	10.99%
60	309,584	449,675	41,611	800,870	1,150,053	-1.70%	14.46%	-15.17%	5.82%	14.27%

Table 3-8: Annual total generation and percentage differences using different time steps for Santiago.

Time step (min)	Annual generation (MWh)					Percentage Difference with respect to 1min results				
	PV	CSP	BESS	Hybrid	Receiver	PV	CSP	BESS	Hybrid	Receiver
1	259,723	263,320	37,342	560,384	687,657	-	-	-	-	-
5	260,412	279,210	35,352	574,973	730,170	0.27%	6.03%	-5.33%	2.60%	6.18%
10	260,634	285,496	34,278	580,408	744,829	0.35%	8.42%	-8.21%	3.57%	8.31%
15	260,993	291,056	32,870	584,919	760,939	0.49%	10.53%	-11.98%	4.38%	10.66%
30	260,339	290,194	33,464	583,997	757,135	0.24%	10.21%	-10.38%	4.21%	10.10%
60	257,950	304,486	31,283	593,719	796,892	-0.68%	15.63%	-16.22%	5.95%	15.88%

3.5.3. Techno-economic results

This section presents the results of the techno-economic analysis performed for different cases of study. In the first instance, the base case results, which considered the same configuration of hybrid plant for two locations, are presented through a comparative analysis of the capacity factor and the LCOE varying the time step. Secondly, three more study cases were included to analyze the impact of time resolution for different plant configurations and dispatch strategies.

3.5.3.1. Base case results

Table 3-9 and Table 3-10 present the simulations' techno-economic results performed as the base case in this study. Results are in terms of the capacity factor and LCOE calculated for the different time steps in both locations, and the percentage differences with respect to 1-minute results. In general, capacity factors between 82 and 86% were obtained in Carrera Pinto, and LCOEs between 85 and 81 USD/MWh, while in Santiago the capacity factors were lower as it was expected, within a range between 60 and 64%, and with higher LCOES between 119 and 112 USD/MWh. Regardless of the location, the LCOE decreases as the time resolution is lower, mainly due to the overestimation of the hybrid plant's annual generation when the time step is increased. Table 3-9 and Table 3-10 also report the simulation time of each time step normalized with respect to the simulation time using the 1-minute time resolution. It is observed that as the time step is increased, the simulation time drops significantly. For instance, only for the simulation using a 5-minute time step, the simulation is about 76.5% faster than with the 1-minute time step, while with the 60-minute time resolution, the simulation duration is decreased a 97.5%. These results are similar in both locations. This reduction in the simulation time is important when fast simulation models are needed; however, the compression of data also leads to a loss of information of the variability, which causes an overestimation in the energy production.

Table 3-9: Techno-economic results for the hybrid plant in Carrera Pinto for different time steps.

Time step (min)	CF (%)	LCOE (USD/MWh)	Hybrid plant generation (MWh)	Normalized Simulation Time (-)	%Diff CF	%Diff LCOE
1	82.08	85.98	756,846	1.000	-	-
5	84.58	83.55	779,923	0.229	3.05%	-2.82%
10	85.66	82.56	789,857	0.128	4.36%	-3.98%
15	86.11	82.15	794,015	0.083	4.91%	-4.46%
30	86.17	82.10	794,621	0.050	4.99%	-4.52%
60	86.85	81.51	800,870	0.023	5.82%	-5.20%

Table 3-10: Techno-economic results for the hybrid plant in Santiago for different time steps.

Time step (min)	CF (%)	LCOE (USD/MWh)	Hybrid plant generation (MWh)	Normalized Simulation Time (-)	%Diff CF	%Diff LCOE
1	60.77	119.29	560,384.28	1.000	-	-
5	62.35	116.37	574,973.27	0.235	2.60%	-2.45%
10	62.94	115.32	580,407.75	0.115	3.57%	-3.33%
15	63.43	114.46	584,919.06	0.090	4.38%	-4.05%
30	63.33	114.63	583,997.16	0.040	4.21%	-3.91%
60	64.39	112.84	593,718.84	0.025	5.95%	-5.41%

In the case of Carrera Pinto, percentage differences in the capacity factor and LCOE were around $\pm 3\%$ with the 5-minute time resolution, between $\pm 4-5\%$ for time steps between 10 and 30 minutes, and the most significant variation was obtained performing hourly simulations between $\pm 5-6\%$. Table 3-10 shows similar percentage differences for the capacity factor and LCOE in Santiago. In this case, percentage differences were between $\pm 2-3\%$ using the 5-minute resolution, $\pm 3-4\%$ for the 10-30 minute time steps, and between $\pm 5-6\%$ with the 60-minute time resolution.

It is crucial to consider that differences between 2-6% in the annual generation of a hybrid plant may be regarded as small; however, they can be decisive when getting funding through PPA or winning a bid. For instance, in Chile's case, energy projects must compete between them to offer the lowest cost of electricity in energy blocks, and even small differences in the offers can lead to different results.

3.5.3.2. Comparison of cases of study

To diversify the results and findings of the methodology raised in this paper, four study cases are presented in this subsection to compare the time resolution impact on modeling different plant configurations and dispatch strategies. Table 3-11: Description of cases of study. shows the description of the configurations considered for this comparative analysis. In first instance, it is included the base case configuration previously simulated in Carrera Pinto, which presents an oversized PV field with a medium CSP plant size (Base Case CP). The second case of study (Hybrid CD) represents a similar configuration of the Cerro Dominador (CD) plant, currently being developed in northern Chile, a 100 MW PV plant, and a molten solar tower with an approximate SM of 3 and 17.5h of TES. This configuration represents an undersized PV with respect to the CSP, and it was added a battery bank of 100MWh. The third case study represents only the CSP part of the CD plant to compare the time resolution impact in a standalone CSP plant (CSP CD). The last configuration (Hybrid 150 peak) presents the same configuration as the base case, but with a peak strategy in which the demand increases to 150 MW_e during peak hours (05:00-09:00, 18:00-21:00) the rest of the day the plant must generate 100 MW_e. All the cases of study in this section were modeled only in Carrera Pinto.

Simulations varying the time step and the meteorological data were performed to obtain the annual results and techno-economic indicators of every case. Results of these simulations are presented in detail in Table 3-12, showing the annual production of only the CSP plant ($E_{CSP(t)}$), the annual hybrid total generation of the plant ($E_{hybrid(t)}$), and the LCOE ($LCOE(t)$). These three values were normalized with respect to the results found with the 1-minute time resolution ($E_{hybrid(t=1min)}$, $E_{CSP(t=1min)}$, $LCOE(t=1min)$, respectively), to be analyzed and compared, as Eq. 3.6, 3.7 and 3.8 indicate. Variables with the “ n ” superscript would represent the normalized values.

$$E_{hybrid(t)}^n = \frac{E_{hybrid(t)}}{E_{hybrid(t=1min)}} \quad (3.6)$$

$$E_{CSP(t)}^n = \frac{E_{CSP(t)}}{E_{CSP(t=1min)}} \quad (3.7)$$

$$LCOE(t)^n = \frac{LCOE(t)}{LCOE(t=1min)} \quad (3.8)$$

Table 3-11: Description of cases of study.

Case of study	Location	Demand (MW)	PV size (MW)	SM (-)	TES capacity (h)	BESS size (MWh)	PV Tracking (-)
Base Case CP	CP	100	190	2	14	400	0
Hybrid CD	CP	100	100	3	17.5	100	1
CSP CD	CP	100	-	3	17.5	-	-
Hybrid 150 peak	CP	150 MW (05:00-09:00, 18:00-21:00) 100MW for the rest	190	2	14	400	0

Table 3-12: Results for different case studies varying the time resolution of the simulation.

Study case	Time Resolution	1	5	10	15	30	60
Base Case CP	CSP generation [MWh]	392,856	418,052	430,588	435,367	437,433	449,675
	Hybrid generation [MWh]	756,846	779,923	789,857	794,015	794,621	800,870
	LCOE [USD/MWh]	85.98	83.55	82.56	82.15	82.10	81.51
Hybrid CD	CSP generation [MWh]	468,768	502,457	515,824	521,864	523,806	535,879
	Hybrid generation [MWh]	746,469	777,364	789,226	794,642	794,270	805,272
	LCOE [USD/MWh]	91.84	88.36	87.09	86.53	86.57	85.45
CSP CD	CSP generation [MWh]	598,543	638,526	656,619	666,307	663,094	685,173
	Hybrid generation [MWh]	-	-	-	-	-	-
	LCOE [USD/MWh]	100.56	94.51	92.02	90.74	91.16	88.35
Hybrid 150 peak	CSP generation [MWh]	406,969	433,389	445,681	451,625	451,401	463,241
	Hybrid generation [MWh]	821,982	848,642	860,814	866,488	865,439	874,183
	LCOE [USD/MWh]	79.37	76.99	75.96	75.49	75.58	74.87

Figure 3-9, Figure 3-10, and Figure 3-11 present the normalized variables for every case at different time steps. Regarding the normalized annual generation ($E_{hybrid(t)}^n$), Figure 3-9 illustrates how the components sizing and the plant configuration influence the time resolution impact. First, results indicate that the most substantial differences in the estimated annual production occur with the standalone CSP plant (CSP-CD). In this case, variations around 7% with respect to the 1-minute results occur even by using the 5-minute time resolution, and differences up to 14% are accounted when the 60-minute time resolution is implemented. In comparison, the cases with a hybrid plant scheme present a lower impact of the time resolution in the annual production, with a maximum difference of 8% obtained with the 60-minute data in the Hybrid-CD case.

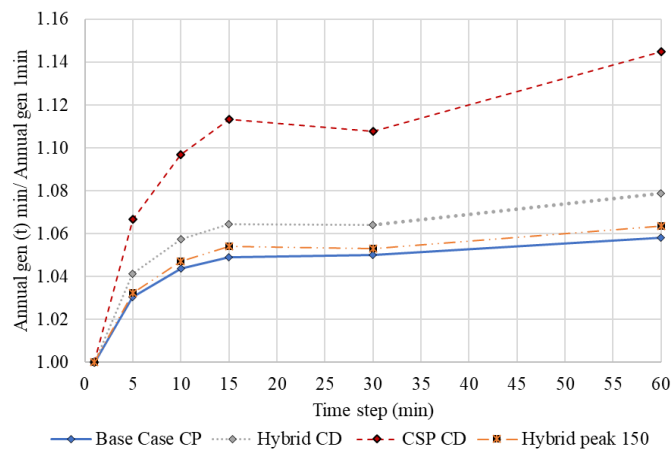


Figure 3-9: Normalized annual generation vs. time step of the simulation for different cases.

In the case of the hybrid plants, it is also observed that the components sizing influences the impact of time resolution on the performance prediction of the system. For instance, both cases with a large and oversized PV system with regards to the CSP (Base case CP and Hybrid 150 peak) obtained the smallest normalized differences as the time step was increased, within a range of 3-6% depending on the time resolution, while the case with an undersized PV plant and a large CSP system (Hybrid CD) was more affected by the temporal resolution than the other two cases for, with differences between 4 and 8% in the annual production. In the case of Hybrid peak 150, the dispatch strategy at peak hours did not cause

any significant in the influence of time resolution since it obtained similar results to the base case. This result shows that varying the sizing of a hybrid plant's components has a higher impact than modifying the dispatch strategy in the evaluation of the time resolution.

Regarding the normalized CSP generation ($E_{CSP(t)}^n$), Figure 3-10 shows that when only the CSP generation is considered (in the case of a hybrid plant, it would be represented by the annual contribution of the CSP-TES plant to the total production, and in the standalone CSP plant, it would be the net yearly generation), the impact of time resolution is within the same range of variation regardless the configuration of the plan. This means the CSP plant's production is affected in the same way by the time resolution, either if it is evaluated in a hybrid scheme or a standalone system. Nevertheless, Figure 3-9 and Figure 3-10 show that differences in the total annual generation are smaller than the variations accounted for only the CSP generation, which indicates that the CSP plant is the system most influenced by the time resolution.

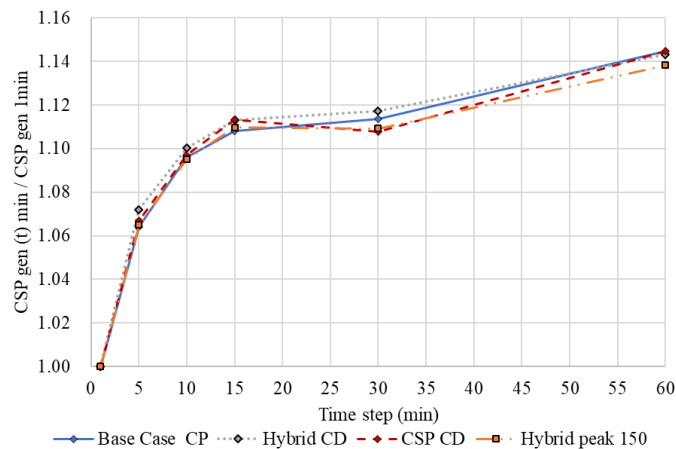


Figure 3-10: Normalized CSP generation vs. time step of the simulation for different cases.

Results also indicate that the sizing of the PV field with respect to the CSP plant plays an important role in the impact that time resolution has on a hybrid plant's performance. Since the PV plant has the priority dispatch on the hybrid plant, it can produce around 40-50% of the total annual generation. Besides this, the yearly PV plant production is barely affected by the time resolution, which helps to attenuate the significant impact that time resolution has on the estimation of the CSP production. Thus, the effect of time resolution on a hybrid

plant's performance prediction is lower when configurations with an oversized PV system with respect to the CSP plant are considered, while the effect is higher when the CSP plant is oversized with regards to the PV system.

Finally, Figure 3-11 shows the variation in the normalized LCOE ($LCOE_{(t)}^n$) for every time step and case. Since the annual generation is overestimated as the time resolution is decreased, the opposite trend is evidenced in the LCOE. This can also be observed in Table 3-12. The $LCOE_{(t)}^n$ is underestimated with respect to the 1-minute result at every case, with the largest difference obtained for the standalone CSP plant using the 60-minute data. This result is in concordance with the tendencies obtained in Figure 3-9. It was also obtained that time resolution impact on the $LCOE_{(t)}^n$ is smaller for the hybrid plant cases, showing the effect that the components sizing and their costs have on the final impact of time resolution on the LCOE estimation.

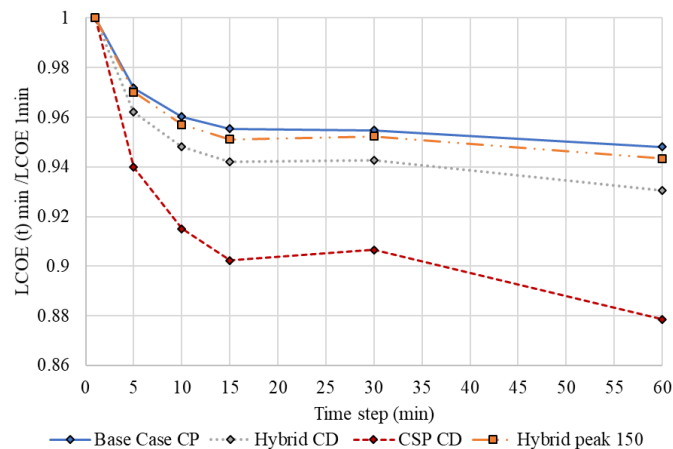


Figure 3-11: Normalized LCOE vs. time step of the simulation for different cases.

3.6. Discussion

This work analyzes the operation, performance, and dispatchability of a hybrid CSP-PV plant integrated with a TES and battery bank under different conditions of time resolution. The main considerations implemented to perform this work and some discussions regarding the results are explained and developed below:

- The operating mode and the sizing of the components can lead to different outcomes of the time resolution impact on the hybrid plant's performance. In this study, the hybrid plant's operating mode prioritizes the PV output, and it dispatches the CSP

plant around the PV, while the BESS is used as a back-up to soft PV variations and to complement the CSP output. The analysis showed in Section 3.5.3.2 indicates that having an oversized or undersized PV plant with respect to the CSP only affects the magnitude of the annual generation's overestimation. Still, the tendency with respect to the time step remains the same. Different dispatch strategies such as baseload and a peak demand were considered between the cases of study, and results showed that the impact of time resolution was more influenced by the sizing of the components than the profile demand.

- Solar data in 1-min resolution implemented in this work comes from ground measurements performed by a sensor located at only one point. This data presents a very high level of DNI variability, which may lead to an underestimation of the incident power on the solar field since the DNI variability may be attenuated if a larger area is considered. The DNI variability has a significant impact on the receiver's control operation and, consequently, the CSP performance. Therefore, more representative data could be obtained if 1-minute data from several measuring points (between 2 to 4) located within the plant area (1-2 km distance) is averaged, which may capture the actual variability that affects the whole solar field area. The 1-minute based data was used to compare the results of different time resolutions due to the lack of data coming from a real power plant. The best way to determine the most appropriate time resolution to simulate the plant would be to compare real data with the results obtained for every time step and then establish which time step captures the operating facility's actual behavior. However, due to the lack of CSP projects operating worldwide, this study's results indicate that the 5-minute based data could be the more appropriate time step to capture the actual variability occurring in the plant's whole area.
- Ground-measured solar and meteorological data of 1-minute has the drawback that is representative of only one particular year. Conversely, a Typical Meteorological Year (TMY) condenses multiyear long-term time series into one representative year, which is created from satellite-based models with a temporal resolution of 30min or 1h that leads to an inevitable loss of the DNI variability information. Discussion regarding if minute-based measurements are better than using the available hourly

TMY data does not have yet a final answer, basically because the use of ground-measurements or TMYs would be influenced by a relationship between the desired precision and the limitations of processing time. For instance, a good practice in the industry is to perform simulations with a TMY and start running a measurement campaign at the site of interest in parallel with the project development. Later, simulations with sub-hourly data shall be performed to determine a more realistic performance of the plant. An interesting research topic could be related to how the hourly TMY data can be adapted to sub-hourly based data to capture the transient effects, as well as assessing how to translate the DNI variability in terms of uncertainty to the hourly data to improve a TMY that could lead to similar results than the 1-minute based data.

- The development of a hybrid CSP-PV project comprises different phases (preliminary feasibility evaluation, a bankability assessment, a real technical-operation simulation, or bid preparation) that present different requirements of the energy models' accuracy. Results obtained in this work have shown the importance of considering the influence of time resolution on energy simulations; therefore, some advantages and drawbacks of using a specific time resolution are discussed. For pre-feasibility evaluations, 1-hour can be the most appropriate time resolution since it provides the fastest simulation time, which is needed to run techno-economic design optimizations that involve a significant number of simulations and to show the potential of different locations; however, the outcomes would lead to an overestimation of the CSP performance, thus, they would be very optimistic. In the development phase, additional simulations using sub-hourly timesteps between 1 to 5 minutes can represent an advantage since they allow to capture the variability effects on energy production. In this way, models with a high time resolution can reduce the uncertainty on estimating the plant generation lowering the risk perception from the financing entities, even though simulations will require a longer computational time. Finally, in bid preparation for electric tenders, simulations with a high time resolution would lead to a conservative approach guaranteeing a minimum energy target. In contrast, if the computational time is a concern, 10-15min timesteps can be implemented to capture the variability effects partially and to set

higher energy targets, nevertheless, this approach can be risky if these targets cannot be accomplished at the time of operating the plant.

3.7. Conclusions

The analysis of the time resolution impact on a hybrid solar power plant's modeling was carried out considering a central-receiver power plant coupled with a two-tank molten salt TES, a PV plant, and a battery bank. The hybrid plant's operation and performance were evaluated, varying the time resolution of the simulation from 1, 5, 10, 15, 30 to 60 minutes. The hybrid plant was modeled in two Chile locations for the base case, and different configurations and dispatch strategies were evaluated as cases of study. The hybrid plant's daily performance, the total annual generation, the capacity factor, and the LCOE were also assessed. Main conclusions which provide the summarized findings of this work are presented as it follows:

- Daily operation analysis showed that the performance of thermal systems such as the receiver and the power block of the CSP plant was the most affected by the time resolution variation, followed by the BESS, while the effect on the daily PV generation was negligible.
- Variation in the receiver operation with the time resolution was a result of the application of operation controls, including start-up, ramp-up, ramp-down, and shut-down procedures that affect the operation time and the energy produced by the receiver. These control procedures of the receiver and power block were more realistically captured with time steps between 1 and 5 minutes, while with higher time steps, information regarding the DNI variability was lost.
- In general, the annual generation of the hybrid plant was overestimated as the time step was increased. Maximum percentage differences in the total yearly hybrid production with respect to the 1-minute results were obtained with the hourly data, reaching 5.83% and 5.95% in Carrera Pinto and Santiago, respectively. Moreover, the largest variations were obtained in the annual CSP generation with 14.27% and 15.88% in both locations, respectively. Regarding the techno-economic results, percentage differences in the capacity factor and LCOE were around ± 2 -3% in both sites using the 5-minute time resolution, while higher differences between ± 4 -6%

were found for time steps between 10 and 60 minutes. In this way, differences about 2-6% may be small, but they can be decisive when evaluating projects to obtain financing or long-term contracts energy contracts in tenders.

- The tendency of overestimation as the time step is increased was also found in the study cases where the components' sizing and the dispatch strategy was varied. Results showed that the impact of time resolution on a standalone CSP plant's performance estimation is much more significant than in a hybrid plant. The time step's effect was lower for oversized PV configurations with respect to the CSP, and variations were higher when the CSP plant is oversized regarding the PV system.
- This work indicates that the 5-minute time resolution can be the most appropriate time step to use in the modeling of a hybrid plant. This time step provides a well-balanced relationship between accuracy and computational time of the simulation; however, authors want to emphasize that temporal resolution will mainly depend on the purpose of the simulation, how much accuracy is expected from the results, and the computational time limitations. In this way, the advantages and drawbacks of implementing different time steps at every phase of the development of a large-scale solar power plant project were discussed and presented in this study.

4. MULTI-OBJECTIVE OPTIMAL DESIGN OF SOLAR POWER PLANTS WITH STORAGE SYSTEMS ACCORDING TO DISPATCH STRATEGY

4.1. Introduction

Nowadays, the energy transition path is being followed by many nations worldwide to achieve more sustainable and flexible electric systems in the future. This brings new challenging goals such as decarbonization scenarios and high renewable energy shares, that would only be possible to reach next to strategies to improve and increase the grid reliability and flexibility. These goals are also pushing forward changes in the electric markets to recognize a variety of benefits from new energy projects, including greater independence of generation and increasing their availability to provide firm power for more hours. In this matter, the integration between variable renewable energy sources and storage systems (like solar and wind) are one of the solutions being assessed. Nonetheless, in the case of solar, the deployment of solar Photovoltaics (PV) projects with Battery Energy Storage Systems (BESS) is limited worldwide due to the relatively high costs of batteries for large-duration storage applications. The development of the Concentrated Solar Power (CSP) technology integrated with Thermal Storage Systems (TES) is also limited to few operational projects in the world, mainly because its Levelized Cost of Electricity (LCOE) is still superior when compared to other energy sources (IRENA, 2020). As a different solution that seizes the low cost of solar PV and dispatchability of CSP-TES plant, a hybrid CSP-PV concept has been evaluated in the literature and by the industry in the last years, since it allows achieving higher capacity factors and lower LCOEs than a standalone CSP plant (Pan & Dinter, 2017; Parrado et al., 2016; Starke et al., 2016). All these systems are considered promising options for providing firm power; however, it is relevant to comprehend and identify the limitations, cost-effectiveness and suitability of these type of solar projects with storage.

In this concern, (Feldman et al., 2016) performed a comparative analysis between a CSP-TES and PV-BESS plant in terms of LCOE, obtaining that for small storage requirements, the PV-BESS presents lower LCOEs, while the CSP-TES tends to produce lower LCOEs for larger sizes. This study has the limitation of only analyzing a fixed 100MW_{ac} power capacity of the systems, and the authors only compared specific design configurations

increasing the solar multiple and DC-AC inverter ratio to provide the same hours of storage. (Jorgenson et al., 2016) also conducted a techno-economic comparison between a CSP-TES plant with a PV plant combined with long-duration BESS or gas turbines, obtaining that the CSP-TES provides the lowest cost, mainly driven by an aggressive heliostat cost decrease for 2030. In this case, the study was focused on the economic comparison of upfront capital and annualized costs considering different load capacities. (Payaro et al., 2018) carried out the optimization of a PV-BESS system and a CSP-TES plant in terms of the LCOE and capacity factor, showing that the CSP plant could be more competitive for capacity factors of 85%, but requiring a significant reduction in the solar field cost. This study presents a good preliminary analysis of the trade-off existing between the LCOE and the capacity factor for these technological solutions, but their results are limited to base generation in which larger capacities of storage are required to meet the demand.

In addition, (Zurita et al., 2018) performed an analysis of a hybrid CSP-PV with TES and BESS, obtaining that the minimum LCOE is achieved for a solution without batteries; however, with a battery cost reduction over 60%, design configurations integrating both TES and BESS could provide a synergetic operation. Separate studies (Bravo & Friedrich, 2018; Starke et al., 2018; Zhai et al., 2017)(Bravo & Friedrich, 2018; Liu et al., 2019; Starke, Cardemil, & Colle, 2018) have also analyzed the economic viability of hybrid CSP-PV plants, in which the hybrid plant has been optimized to provide energy in baseload demand, minimizing the LCOE, maximizing the energy production and minimizing the total installation cost. Nevertheless, these studies have the limitation of not considering the effect of different dispatch strategies than baseload on the optimal design configurations. Based on this literature review, it is evidenced that the techno-economic performance of PV, CSP, and hybrid CSP-PV plants with TES and battery storage has been widely studied, considering technical and financial objective functions. However, it has not also been found any study in the literature that integrates the comparison among all the currently available solar technology combinations, for instance PV-BESS, CSP-TES, hybrid CSP-PV with TES, and hybrid CSP-PV with TES and BESS, as well as little research has been performed concerning how the dispatch strategy affects these storage-integrated technology optimal configurations. Additionally, only few studies have analyzed the importance of achieving high sufficiency factors beyond reaching low LCOEs.

In this concern, the study presented herein analyses the influence that dispatch strategies have on the optimal design of solar power plants integrated with storage, for a case of study in the Chilean electric market. This work also aims to address how the design requirements of solar systems with storage represent a location-specific problem, and how their viability depends on the economic environment and the dispatch profile chosen to provide. In this manner, a multi-objective optimization approach with a genetic algorithm was performed to obtain the set of Pareto-optimal solutions that minimize the LCOE and maximize the sufficiency factor, considering four dispatch strategies (baseload, night and evening, daylight and evening, and only daylight hours), and four technology combinations: a PV-BESS, a CSP-TES based on a molten salt central receiver, a CSP-PV with TES, and a CSP-PV-TES-BESS. The study also considers a cost scenario for 2020 and future projections for 2030, and two locations with different solar resource conditions are analyzed. This enables to provide insights about which is the least-cost technological option that allows meeting a dispatch strategy with a certain level of supply guarantee, filling the knowledge gap regarding the limitations and suitability ranges among solar and storage-integrated technologies for different dispatch profiles, cost scenarios and solar resource conditions.

4.2. System Description

Figure 4-1 illustrates the scheme of the systems considered. Four technological combinations were studied:

- 1) PV-BESS: A PV plant with a single-axis tracking system coupled to a Battery Energy Storage System (BESS) based on lithium-ion technology.
- 2) CSP-TES: A CSP plant based on a molten salt central receiver technology coupled to two-tank molten salt direct TES.
- 3) CSP-PV-TES: A hybrid scheme composed of a central receiver power plant with TES coupled to a single-axis PV plant.
- 4) CSP-PV-TES-BESS: A hybrid plant same as the previous one but including a lithium-ion battery bank.

The PV plant consists of a horizontal single-axis tracking system oriented in a north-south line with a silicon mono-crystalline modules of $330W_p$ (SunEdison, 2015). The inverter was selected with a maximum AC power of $1 MW_{ac}$ (ULTRA-TL-1100 of ABB (ABB, 2017)).

The PV plant is designed with a scalable size in terms of the number of inverters to reach the nominal PV capacity (from 0 to 500 MW), with a fixed DC-AC ratio of 1.04. The PV-BESS combination considers an AC-coupling system, in which a PV inverter and a power conversion system for the battery bank are included (Figure 4-1). This configuration allows upgrading the PV and battery separately since the systems are independent of one another (Fu et al., 2018). Regarding the BESS, it was considered a lithium-ion battery bank with an overall efficiency of 94%, 5000 lifecycles, 20 years of calendar lifetime and a Depth of Discharge (DoD) of 84% (IRENA, 2017).

The CSP plant is based on a molten salt central-receiver technology integrated with a two-tank direct TES system. The central-receiver and TES section operate with a mixture of molten salts as heat transfer fluid and storage media, composed of 60% NaNO_3 and 40% KNO_3 . Cold and hot tank temperatures of the TES system were set at 295°C and 565°C, respectively. Regarding the solar field design, the heliostats field configuration and efficiency, the receiver height, receiver diameter, and tower height were optimized in terms of the Solar Multiple (SM) for every study case. The CSP's power block consists of a steam cycle with a gross power output of 110 MW_e and a nominal efficiency of 39.12% (Zurita et al., 2020). The Rankine cycle is composed of a steam generator with a reheating stage, two closed feed-water heaters, a deaerator, two feed-water pumps, and a turbine with a high-pressure phase and three low-pressure stages. The minimum turbine load was set at 30% of the gross power. The power block operates with a maximum design temperature of 550°C, and it integrates an Air-Cooled Condenser (ACC) with a design dry ambient temperature of 30°C. Main design parameters of the CSP plant and the power block can be found in a previous study developed by the authors (Zurita et al., 2020).

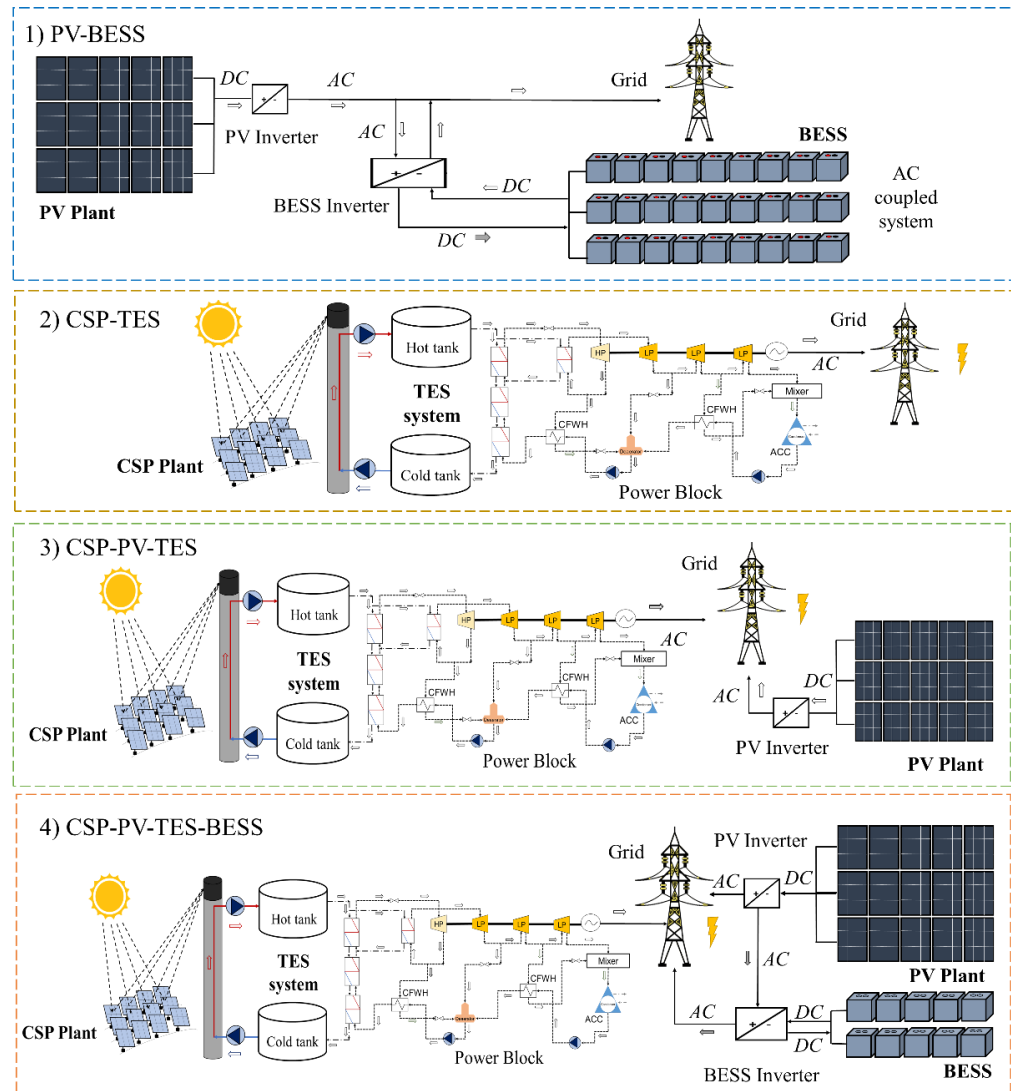


Figure 4-1: Technology combinations of storage and solar power plants considered in this study.

4.2.1. Locations

The study considers two locations in Chile that represent different solar resource conditions: Carrera Pinto (27.08° S, 69.93° W), and Santiago (33.50° S, 70.61° W), both with meteorological data from ground stations. The data includes measurements of Global Horizontal Irradiance (GHI), Direct Normal Irradiance (DNI), ambient temperature, relative humidity, and wind velocity with a 5-minute time resolution. Details regarding the meteorological stations can be found in (Zurita et al., 2020). Carrera Pinto shares the excellent solar resource conditions of Northern Chile, with a total annual DNI of 3462

kWh/m²-yr and a GHI of 2519 kWh/m²-yr, presenting extremely arid conditions and high clear-sky indexes throughout the year since it is in the Altiplano desert at 1640m above sea level (Escobar et al., 2015). In contrast, Santiago represents a site with a solar resource that can be comparable to other locations around the world, with yearly totals of DNI (2153 kWh/m²-yr) and GHI (1941 kWh/m²-yr) values, presenting a dry climate but a stronger variability and seasonality throughout the year (Escobar et al., 2015; Zurita et al., 2020).

4.2.2. Dispatch strategies

The Chilean electricity market is considered as a reference for the techno-economic analysis and multi-objective optimization. Usually, the generation companies negotiate long-term Power Purchase Agreements (PPA) with clients to secure an income from their operation. Among them, the regulated clients are supplied by the distribution companies, which must back the projected demand with PPAs that are granted through public tenders (Central Energía, 2020). The public power supply tenders in Chile aim to award energy supply blocks plus their associated power with a supply period typically set at 20-25 years. These power hourly blocks are commonly divided into three time bands (depicted in Figure 4-2) to deliver a yearly demand of GWh per year (Empresas Eléctricas A.G., 2019). Supply block “A” only includes the consumptions made between 00:00-07:59 h and 23:00-23:59 h (9 hours at night). Supply block “B” comprehends the period between 08:00-17:59 h (10 hours during daytime), and the supply block “C” represents the dispatch period between 18:00-22:59 h (5 hours in the evening). Following this, four dispatch strategies were considered by combining the supply blocks described above. Table 4-1 shows in detail the combinations made for each case. A fixed 100 MW_e dispatch power was chosen for all the cases.

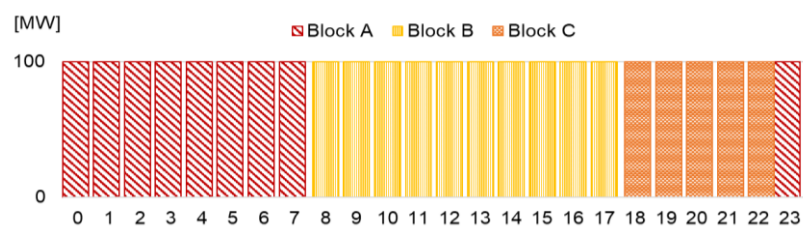


Figure 4-2: Typical hourly blocks implemented in electric tenders of Chile.

Table 4-1: Dispatch strategies chosen for each case of study.

Supply blocks	Time [h]	Demand hours per day [h]	Annual energy demand [GWh/yr]
A+B+C (baseload)	00:00-23:59	24 (baseload generation)	876
B+C	08:00-22:59	15 (daytime+evening)	547
A+C	00:00-07:59 18:00-23:59	14 (evening+night)	511
B	08:00-17:59	10 (daytime)	365

4.3. Cost Scenarios

Different cost scenarios of solar technologies and energy storage were employed to evaluate their impact on the optimal design configurations. This work's cost trends are based on a review of molten salt central-receiver CSP plants, solar PV, and lithium-ion battery costs. Literature data was used to develop a base case cost scenario for 2020, with a low and high-cost projection for 2030.

4.3.1. CSP costs

For the base case cost scenario, the investment and Operational and Maintenance (O&M) costs are based on the values reported in (CORFO, 2019; Dieckmann et al., 2017; Turchi et al., 2019). The cost functions used for the analysis are shown in APPENDIX C: APPENDIX FOR CHAPTER 4, and the reference values are described in detail in Table 4-2. Literature data and a learning curve approach were used to create high and low-cost scenarios for 2030. The learning curve method was implemented to generate the cost scenarios for the Balance of Plant (BoP), power block, tower, and receiver, while the remaining costs are based on future projections found in the literature. A learning rate of 10% was used for the high-cost scenario (Breyer et al., 2016; Feldman et al., 2016; Köberle et al., 2015; Turchi et al., 2019), and an average learning rate of 15% was implemented for the low-cost scenario (Breyer et al., 2016; Turchi et al., 2019). The cost data is based on the values and projections reported in (Breyer et al., 2016; CORFO, 2019; Dieckmann et al., 2017; Estela et al., 2016; Jorgenson et al., 2016; Pfahl et al., 2017; Turchi et al., 2019).

Table 4-2: Current and specific CSP cost scenarios data.

Description	Unit	Base case 2020	High cost 2030 (HC)	Low cost 2030 (LC)
<i>Investment costs</i>				
Heliostats field	USD/m ²	140 (CORFO, 2019)	120	100 (Pfahl, Coventry, Röger, Wolfertstetter, Vásquez-Arango, et al., 2017)
BoP & power block	USD/kW _e	1000 (Turchi et al., 2019)	900 (Turchi et al., 2019)	850 (Breyer et al., 2016; Turchi et al., 2019)
Storage	USD/kWh-t	22 (CORFO, 2019)	18 (Estela et al., 2016)	15 (Jorgenson et al., 2016)
Tower ref. cost	USD/m	90,000 (Dieckmann et al., 2017)	72,000 (Breyer et al., 2016; Dieckmann et al., 2017)	65,000 (Breyer et al., 2016; Turchi et al., 2019)
Receiver ref. cost	USD/kWt	125 (Dieckmann et al., 2017)	100 (Breyer et al., 2016; Dieckmann et al., 2017)	90 (Breyer et al., 2016; Turchi et al., 2019)
Contingency	%	5 (CORFO, 2019)	5	5
EPC	% direct cost	13 (Turchi et al., 2019)	10 (CORFO, 2019; Jorgenson et al., 2016)	10
<i>O&M costs</i>				
Fixed cost by capacity	USD/kW-yr	60 (CORFO, 2019)	45 (Jorgenson et al., 2016)	45
Variable cost by generation	USD/MWh-yr	3.5 (Turchi et al., 2019)	3.5	3.5

4.3.2. PV and BESS costs

The base case scenario for 2020 considers the inverter, balance of system (BoS), and O&M costs reported by NREL for utility-scale PV plants with a one-axis tracking system in (Fu et

al., 2018), while the PV module cost is based on the spot market price (PVInsights, 2020). These values were used as reference costs for a PV plant of 100MW, and they were adjusted to the nominal power of the PV plant following the cost functions described in APPENDIX C: APPENDIX FOR CHAPTER 4. Regarding the cost scenarios for 2030, the learning curve approach was applied to estimate the cost reduction in both PV module and inverter (considering the PV installed capacity projection for 2030 by IRENA (IRENA, 2019a)), while the other costs were assumed to remain the same by 2030. A learning rate of 20% was considered for both PV module and inverter costs (Breyer et al., 2016) in the high-cost scenario, while a learning rate of 24% was considered for the PV module and 20% for the inverter in the low-cost scenario (Fraunhofer ISE, 2020; Köberle et al., 2015). The cost data for the PV plant and BESS is described in Table 4-3.

Regarding the BESS, the base cost scenario is based on the capital breakdown costs reported by (Fu, Remo, et al., 2018). The reference values in Table 4-3 for the power conversion system, the BoS, installation, and the EPC overhead costs were adjusted in terms of the battery bank's energy-to-power ratio (APPENDIX C: APPENDIX FOR CHAPTER 4). The reduction was only applied to the battery pack price due to the scarce information about the detailed cost breakdown of the lithium-ion batteries into the future (BloombergNEF, 2019; W. Cole & Frazier, 2019; W. J. Cole et al., 2016; IRENA, 2017, 2019b; Zakeri & Syri, 2015). The high-cost scenario considers the 2030 value from the low-cost scenario reported by Cole and Frazier (Feldman et al., 2016), and the low-cost scenario is based on the price declared by BloombergNEF (BloombergNEF, 2019) for 2030. Additionally, the replacement cost is only introduced in operational years at which the lifecycles are exceeded, or when the calendar lifetime of the batteries is reached. If a replacement period superior to the calendar life were obtained, at least one replacement is introduced in the 20th year of the analysis. This means the batteries are replaced once or twice over a 30-year analysis period of the project. Finally, due to the DoD of the batteries, the battery system costs consider an oversize of the battery capacity of 16% (DoD of 84%) to compensate lifetime reasons, which is the standard in commercial BESS projects.

Table 4-3: PV and BESS cost scenarios data.

Description	Unit	Base case 2020	High cost 2030 (HC)	Low cost 2030 (LC)
<i>PV plant</i>				
Module price	USD/W _{dc}	0.28 (PVInsights, 2020)	0.19 (Breyer et al., 2016)	0.15 (Fraunhofer ISE, 2020; IRENA, 2019a)
Inverter cost	USD/W _{ac}	0.05 (Fu, Feldman, et al., 2018)	0.03 (Breyer et al., 2016)	0.02 (Breyer et al., 2016; IRENA, 2019a)
Electrical BoS ref. cost	USD/W _{dc}	0.08 (Fu, Feldman, et al., 2018)	0.08	0.08
Mechanical BoS ref. cost	USD/W _{dc}	0.13 (Fu, Feldman, et al., 2018)	0.13	0.13
Installation labor ref. cost	USD/W _{dc}	0.10 (Fu, Feldman, et al., 2018)	0.10	0.10
EPC overhead ref. cost	USD/W _{dc}	0.06 (Fu, Feldman, et al., 2018)	0.06	0.06
Developer overhead ref. cost	USD/W _{dc}	0.02(Fu, Feldman, et al., 2018)	0.02	0.02

O&M costs

Fixed O&M cost	USD/kW-yr	14 (Fu, Feldman, et al., 2018)	14	14
----------------	-----------	--------------------------------	----	----

*BESS**Capital cost*

Battery pack price	USD/kWh	209 (Fu, Remo, et al., 2018)	124 (Feldman et al., 2016)	62 (BloombergNEF, 2019)
Power conversion system cost	USD/kW	70 (Fu, Remo, et al., 2018)	70	70
Structural BoS ref. cost	USD/kW	20 (Fu, Remo, et al., 2018)	20	20
Electrical BoS ref. cost	USD/kW	75 (Fu, Remo, et al., 2018)	75	75
Installation ref. cost	USD/kW	60 (Fu, Remo, et al., 2018)	60	60
EPC overhead ref. cost	USD/kW	30 (Fu, Remo, et al., 2018)	30	30

O&M costs

Fixed O&M cost	USD/kW- yr	6.9 (Zakeri & Syri, 2015)	6.9	6.9
Variable O&M cost	USD/MWh	2.1 (Zakeri & Syri, 2015)	2.1	2.1

Replacement

Replacement cost	USD/kWh	139	83	41
------------------	---------	-----	----	----

4.4. Methodology

The plant models were developed in the Transient System Simulation Program (TRNSYS) to determine every technology combination's annual energy production. The TRNSYS model was coupled to MATLAB to compute the techno-economic indicators. Then, a surrogate model substituting the physical model was created. A multi-objective optimization problem was formulated to minimize the LCOE and to maximize the sufficiency factor. Finally, a multi-criteria decision-making method was implemented to select the best optimal solution among the Pareto front points. These steps are illustrated in Figure 4-3 and explained in detail below.

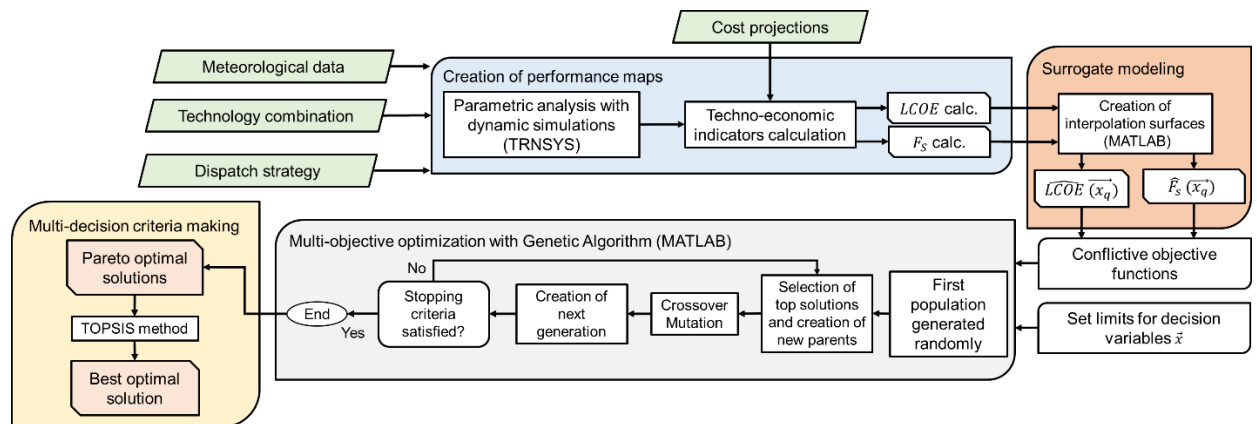


Figure 4-3: Scheme of the methodology followed for the multi-objective analysis.

4.4.1. Modeling and Simulation

Each section of the plant (the PV system, the battery bank, the CSP field, the power block, and the TES section) was modeled in TRNSYS. Each technological combination was simulated in a unique deck, and simulations were developed using a 5-minute time step. The systems' modeling is based on available components from the TRNSYS library and new models created by the authors. These models have been used and validated in previous works (Zurita et al., 2020; Zurita et al., 2018), where is described the assumptions regarding the modeling and control procedures that rule the systems operation. Therefore, only a summary of the models is described below.

The PV plant model considering a one-axis tracking is based on Type 190 of TRNSYS that introduces the inverter efficiency curve as input. The PV field was modeled with a scalable size in terms of the number of inverters (Zurita et al., 2018). The BESS model is based on a balance of State of Charge (SOC), which allows varying both power and energy capacities of the BESS, considering the DoD to obtain the minimum energy capacity (Zurita et al., 2018). The CSP plant model consists of the solar field, the central receiver, the TES tanks, and the power block. The heliostats field considers a field efficiency matrix in terms of the solar position, heliostat reflectivity, and soiling rate to calculate the receiver's incident power. The central receiver was based on a cylindrical tubular central receiver model, that calculates the thermal power absorbed by the HTF in the receiver, considering energy balances on a receiver tube element and including thermal losses (radiation, natural and forced convection) (Wagner, 2008). It also incorporates the modeling of a thermal capacitance that represents the receiver's thermal inertia to simulate the effects of intermittent solar irradiance (Zurita et al., 2020). The TES system was modeled using variable volume tanks with its respective energy losses (Type 39). The power block model consists of a polynomial multi-variable regression model that considers the nominal and off-design performance of the Rankine cycle. This model was employed to create a new type in TRNSYS (Zurita et al., 2020).

Regarding the plants' operating modes, it was used the previous one developed in (Zurita et al., 2020) which considers that the system must deliver a maximum rate power of 100 MW_e. Technological combinations that include the PV system have a priority to dispatch first the PV output. If the electrical output surpasses the 100 MW_e, a spillage of energy is produced, which may be used to charge the battery system, or it becomes dumped energy. In the hybrid plants, the CSP plant operates as a back-up of the PV, and the BESS acts as a back-up when the CSP-PV production is not enough to cover the demand. Controls and procedures that rule the TES and power block's operation are explained in detail in (Zurita et al., 2020; Zurita et al., 2018). For the rest of the technology combinations, the same operation controls developed for the hybrid plant were adapted. In the case of the CSP-TES plant, the TES system and the power block operate considering a null output of the PV plant; while for the PV-BESS plant, the charge and discharge of the batteries are controlled monitoring the PV

output. Lastly, the dispatch strategy profiles were implemented in TRNSYS using the Type 109. Dispatch strategies were introduced to the model as the profile demand.

4.4.2. Multi-objective optimization

A Genetic Algorithm (GA) was implemented to solve the multi-objective problem. GAs use evolutionary strategies based on the principals of natural selection and genetics to obtain a set of trade-off optimal solutions known as Pareto solutions (Burke & Kendall, 2014; MathWorks, 2020). This optimization algorithm has been frequently used to solve similar optimization problems (Abdelkader et al., 2018; Cui et al., 2017; Fadaee & Radzi, 2012; Starke et al., 2018). The multi-objective optimization in this work considers two objective functions: minimizing the LCOE and maximizing the sufficiency factor. The LCOE allows quantifying the cost per unit of energy produced throughout the lifetime of a power plant (IRENA, 2018). It is often used to compare the techno-economic performance of different technologies that present different operational and investment costs. The LCOE was estimated through discounted cash flows to present value following Eq. 4.2 (Guédez, 2016):

$$LCOE = \frac{CAPEX + \sum_{i=n_{oper}}^T \frac{OPEX(i)}{(1+WACC)^i} + \sum_{i=n_{oper}}^T \frac{C_{rep,BESS}(i)}{(1+WACC)^i}}{\sum_{i=n_{oper}}^T \frac{[E_{PV(i)} \cdot (1-DR_{PV})^i + E_{CSP(i)} \cdot (1-DR_{CSP})^i + E_{disch,BESS(i)} \cdot (1-DR_{BESS})^i] \cdot F_a}{(1+WACC)^i}} \quad (4.2)$$

where $CAPEX$ is the capital expenditures, $OPEX$ is the annual O&M cost, $C_{rep,BESS}$ is the annual replacement cost of the BESS, E is the annual energy production of the PV, CSP and BESS plant, DR is the annual degradation rate of each component of the plant, F_a is the availability factor set at 95%, the $WACC$ is the Weighted Average Capital Cost set at 7%, and T is the lifetime of the project (30 yrs). An annual degradation rate of 0.7% (Fu et al., 2018), 0.4% (Pfahl et al., 2017), and 1% were considered for the PV, CSP and BESS sections, respectively. Evaluating the degradation rate for every component of the plant allows capturing and analyzing the degradation effects of different components at the same time.

Additionally, the sufficiency factor (F_s) was defined following Eq. 4.3, which allows to measure the overall energy production of the hybrid plant and the demand fulfillment for

different dispatch strategies, and it is defined as the ratio between the annual production (E_{annual}) and the annual demand in terms of energy (D_{annual}):

$$F_s = \frac{E_{annual}}{D_{annual}} \cdot F_d \quad (4.3)$$

The optimization problem was formulated as follows:

$$\text{Min. } f_1(\vec{x}) = LCOE(\vec{x}),$$

$$\text{Max. } f_2(\vec{x}) = F_s(\vec{x}),$$

$$\text{Subject to: } x_j^l \leq x_j \leq x_j^u, \quad j = 1, 2, \dots, N_{var} \quad (4.4)$$

where $f_1(\vec{x})$ and $f_2(\vec{x})$ are the two objective functions and \vec{x} is a vector of independent decision variables with a length of N_{var} . This optimization problem is only subject to the lower (x_j^l) and upper (x_j^u) boundaries of the decision variables, which delimit the solution space. Regarding the decision variables, the \vec{x} vector is different depending on the technology combination evaluated, as Table 4-4 indicates. Hence, decision variables can be the nominal size of the PV power plant (P_{PV}^{nom}), the Solar Multiple (SM) of the CSP plant, the size of the TES system in terms of hours (TES_h), the energy capacity of the battery bank (S_{BESS}) and the power rate of the BESS' inverter (P_{BESS}^{inv}).

Table 4-4: Decision variables for every optimization problem, depending on the technology combination.

Technology	N_{var}	Decision variables (\vec{x})
PV-BESS	3	$P_{PV}^{nom}, S_{BESS}, P_{BESS}^{inv}$
CSP-TES	2	SM, TES_h
CSP-PV-TES	3	P_{PV}^{nom}, SM, TES_h
CSP-PV-TES-BESS	5	$P_{PV}^{nom}, SM, TES_h, S_{BESS}, P_{BESS}^{inv}$

4.4.3. Surrogate model

At the time of solving the optimization problem, the GA requires a high amount of simulations that are high-costly in computational time since thousands of generations could be needed to meet the convergence in the optimal solutions. To address this problem, a surrogate model was created to substitute physical modeling. The surrogate model was

created following the methodology developed by (Starke et al., 2018). First, a parametric analysis in TRNSYS varying the design variables within the ranges reported in Table 4-5 was performed for every case of study, then, the LCOE and sufficiency factor were calculated, and an interpolation surface was built to create the surrogate models with the calculated values using the *griddedInterpolant* function in Matlab. The surrogate models were validated with a random sample of 10% of the simulations within the original decision-variable space. Results of the validation indicated a good agreement of the surrogate models since they presented a dispersion lower than $\pm 3\%$ with respect to the simulated results, and Normalized Root-Mean-Square Deviations between 0.5% and 0.9%.

Table 4-5: Variables in parametric analyses performed for every technology combination and dispatch strategy.

Technology combination	N_{sim}	P_{PV}^{nom} [MW]	SM [-]	TES_h [h]	S_{BESS} [MWh]	P_{BESS}^{inv} [MW]
CSP-PV-TES-BESS	48,510	[0:250]	[0.4:3.0]	[2:18]	[0:500]	[0:100]
CSP-PV-TES	6,171	[0:300]	[0.4:3.6]	[2:18]	-	-
CSP-TES	561	-	[0.4:3.6]	[2:18]	-	-
PV-BESS	4,655	[50:500]	-	-	[0:1500]	[0:100]

4.4.4. Optimization parameters and decision-making process

The multi-objective optimization problem was solved using the *gamultiobj* algorithm in Matlab, which uses a variant of Non-Dominated Sorted GA-II (Mathworks, 2020). The optimization parameters such as the population size, the number of generations, the tolerance of the fitness values, were adequately set from default values, presented in Table 4-6. Finally, the Technique for Order of Preference by Similarity to Ideal Solution (TOPSIS) algorithm was implemented to select the best solution among the set of Pareto-optimal solutions. This method allows choosing a point with the better fitness considering the lower minimum geometric distance from the ideal solution (lowest LCOE and highest F_s) and the highest geometric distance from the non-ideal point (highest LCOE and lowest F_s). This algorithm

has been frequently used to select the final optimum design point in similar optimization problems (Cui et al., 2017; Nasruddin et al., 2019).

Table 4-6: Multi-objective optimization parameters.

Parameter set	Value
Solver	<i>gamultiobj</i> of Matlab
Population size	600
Crossover fraction	0.8
Pareto fraction	1
Function tolerance	1×10^{-4}
Maximum stall generations	100
Maximum number of generations	3000

4.5. Results and Discussions

This section describes the results obtained for different cases of study, which include four technology combinations (PV-BESS, CSP-TES, CSP-PV-TES, and CSP-PV-TES-BESS), four dispatch strategies (baseload, blocks B+C, blocks A+C, and block B), and three cost scenarios (base case for 2020, high and low-cost for 2030) for two locations in northern Chile (Carrera Pinto and Santiago). In first instance, a base case of study is considered in Carrera Pinto with the 2020's costs to evaluate the dispatch strategy's influence on the Pareto curves of all the technology combinations. The optimal configurations along the Pareto fronts are also studied to evaluate the design variables being selected in the multi-objective optimization. Subsequently, it is analyzed the impact of the high and low-cost scenarios for 2030 on the Pareto curves of the technology combinations, and finally, a comparative analysis among the Pareto curves obtained in Carrera Pinto and Santiago (two locations with different solar resource) is performed, considering all the technology combinations in baseload and Block A+C.

4.5.1. Pareto front results

Figure 4-4 shows the Pareto fronts obtained for each technology combination and dispatch strategy considering the base cost scenario of 2020 in Carrera Pinto (DNI of $\sim 3400 \text{ kWh/m}^2\text{-yr}$). The optimal points selected by the TOPSIS algorithm among the Pareto solutions are also illustrated in these graphs.

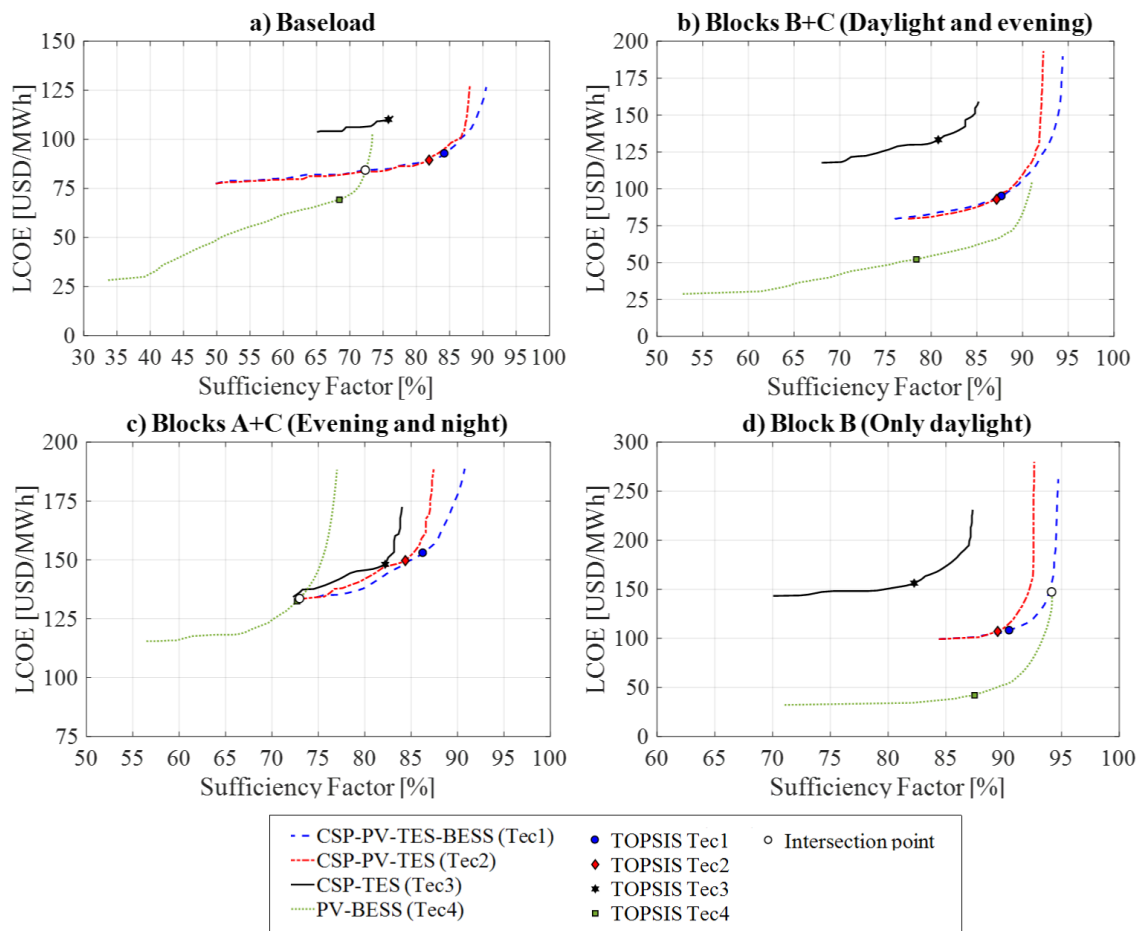


Figure 4-4. Pareto fronts for every technology combination and the base cost scenario of 2020 to provide energy in a) baseload, b) Block B+C (daytime and evening), c) Block A+C (evening and night), d) Block B (daytime) in Carrera Pinto.

Regarding the comparison between dispatch strategies, the lowest LCOEs are obtained for baseload dispatch, in which the plant production is not limited to specific hourly blocks. In contrast, the highest LCOEs are obtained for the block A+C, because covering

the night dispatch requires an investment in larger capacities of storage which leads to higher costs. The highest sufficiency factors are also achieved in the block B and B+C, mainly because these dispatch strategies only consider supplying energy during 10 daylight hours (block B) or including 5 hours in the evening (block B+C); therefore, the dispatch profile perfectly matches with the solar resource availability, and sufficiency factors up to 95% can be achieved.

4.5.2. Comparison between technology combinations

Figure 4-4 exhibits a clear advantage of the PV-BESS plant in LCOE for all the dispatch strategies; however, the PV-BESS plant obtained the lowest sufficiency factors, except on blocks B and B+C. It is also noticed that the hybrid CSP-PV plants (with and without BESS) present more favorable optimal solutions in terms of cost and demand fulfillment than the standalone CSP-TES plant, due to the PV plant's hybridization allows reaching optimal solutions with higher sufficiency factors and lower LCOEs. In addition, the optimal solutions of the CSP-PV-TES-BESS and the CSP-PV-TES plants are quite similar, and the main difference between them relies on the possibility of including a battery bank. The BESS inclusion allows obtaining design configurations with higher sufficiency factors (between 1-5%) than the CSP-PV-TES plant but with similar LCOEs.

The graphs also show that the Pareto curve of the PV-BESS plant intersects with the fronts of the hybrid CSP-PV-TES-BESS plant in almost all the dispatch strategies. Before this point, the PV-BESS plant presents the optimal solutions with the lowest LCOEs among the technology combinations. The intersection point varies with the dispatch strategy presenting different optimal configurations. For instance, the optimal configuration of the PV-BESS plant that intersects with the hybrid CSP-PV-TES-BESS plant's Pareto front in baseload (Figure 4-4a) considers a 350MW PV plant with a 1000MW/ 75MW BESS (~13h of storage in batteries), while the configuration of the hybrid plant includes a 150MW PV plant and a CSP plant with 1.4 of SM and 10h of TES without batteries. Both technology combinations can provide a sufficiency factor of 72% with an LCOE of 84 USD/MWh, with highly similar installation costs of 5.01 USD/W and 5.26 USD/W, respectively. In these cases, the choice of a technology

combination will depend on the financial conditions of the project. Financial structures play a crucial role in the cost-effectiveness of each technology combination, which are given by the debt conditions (the equity-debt ratio, the debt rate), the project lifetime, the depreciation, among others (Lilliestam & Pitz-Paal, 2018). The variation of these conditions is not within the scope of this study, but it is worth mentioning that they also play a critical role on obtaining competitive internal interest rates of the projects and lower LCOEs.

This decision will also depend on the selection of a sufficiency factor. After the intersection point, the PV-BESS plant starts increasing its cost without benefiting the sufficiency factor, while the plants including a CSP section become a more competitive solution since they can achieve higher sufficiency factors at a similar cost than the PV-BESS plants, especially in baseload and the blocks A+C. In this manner, the PV-BESS plant represents the best fit to provide energy during daylight hours that require short storage durations (<5h) with the highest sufficiency factors (between 90-95%), providing trade-offs with the lowest LCOEs (between 84-100 USD/MWh and 52-144 USD/MWh in the Blocks B+C and Block B). In contrast, if sufficiency factors above 80% are required in baseload and the block A+C, only the hybrid CSP-PV plants can fulfill these requirements, providing LCOEs between 87-120 USD/MWh and 138-177 USD/MWh, respectively. This is because the PV-BESS plant presents sufficiency factors up to 75% due to technical limitations concerning the amount of energy that can be stored, while the CSP-TES plant can only reach a demand fulfillment up to 75-85% in this location.

4.5.3. Design configurations along the Pareto curves

Figure 4-5 illustrates the variation on the design configurations along the Pareto curve of the hybrid CSP-PV-TES-BESS and the PV-BESS plants for the base case scenario of 2020 in Carrera Pinto. These technology combinations were selected since they present the highest sufficiency factors and the lowest LCOEs, respectively. For the hybrid CSP-PV-TES-BESS plant (Figure 4-5a), large PV plant sizes (above 100MW) are selected in all the dispatch strategies except on the block A+C. This occurs because the PV plant's dispatch is prioritized in the profiles that include supply blocks during the daytime. In this case, the CSP plant only

operates during the day to charge the molten salts tanks, and the stored energy in the TES is mainly used during the non-sunlight hours to operate the power block. In consequence, the smallest SMs (between 0.4-0.9) and TES sizes (between 2-6h) are selected in the block B+C and B since they do not require long storage durations. In contrast, the block A+C present design configurations with small PV plants (25-50MW) and large CSP plants (SM: 2-3, and TES sizes: 12-18h), mainly because the PV plant's output is only required to supply the parasitic consumptions of the CSP plant and to charge the BESS during the day to be used at the evening and night.

In the case of the PV-BESS plant (Figure 4-5b), both PV nominal power and BESS capacity gradually increase in all the dispatch strategies as higher sufficiency factors are reached, but the demand fulfillment differs with the dispatch strategy considered. For instance, in the blocks B and B+C, sufficiency factors above 85% can be achieved, but for baseload and the block A+C, the maximum demand fulfillment is up to 73 and 77%, respectively. In the block A+C, sufficiency factors above 70% can be reached with PV configurations above 200 MW, BESS sizes above 1200 MWh, and inverter power rates of 100 MW. Nevertheless, in this dispatch strategy, the BESS's inverter power rate plays a critical role, since there is a limit in the energy that can be stored throughout the day that is given by the BESS's inverter power rate (maximum 100MW_{AC}). This power limitation does not allow exploiting the extra energy surplus of the largest PV plants ($>200\text{ MW}$). As consequence, there is a limit from which if larger PV and BESS sizes are added, the LCOE highly rises without benefiting the sufficiency factor.

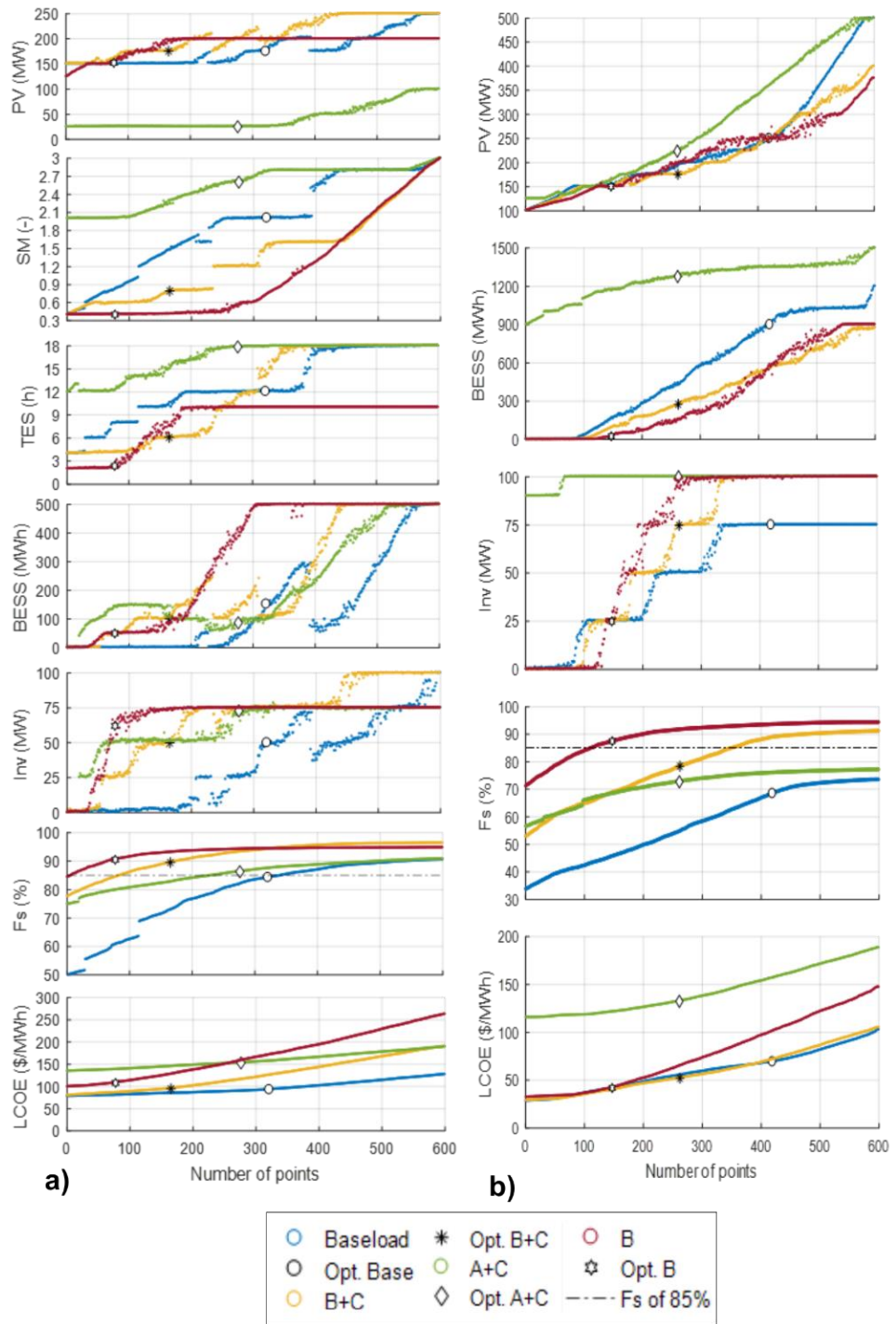


Figure 4-5. Design configurations along the Pareto curve of the a) hybrid CSP-PV-TES-BESS plant and b) PV-BESS plant, for all the dispatch strategies, considering the base case cost scenario of 2020 in Carrera Pinto.

Figure 4-5 also evidences that the solutions with the minimum LCOE present smaller plant configurations with non or small storage size when compared against the optimal solutions selected by TOPSIS, which considers medium/large amount of storage (TES and BESS). For instance, the minimum LCOE solution of the PV-BESS and CSP-PV-TES-BESS plants for the baseload achieve 33% and 50% of demand fulfillment, respectively, with an LCOE of 28 USD/MWh and 77 USD/MWh, presenting a lack of availability for this dispatch strategy. Conversely, the TOPSIS solutions reach 68% and 84%, with LCOEs of 69 USD/MWh and 93 USD/MWh, respectively. These results indicate that the concept of designing solar power plants for only achieving the minimum LCOE (which is frequently used in the industry and literature) may not be the most appropriate when a certain level of supply wants to be guaranteed.

In this manner, more suitable and dispatchable solar power plants configurations could be obtained considering the sufficiency factor as an objective function, in detriment of having a moderate higher LCOE. It also becomes evident that an investment on energy storage systems is required to cover the evening and night dispatch, such as baseload and the block A+C. For these dispatch strategies, the solutions with this approach consider large BESS capacities between 900-1200 MWh/75-100 MW for the PV-BESS plant, while the CSP-PV plants include large capacities of TES (13-18h) and small BESS sizes (100-150 MWh/50-75MW).

4.5.4. Cost reduction scenarios

When the cost projections for 2030 are considered, the Pareto curves of every case of study are displaced further down with respect to the base case scenario, and all the tendencies described above remain similar. Figure 4-6 illustrates the Pareto curves obtained for the hybrid CSP-PV-TES-BESS and the PV-BESS plant for all the cost scenarios in Carrera Pinto. It is observed that the most significant reduction in the LCOE occurs for baseload and the block A+C. The 2030 cost reductions are also more favorable for the PV-BESS plant, reaching a larger LCOE decrease at higher sufficiency factors, mainly because the costs projections considered for the batteries are aggressive. When the TOPSIS optimal solutions are compared, it is observed that the LCOE of the PV-BESS plant decreased 39% in baseload and 45% in the Block A+C in the low-cost scenario (with respect to the base case), while in

the high-cost scenario, the average decrease is around 25% in both dispatch strategies. For the CSP-PV-TES-BESS plant, a LCOE reduction of 24% (baseload) and 28% (A+C block) is achieved in the low-cost scenario, while in the high-cost scenario the LCOE is only reduced 16% in both dispatch strategies. In the cases of both block B and B+C, the LCOE reduction for the LC and HC scenarios is about 27% and 20%, since these dispatch strategies include small capacities of BESS within their optimal configurations.

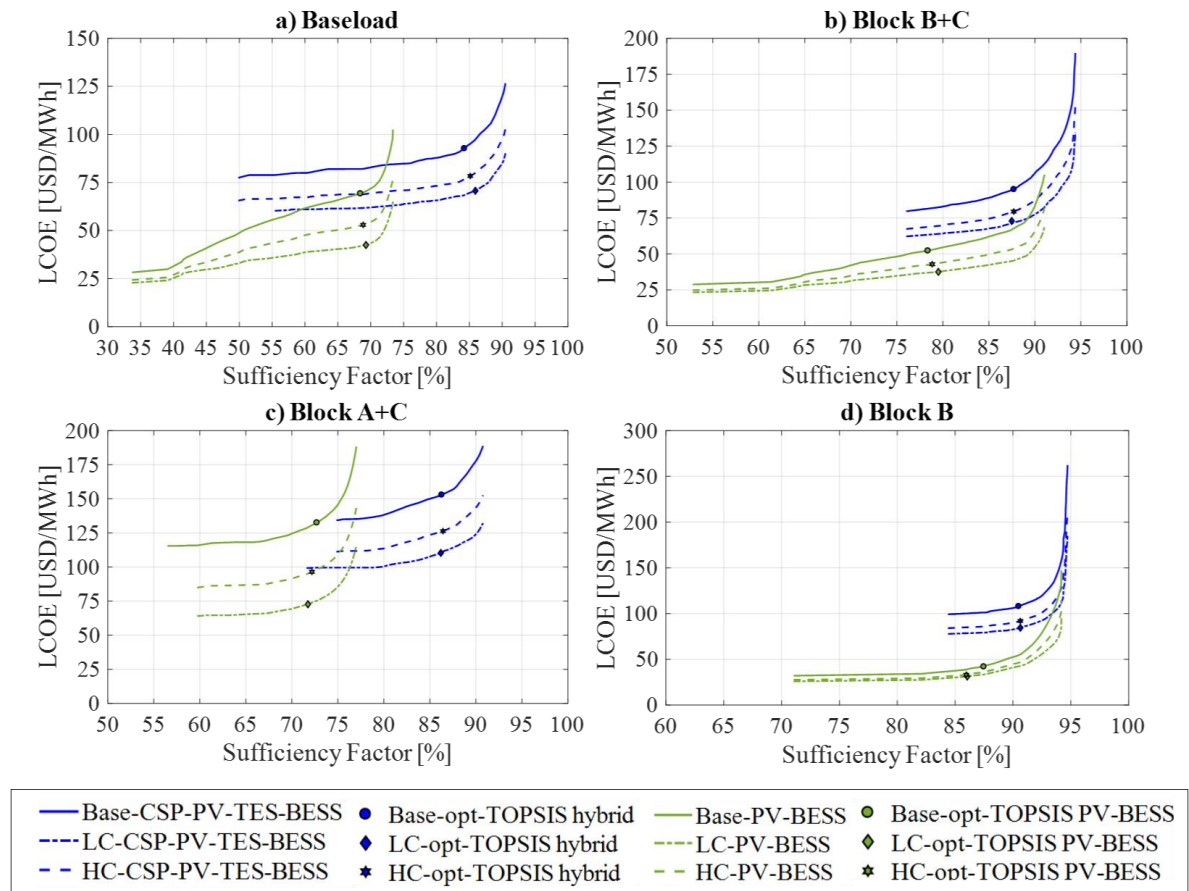


Figure 4-6. Pareto fronts for every technology combination and cost scenarios to provide energy in a) Baseload, b) Block B+C (daytime and evening), c) Block A+C (evening and night), d) Block B (daytime) in Carrera Pinto.

These results evidence that the PV-BESS plant continues to be the most competitive option in terms of LCOE when the 2030 cost projections are considered in all the dispatch strategies, while the hybrid CSP-PV-TES-BESS plant provides the highest sufficiency factors. In the case of the hybrid CSP-PV-TES-BESS plant, a significant LCOE reduction is

observed with the cost projections, however, their impact is lower than in the PV-BESS plant. The CSP cost scenarios implemented in this work for 2020 and 2030 are conservative, mainly because the information reported in the literature does not accurately represent the current tendencies in the industry, and the cost data is often confidential among the players in the CSP sector. Current trends evidenced in different CSP projects around the world (DEWA IV project in Dubai was awarded a PPA of 73 USD/MWh (Lilliestam & Pitz-Paal, 2018) and installation costs of molten salt towers in China (Turchi et al., 2019) were around 3300-4900 USD/kW) indicate that the CSP industry is betting on more aggressive short-term future projections, being able to estimate that these costs could be achieved even before 2025. In this context, a further reduction could be achieved considering a significant enhancement in the supply chain of the CSP technology, and an increase of the suppliers and the number of projects worldwide which will allow to push forward its competitiveness, mainly in long-duration storage applications (>12h) such as baseload and night dispatch.

4.5.5. Location and solar resource conditions impact

Figure 4-7 illustrates the variation on the Pareto curves for two technology combinations (the hybrid CSP-PV-TES-BESS and the PV-BESS plants) considering the low-cost scenario of 2030 in two locations: Carrera Pinto (CP - DNI of ~ 3400 kWh/m²-yr), and Santiago (SG - DNI of ~ 2100 kWh/m²-yr). In general, it is observed that the Pareto fronts of all the technology combinations in SG present lower sufficiency factors and higher LCOEs than in CP, especially the plants including a CSP section. This occurs because the CSP performance is strongly affected by the DNI levels and solar resource variability, producing less energy (especially in winter season) and reducing its ability to deliver overnight storage. The evident lower levels of DNI in SG cause a decrease of 20-30% in the sufficiency factors of the hybrid CSP-PV and CSP-TES plants with respect to CP. In contrast, the PV-BESS plant in SG only decreases 5-10% its sufficiency factors when compared to the CP location, mainly because the reduction in the GHI levels in SG is less significant than in the DNI.

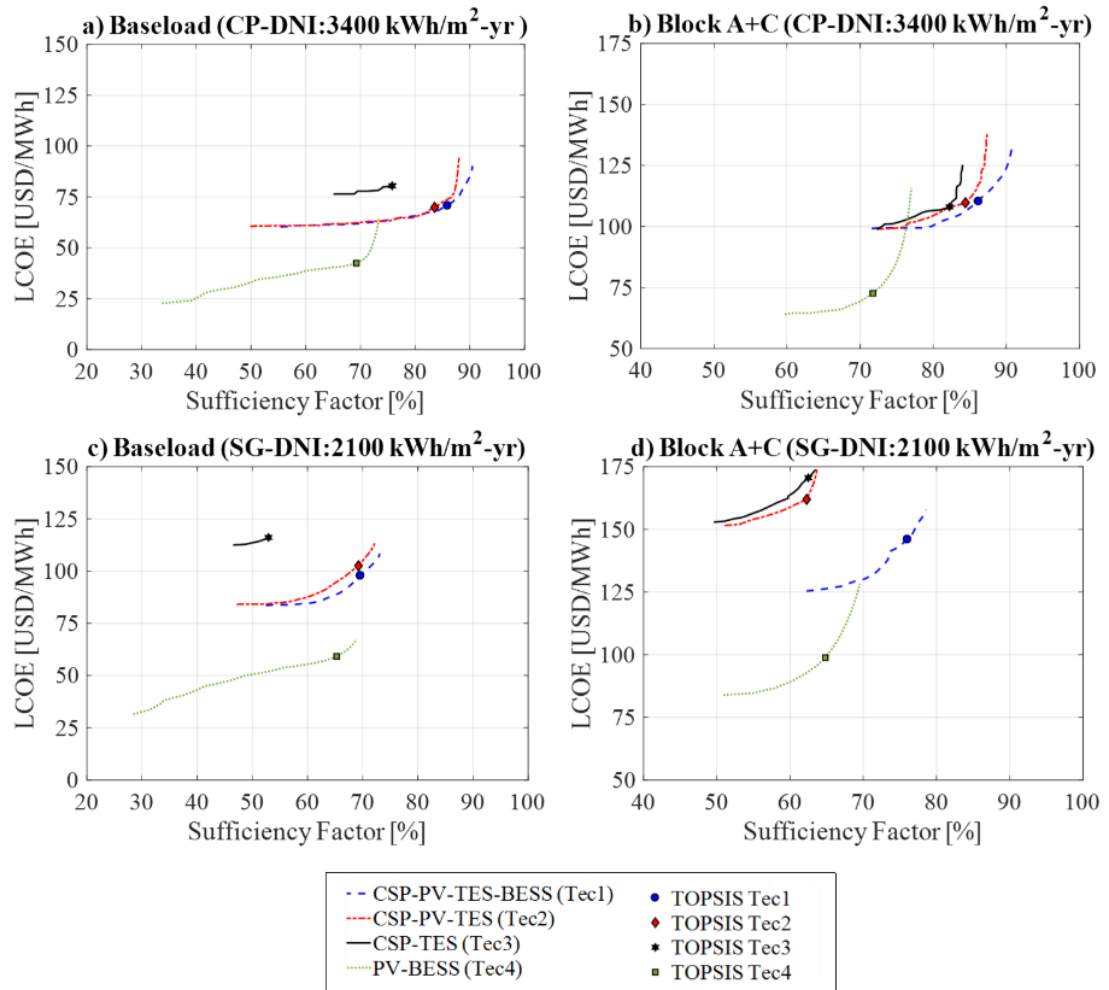


Figure 4-7. Pareto curves for baseload and night dispatch (Block A+C) considering two solar resource conditions: (a)-(b) in Carrera Pinto (DNI of ~ 3400 kWh/m²-yr), and (c)-(d) in Santiago (DNI of ~ 2100 kWh/m²-yr) for the low-cost scenario of 2030.

For baseload, the PV-BESS plant becomes the most suitable technology combination in locations that present DNI values around 2000 kWh/m²-yr, due to the CSP technology losses its advantage of achieving large sufficiency factors ($>75\%$) under these conditions. In contrast, the hybrid CSP-PV-TES-BESS's Pareto-front in SG shows a different tendency than the hybrid CSP-PV-TES plant in the block A+C, which usually were quite similar. This variation is related to the optimal design configurations. The Topsis optimal solution in CP includes a hybrid plant where the BESS acts as a back-up of the CSP-PV, with a small PV

plant (75MW), a medium CSP sections (SM of 2 and 15h of TES) and small to medium BESS (500MWh/75MW), but in SG, the CSP supports the PV-BESS generation, since the TOPSIS solution includes a large PV plant of 250MW, a CSP plant with 1.6 of SM and 6h of TES, and a large BESS with 1000MWh/100MW. In this case, a bulky battery bank is preferred to provide the hours of storage that the TES cannot supply due to the detriment in the CSP's generation. Under these conditions, the results obtained in SG emphasize the competitiveness that the batteries can provide over the TES for long-duration storage applications (>12h) in locations with less favorable solar conditions, reaching almost 70% of sufficiency factor with the PV-BESS plant in baseload, and almost 80% with the hybrid CSP-PV-TES-BESS plant in the block A+C.

4.6. Conclusions

A comprehensive analysis evaluating the dispatch strategy's impact on the optimal design configurations of different solar and storage combinations was carried out. The study considered four technology combinations: a solar PV plant with batteries, a CSP plant with TES based on a molten salt central receiver system, a hybrid CSP-PV plant with TES, and a hybrid CSP-PV plant with TES and batteries. Four dispatch strategies with different profiles were also considered, with three cost scenarios based on current values and future projections for 2030, and two locations in Chile to represent different solar resource conditions. A multi-objective optimization approach with a genetic algorithm was followed to obtain the set of optimal configurations of each system, showing the trade-off curves between minimizing the LCOE and maximizing the sufficiency factor. Main conclusions which provide the summarized findings of this work are presented as follows:

- The lowest LCOEs were obtained in baseload for all the technology combinations, followed by the dispatch strategies with profiles only during sunlight hours or with few hours in the evening (Block B and B+C). In contrast, the highest LCOEs were achieved in the Block A+C, that only considers evening and night hours.
- The PV-BESS plant provides the lowest LCOE optimum solutions in all the cases analyzed, but its ability to guarantee the energy supply varies with the dispatch strategy considered. This work indicates that PV-BESS plants are the most competitive technology when covering daylight and evening dispatch (<5h of

storage), since sufficiency factors above 90% can be reached. In contrast, for baseload and night dispatch, the PV-BESS configurations that meet levels of 60-70% of sufficiency present oversized PV plants (>200MW), with 10-12h BESS (800-1300 MWh) and power rates of 75-100MW.

- The hybrid CSP-PV plants (with or without BESS) are the most competitive option when long duration storage is required (>12h), like in baseload and night dispatch. They represent the only option that can reach sufficiency factors above 85% with moderate costs in these dispatch strategies. For baseload (in CP), the optimum design configurations consist of large PV plants (150-200MW) with medium CSP plants (2.0 of SM and 12h of TES) and small BESS (100-300 MWh/25-75MW), while the optimum solutions for the night dispatch (Block A+C) present small PV plants (25-50MW) with large CSP sections (SMs between 2.6-3.0, 15-18h of TES) and small BESS (100MWh/50-75MW).
- The concept of designing solar power plants to achieve the minimum LCOE is frequently used in the industry and in the literature. This work shows that this approach may not be the most appropriate when a certain level of supply wants to be guaranteed, especially for baseload and night dispatch. The minimum LCOE solutions usually consider design configurations that only reach 30-50% of sufficiency factor, while the optimal solutions obtained in the multi-objective optimization integrate storage systems as a crucial part to achieve sufficiency factors above 70%. These types of plants (despite of being a little more expensive due to the investment on storage) can provide an added value of dispatchability and energy availability, which are features that could increase the incomes of the project through other remuneration mechanisms such as ancillary services and flexibility.
- When the 2030 cost projections are considered, the impact on the reduction of the LCOE is more significant in the PV-BESS plant than in the hybrid CSP-PV-TES-BESS plant, mainly because the cost scenarios implemented for the BESS are aggressive, while for the CSP plant are more conservative (based on the available literature). In this context, if current trends evidenced in the CSP industry were considered (lower installation costs of the CSP technology like those reported in China, and more favorable financial conditions for the projects), lower LCOEs could

be achieved in the short-term future (even before 2030), which would enhance the competitiveness of the CSP technology, mainly in long-duration storage applications (>12h) such as baseload and night dispatch.

- In locations endowed with high solar resource ($\text{DNI} > 3000 \text{ kWh/m}^2/\text{yr}$), the optimal solutions for long-duration storage applications (>12h) consider hybrid CSP-PV plants in which the BESS primarily acts as a back-up of the CSP-PV plant, with the TES providing most of the overnight storage. In contrast, the PV-BESS plant becomes the most suitable technology combination under less favorable solar resource conditions ($\text{DNI} \sim 2000 \text{ kWh/m}^2/\text{yr}$). This occurs due to the CSP performance is strongly affected by the decrease in the DNI levels, reducing its cost-effectiveness to provide long duration storage. Because of this, large BESS capacities are preferred in the optimal solutions of the hybrid CSP-PV plants, with medium CSP sections supporting the PV-BESS plant. These results highlight the competitiveness that the BESS can provide over the TES under these conditions.

5. CONCLUSIONS

This thesis presents a methodology to identify the set of optimal design configurations of solar power plants integrated with storage, in particular, PV, CSP, TES systems, BESS, and hybrid CSP-PV plants, according to a specific dispatch strategy and location in Chile. Specific objectives of this thesis have been answered in Chapters 2, 3, and 4, respectively, through the publication of three original scientific articles. This work provides a meaningful contribution to the state-of-art of modeling, simulation, and techno-economic analysis of hybrid CSP-PV-TES-BESS plants and multi-objective optimization of solar power plants integrated with storage.

The physical and techno-economic model created for the hybrid plant allows evaluating its performance, providing a new insight into its techno-economic viability, and the design configurations required to integrate both TES and BESS to achieve a synergetic operation. The analysis performed for the hybrid CSP-PV-TES-BESS plant in Paper-I (Chapter 2) shows that minimum LCOE design configurations do not include batteries due to their high investment costs, however, under a cost reduction between 60-90% of the battery pack price, both TES and BESS can provide an integrated operation for fulfilling a baseload demand. It also shows that the integration can provide sufficiency factors above 80%.

It is also discussed and quantified the impact of time resolution on the hybrid plant's energy production estimation in Paper-II (Chapter 3). A new physical model of a molten salt central receiver that integrates a thermal capacitance to capture the effects of DNI variability and the thermal inertia is developed, that allows evaluating the solar variability's influence on the dispatchability and control procedures of the hybrid plant at a component level (PV, CSP-TES, and BESS). In this concern, this work identifies the need to capture the effects of the solar irradiance variability on the performance of the solar and storage systems more realistically by performing sub-hourly simulations and implementing all the control procedures required.

In the PV plants case, their production is highly susceptible to variations in the solar irradiance. The BESS are flexible systems that can respond very quickly to changing conditions, but the CSP plants present more constraints due to steam turbines generators' operational limits, which include minimum running levels and start-up, ramp, and shut-down

procedures of the systems. These control procedures rule the steam turbines' operation in the power block and the central receiver in the CSP plant to protect them from stress and fatigue effects and avoid major failures. This work shows how the CSP plant's operation is one of the most critical points during the simulation since the thermal power generation does not follow the solar irradiation changes, mainly due to the thermal inertia provided by a large amount of molten salts and pipes within the system. The inclusion of the thermal systems' operational constraints represents a complex process in the modeling phase; however, this thesis's results highlight that the thermal systems' operation prediction is the most influenced by the time resolution, such as the CSP plant's central receiver. For instance, a high overestimation of the CSP's plant annual production between 14-15% is obtained with an hourly time resolution (with respect to the 1-min results), which leads to an overestimation of the annual production of the hybrid plant (and underestimation of the LCOE) between 2-6%. In this manner, this work aims to emphasize the importance of choosing an appropriate time step when modeling solar power plants with storage, first identifying the simulation's purpose, to evaluate how much accuracy is expected from the results, and to establish the computational time constraints, if any.

The advantages and drawbacks of using a time resolution along the different stages of a hybrid CSP-PV plant's project development value chain are also discussed in this thesis. Concerning this, the thesis highlights that the new developments implemented in the models could support the process of establishing standard design criteria for the modeling and simulation of solar power plants, especially in the CSP industry, in which the standardization of guidelines to simulate CSP plants is still a work in progress. Besides, the quantification of the time resolutions' impact on the energy production estimation provides valuable information for the actors involved in the early phases of a project pre-design and the Engineering and Procurement and Construction (EPC) stage in which the project's detail engineering is performed.

Furthermore, this research implements a multi-variable and multi-objective techno-economic approach for obtaining the optimal design of different technology combinations in Paper-III (Chapter 4). Relevant information concerning under which conditions a technology combination is preferable over another, and a quantification of the influence that dispatch strategy, solar resource conditions, and cost projections have on the

competitiveness of storage-integrated technology options in terms of cost and demand fulfillment is provided in this work. This section also provides a new insight concerning the need to include the sufficiency factor as an objective function in the techno-economic design optimization of energy projects. In this concern, this research establishes that designing solar power plants with storage to achieve only the minimum LCOE may not be the most adequate when a certain supply level needs to be guaranteed.

This thesis addresses some of the issues currently being discussed in the electricity generation context. The dramatic cost reduction that renewable energies have experienced in the last years has led to this market's imminent growth worldwide. In Chile's case, the largest part of the renewable energy installed capacity consists of solar PV or wind that present the lowest installation costs and LCOEs, even below the fossil fuels range. Nonetheless, the massive deployment of variable renewable energies has created new electric sector issues due to the variability and instability of these natural resources. Thus, the energy transition scenarios being studied are starting to recognize the efforts that must be done to increase the flexibility and adaptability of the electric grid to guarantee the minimum standards of security, reliability, and quality that the electric supply requires. In this context, the solar projects endowed with capacities to manage their production on-demand will start playing a more crucial role in the future. The discussion on this topic has become more urgent now that a decarbonization plan has been signed to phase out all the coal power plants in Chile by 2040. In this context, solar technologies endowed with capacities to manage their production on-demand will start playing a more critical role in the future.

Based on this research, the PV-BESS integration at utility-scale represents the most competitive option in terms of costs in most of the scenarios studied. However, the CSP-PV hybridization with TES and BESS is the most promising option in cases where a high supply sufficiency is required, such as in baseload and night dispatch. These results highlight the importance of recognizing supply sufficiency as one of the features that new energy projects must-have. In this regard, the capability of the plants to provide high sufficiency factors should be properly encouraged through new policies and regulations of the electric markets and the new auctions that award long-term energy contracts such as PPAs. In Chile, energy auctions are currently designed to incentive the entry of projects that provide the lowest

electricity generation costs. This is a mechanism used to ensure that distribution companies will procure power at the least possible cost for retail consumers; however, it also results in installing more inefficient power plants that, by cost optimization, do not include storage capacities (being unable to provide dispatchability).

Including the supply sufficiency as a relevant factor in new auctions will incentive the deployment of storage systems and dispatchable technologies to the electric system. These changes are important to ensure well-functioning electricity markets in the future. On one side, the BESS does not have charge or discharge restrictions, and they can be implemented to provide a fast response to variations in the electric supply. In contrast, CSP plants and hybrid CSP-PV plants offer constant energy generation throughout non-sunlight hours integrating storage systems such as thermal storage, batteries, or even both. In the case of CSP technology, this thesis's results confirm that hybrid CSP-PV plants present more favorable optimal solutions than the standalone CSP-TES plants since they can provide larger capacity factors at similar costs. Nonetheless, the CSP technology's cost-effectiveness is studied employing conservative cost data found in the literature, mainly because CSP industrial actors are very reserved with providing their own operational and cost data for publication with academic purposes. In this context, the challenges of CSP technology in the future are related to achieving further cost reductions. This requires a significant enhancement in the supply chain and an increase of the suppliers and installed capacity worldwide to push forward its competitiveness, mainly in long-duration storage applications (>12h) such as baseload and night dispatch.

This thesis also emphasizes that plants, including a CSP-TES section, are only competitive under favorable solar conditions, like those shared in northern Chile. In contrast, the integration of large-scale battery banks takes the lead in locations with less favorable solar conditions (DNI values around 2000 kWh/m²-yr), which occurs because the CSP plants lose their advantage of achieving large sufficiency factors (>80%) under these conditions. In comparison, the PV plants integrated with BESS can provide almost 70% of sufficiency factors in long-duration storage applications (>12h) at the lowest LCOEs.

Conclusively, this research shows that CSP technology integrated with TES systems, the PV-BESS plants, and the hybrid CSP-PV plants are all valid options to be part of the set of solutions that face the electric production dispatchability problem. However, energy policy

creators and decision-makers such as ministries and government entities should encourage flexibility and dispatchability as relevant features. This can be achieved by recognizing storage as a crucial part of achieving a sustainable energy transition and distinguishing their value in the new policies tender processes currently being developed. In this line, this research thesis demonstrates the value that solar energy can have in Chile to increase the diversity in the future energy matrix. It provides methods and guidelines to identify the most cost-effective technology combinations of solar power plants with storage. It also highlights the value of hybridization to complement technologies, providing flexibility to the dispatch, and achieving cheaper electricity costs. In this manner, more applied research, as the one presented in this thesis, is still needed to keep studying new technology combinations to add more value to the future solar generation systems.

BIBLIOGRAPHIC REFERENCES

- ABB. (2017). *ULTRA-750/1100/1500 (North America)*. <http://new.abb.com/power-converters-inverters/solar/central/ultra/750kw-1100kw-1500kw>
- Abdelkader, A., Rabeh, A., Ali, M., & Mohamed, J. (2018). Multi-objective genetic algorithm based sizing optimization of a stand-alone wind/PV power supply system with enhanced battery/ supercapacitor hybrid energy storage. *Energy*, *163*, 351–363. <https://doi.org/10.1016/j.energy.2018.08.135>
- Aly, A., Bernardos, A., Fernandez-Peruchena, C. M., Solvang Jensen, S., & Pedersen, A. B. (2019). Is Concentrated Solar Power (CSP) a feasible option for Sub-Saharan Africa?: Investigating the techno-economic feasibility of CSP in Tanzania. *Renewable Energy*, *135*, 1224–1240. <https://doi.org/10.1016/j.renene.2018.09.065>
- Antonanzas-Torres, F., Antonanzas, J., Urraca, R., Alia-Martinez, M., & Martinez-De-Pison, F. J. (2016). Impact of atmospheric components on solar clear-sky models at different elevation: Case study Canary Islands. *Energy Conversion and Management*, *109*, 122–129. <https://doi.org/10.1016/j.enconman.2015.11.067>
- Ayala-Gilardón, A., Sidrach-de-Cardona, M., & Mora-López, L. (2018). Influence of time resolution in the estimation of self-consumption and self-sufficiency of photovoltaic facilities. *Applied Energy*, *229*, 990–997. <https://doi.org/10.1016/j.apenergy.2018.08.072>
- BloombergNEF. (2019). *A Behind the Scenes Take on Lithium-ion Battery Prices*. <https://about.bnef.com/blog/behind-scenes-take-lithium-ion-battery-prices/>
- Boretti, A. (2018). Cost and production of solar thermal and solar photovoltaics power plants in the United States. *Renewable Energy Focus*, *26*(September), 93–99. <https://doi.org/10.1016/j.ref.2018.07.002>
- Bravo, R., & Friedrich, D. (2018). Two-stage optimisation of hybrid solar power plants. *Solar Energy*, *164*(September 2017), 187–199. <https://doi.org/10.1016/j.solener.2018.01.078>
- Breyer, C., Afanasyeva, S., Brakemeier, D., Engelhard, M., Giuliano, S., Puppe, M., Schenk, H., Hirsch, T., & Moser, M. (2016). Assessment of Mid-Term Growth Assumptions and Learning Rates for Comparative Studies of CSP and Hybrid PV-

- Battery Power Plants. *AIP Conference Proceedings 1850, 1850*(October), 160001.
<https://doi.org/10.1063/1.4984535>
- Burke, E. K., & Kendall, G. (2014). *Search Methodologies: introductory tutorials in optimization* (E. K. Burke & G. Kendall (eds.); Second). Springer.
https://doi.org/10.1007/978-1-60761-842-3_19
- Center for Clean Energy Policy. (2019). *Chile launches ambitious decarbonization plan ahead of COP25 presidency*. <https://ccap.org/chile-launches-ambitious-decarbonization-plan-ahead-of-cop25-presidency/>
- Central Energía. (2020). *Regulation*. <http://www.centralenergia.cl/en/electric-market-regulation-chile/>
- Cerro Dominador project. (2018). *Cerro Dominador: Photovoltaic Plant*. Technology.
<https://cerrodominador.com/tecnologia/photovoltaic-plant/?lang=en>
- CNE. (2018a). *Reporte Mensual ERNC Junio 2018*. https://www.cne.cl/wp-content/uploads/2015/06/RMensual_ERNC_v201806.pdf
- CNE. (2018b). *Reporte Mensual Sector Energético Febrero 2018*.
- Cocco, D., Migliari, L., & Petrollese, M. (2016). A hybrid CSP-CPV system for improving the dispatchability of solar power plants. *Energy Conversion and Management, 114*, 312–323. <https://doi.org/10.1016/j.enconman.2016.02.015>
- Cole, W., & Frazier, A. W. (2019). Cost Projections for Utility- Scale Battery Storage. In *National Renewable Energy Laboratory* (Issue NREL/TP-6A20-73222).
<https://www.nrel.gov/docs/fy19osti/73222.pdf>
- Cole, W. J., Marcy, C., Krishnan, V. K., & Margolis, R. (2016). Utility-scale lithium-ion storage cost projections for use in capacity expansion models. *NAPS 2016 - 48th North American Power Symposium, Proceedings*.
<https://doi.org/10.1109/NAPS.2016.7747866>
- Comisión Nacional de Energía. (2019). *Anuario Estadístico de Energía 2019*.
<https://bit.ly/2ZZqoRo>
- CORFO. (2019). *Reporte de relación y magnitud de costos de inversión (CAPEX) y Operación y Mantenimiento (OPEX)*. <https://www.comitesolar.cl/wp-content/uploads/2019/12/Reporte-Capex-Opex-Plantas-CSP-final-Publicado.pdf>
- Cui, Y., Geng, Z., Zhu, Q., & Han, Y. (2017). Review: Multi-objective optimization

- methods and application in energy saving. *Energy*, *125*, 681–704.
<https://doi.org/10.1016/j.energy.2017.02.174>
- De Soto, W., Klein, S. A., & Beckman, W. A. (2006). Improvement and validation of a model for photovoltaic array performance. *Solar Energy*, *80*(1), 78–88.
<https://doi.org/10.1016/j.solener.2005.06.010>
- Dieckmann, S., Dersch, J., Giuliano, S., Puppe, M., Lüpfert, E., Hennecke, K., Pitz-Paal, R., Taylor, M., & Ralon, P. (2017). LCOE reduction potential of parabolic trough and solar tower CSP technology until 2025. *AIP Conference Proceedings*, *1850*, 160004.
<https://doi.org/10.1063/1.4984538>
- Empresas Eléctricas A.G. (2019). *Licitaciones Vigentes*.
<http://www.licitacioneselectricas.cl/licitaciones-vigentes/>
- Engelhard, M., Hurler, S., Weigand, A., Giuliano, S., Puppe, M., Schenk, H., & Hirsch, T. (2016). Techno-Economic Analysis and Comparison of CSP with Hybrid PV-Battery Power Plants Results from the THERMVOLT Study Motivation and Goals for THERMVOLT Study : Dispatchable Solar Power. In *22nd SolarPACES, Abu Dhabi* (pp. 1–15). SolarPaces 2016.
https://www.researchgate.net/publication/309011409_Techno-Economic_Analysis_and_Comparison_of_CSP_with_Hybrid_PV-Battery_Power_Plants_-_Results_from_the_THERMVOLT_Study
- Escobar, R. A., Cortés, C., Pino, A., Salgado, M., Pereira, E. B., Martins, F. R., Boland, J., & Cardemil, J. M. (2015). Estimating the potential for solar energy utilization in Chile by satellite-derived data and ground station measurements. *Solar Energy*, *121*, 139–151. <https://doi.org/10.1016/j.solener.2015.08.034>
- Estela, Greenpeace, & SolarPACES. (2016). *Solar Thermal Electricity - Global Outlook 2016*.
- Fadaee, M., & Radzi, M. A. M. (2012). Multi-objective optimization of a stand-alone hybrid renewable energy system by using evolutionary algorithms: A review. *Renewable and Sustainable Energy Reviews*, *16*(5), 3364–3369.
<https://doi.org/10.1016/j.rser.2012.02.071>
- Feldman, D., Margolis, R., & Stekli, J. (2016). Exploring the Potential Competitiveness of Utility-Scale Photovoltaics plus Batteries with Concentrating Solar Power, 2015 –

- 2030 (NREL). In *U.S. Department of Energy* (Issue August).
- Fraunhofer ISE. (2020). *Photovoltaics Report*. Fraunhofer.
<https://www.ise.fraunhofer.de/content/dam/ise/de/documents/publications/studies/Photovoltaics-Report.pdf>
- Fu, R., Feldman, D., & Margolis, R. (2018). U.S. Solar Photovoltaic System Cost Benchmark: Q1 2018 (NREL). In *NREL* (Issue November).
<https://www.nrel.gov/docs/fy19osti/72399.pdf>
- Fu, R., Remo, T., & Margolis, R. (2018). 2018 U. S. Utility-Scale Photovoltaics- Plus-Energy Storage System Costs Benchmark (NREL). In *NREL* (Issue November).
<https://www.nrel.gov/docs/fy19osti/71714.pdf>.%0Ahttps://www.nrel.gov/docs/fy19osti/71714.pdf
- Giuliano, S., Puppe, M., Schenk, H., Hirsch, T., Moser, M., Fichter, T., Kern, J., Franz, T., Engelhard, M., Hurler, S., Weigand, A., Brakemeier, D., Kretschmer, J., Haller, U., Klingler, R., Breyer, C., & Afanasyeva, S. (2016). *THERMVOLT Systemvergleich von solarthermischen und photovoltaischen Kraftwerken für die Versorgungssicherheit* (Issue December 2016).
<https://doi.org/10.2314/GBV:100051305X>
- Green, A., Diep, C., Dunn, R., & Dent, J. (2015). High Capacity Factor CSP-PV Hybrid Systems. *Energy Procedia*, 69, 2049–2059.
<https://doi.org/10.1016/j.egypro.2015.03.218>
- Guédez, R., Spelling, J., Laumert, B., & Fransson, T. (2014). Optimization of Thermal Energy Storage Integration Strategies for Peak Power Production by Concentrating Solar Power Plants. *Energy Procedia*, 49(0), 1642–1651.
<https://doi.org/10.1016/j.egypro.2014.03.173>
- Guédez, Rafael. (2016). *A Techno-Economic Framework for the Analysis of Concentrating Solar Power Plants with Storage* [KTH Royal Institute of Technology].
<http://www.diva-portal.org/smash/get/diva2:956167/FULLTEXT01.pdf>
- Guédez, Rafael, Spelling, J., & Laumert, B. (2014). Thermo-economic optimization of solar thermal power plants with storage in high-penetration renewable electricity markets. *Energy Procedia*, 57(0), 541–550. <https://doi.org/10.1016/j.egypro.2014.10.208>
- Guédez, Rafael, Topel, M., Conde, I., Ferragut, F., Callaba, I., Spelling, J., Hassar, Z.,

- Perez-Segarra, C. D., & Laumert, B. (2016). A Methodology for Determining Optimum Solar Tower Plant Configurations and Operating Strategies to Maximize Profits Based on Hourly Electricity Market Prices and Tariffs. *Journal of Solar Energy Engineering*, 138(2), 021006. <https://doi.org/10.1115/1.4032244>
- Hamilton, W. T., Husted, M. A., Newman, A. M., Braun, R. J., & Wagner, M. J. (2019). Dispatch optimization of concentrating solar power with utility-scale photovoltaics. In *Optimization and Engineering*. Springer US. <https://doi.org/10.1007/s11081-019-09449-y>
- Hirsch, T., Dersch, J., Fluri, T., Garcia-Barberena, J., Giuliano, S., Hustig-Diethlem, F., Meyer, R., Schmidt, N., Seitz, M., & Yildiz, E. (2017). SolarPACES guideline for bankable STE yield assessment. In *IEA-SolarPACES*.
- Hlusiak, M., Götz, M., Díaz, H. A. B., & Breyer, C. (2014). Hybrid Photovoltaic (PV) - Concentrated Solar Thermal Power (CSP) Power Plants: Modelling , Simulation and Economics. *29th European Photovoltaic Solar Energy Conference and Exhibition - Proceedings of the International Conference, September 2014*. <https://doi.org/10.4229/29thEUPVSEC2014-7AV.6.20>
- Instituto de Ecología Política. (2013). *Aprobado El Proyecto De Ley 20/25 De Energías Renovables No Convencionales En Chile*. <http://www.iepe.org/2013/06/aprobado-el-proyecto-de-ley-2025-de-energias-renovables-no-convencionales-en-chile/>
- IRENA. (2012). *Renewable Energy Technologies: Cost Analysis Series Concentrating Solar Power* (Vol. 3, Issue 2). <https://doi.org/10.1016/B978-0-08-087872-0.00319-X>
- IRENA. (2017). *Electricity Storage and Renewables: Costs and Markets to 2030* (Issue October). www.irena.org
- IRENA. (2018). Renewable Power Generation Costs in 2017. In *International Renewable Energy Agency*. https://doi.org/10.1007/SpringerReference_7300
- IRENA. (2019a). *Future of Solar Photovoltaic. Deployment, investment, technology, grid integration and socio-economic aspects*. www.irena.org/publications.
- IRENA. (2019b). *Innovation landscape brief: Utility-scale batteries*.
- IRENA. (2019c). *Renewable Power Generation Costs in 2018*. https://doi.org/10.1007/SpringerReference_7300
- IRENA. (2020). *How Falling Costs Make Renewables a Cost-effective Investment*.

<https://www.irena.org/newsroom/articles/2020/Jun/How-Falling-Costs-Make-Renewables-a-Cost-effective-Investment>

- Jorgenson, J., Mehos, M., & Denholm, P. (2016). Comparing the net cost of CSP-TES to PV deployed with battery storage. *AIP Conference Proceedings*, 1734, 080003. <https://doi.org/10.1063/1.4949183>
- Kassem, A., Al-Haddad, K., & Komljenovic, D. (2017). Concentrated solar thermal power in Saudi Arabia: Definition and simulation of alternative scenarios. *Renewable and Sustainable Energy Reviews*, 80, 75–91. <https://doi.org/10.1016/j.rser.2017.05.157>
- Köberle, A. C., Gernaat, D. E. H. J., & van Vuuren, D. P. (2015). Assessing current and future techno-economic potential of concentrated solar power and photovoltaic electricity generation. *Energy*, 89, 739–756. <https://doi.org/10.1016/j.energy.2015.05.145>
- Li, R., Dai, Y., & Cui, G. (2019). Multi-objective optimization of solar powered adsorption chiller combined with river water heat pump system for air conditioning and space heating application. *Energy*, 189. <https://doi.org/10.1016/j.energy.2019.116141>
- Lilliestam, J., & Pitz-Paal, R. (2018). Concentrating solar power for less than USD 0.07 per kWh: finally the breakthrough? *Renewable Energy Focus*, 26(September), 17–21. <https://doi.org/10.1016/j.ref.2018.06.002>
- Liu, H., Zhai, R., Fu, J., Wang, Y., & Yang, Y. (2019). Optimization study of thermal-storage PV-CSP integrated system based on GA-PSO algorithm. *Solar Energy*, 184(April), 391–409. <https://doi.org/10.1016/j.solener.2019.04.017>
- Mata-Torres, C., Escobar, R. A., Cardemil, J. M., Simsek, Y., & Matute, J. A. (2017). Solar polygeneration for electricity production and desalination: Case studies in Venezuela and northern Chile. *Renewable Energy*, 101, 387–398. <https://doi.org/10.1016/j.renene.2016.08.068>
- Mata-Torres, C., Zurita, A., Cardemil, J. M., & Escobar, R. A. (2019). Exergy cost and thermoeconomic analysis of a Rankine Cycle + Multi-Effect Distillation plant considering time-varying conditions. *Energy Conversion and Management*, 192, 114–132. <https://doi.org/10.1016/j.enconman.2019.04.023>
- Mathworks. (2020). *gamultiobj Algorithm*. <https://www.mathworks.com/help/gads/gamultiobj-algorithm.html>

- MathWorks. (2020). *How the Genetic Algorithm Works*.
<https://www.mathworks.com/help/gads/how-the-genetic-algorithm-works.html>
- Meybodi, M. A., & Beath, A. C. (2016). Impact of cost uncertainties and solar data variations on the economics of central receiver solar power plants: An Australian case study. *Renewable Energy*, 93, 510–524. <https://doi.org/10.1016/j.renene.2016.03.016>
- Ministerio de Energía. (2014). *Energía 2050 - Política Energetica De Chile* (p. 158).
http://eae.mma.gob.cl/uploads/D03_Politica_Energetica_de__Chile_2050_Anteproyecto2.pdf
- Ministerio de Energía. (2019). *Estrategia de Descarbonización: Retiro y/o Reconversión de Unidades a Carbón*.
https://energia.gob.cl/sites/default/files/folleto_estrategia_descarbonizacion_cast.pdf
- Ministerio de Energía. (2020). *Plan de Descarbonización de la Matriz Eléctrica*.
<https://www.energia.gob.cl/mini-sitio/plan-de-descarbonizacion-de-la-matriz-electrica>
- Nasruddin, Sholahudin, Satrio, P., Mahlia, T. M. I., Giannetti, N., & Saito, K. (2019). Optimization of HVAC system energy consumption in a building using artificial neural network and multi-objective genetic algorithm. *Sustainable Energy Technologies and Assessments*, 35(June), 48–57.
<https://doi.org/10.1016/j.seta.2019.06.002>
- NREL. (2013). *System Advisor Model (SAM) Case Study : Gemasolar*.
- NREL. (2014). *System Advisor Model , SAM 2014 . 1 . 14 : General Description*.
<https://www.nrel.gov/docs/fy14osti/61019.pdf>
- NREL. (2017). U.S. Solar Photovoltaic System Cost Benchmark : Q1 2017. In *NREL* (Issue September). <https://doi.org/10.2172/1390776>
- NREL. (2018). *Solar Power tower Integrated Layout and Optimization Tool*.
<https://www.nrel.gov/csp/solarpilot.html>
- Pan, C. A., & Dinter, F. (2017). Combination of PV and central receiver CSP plants for base load power generation in South Africa. *Solar Energy*, 146, 379–388.
<https://doi.org/10.1016/j.solener.2017.02.052>
- Paravalos, C., Koutroulis, E., Samoladas, V., Kerekes, T., Sera, D., & Teodorescu, R. (2014). Optimal design of photovoltaic systems using high time-resolution meteorological data. *IEEE Transactions on Industrial Informatics*, 10(4), 2270–2279.

<https://doi.org/10.1109/TII.2014.2322814>

Parrado, C., Girard, A., Simon, F., & Fuentealba, E. (2016). 2050 LCOE (Levelized Cost of Energy) projection for a hybrid PV (photovoltaic)-CSP (concentrated solar power) plant in the Atacama Desert, Chile. *Energy*, *94*, 422–430.

<https://doi.org/10.1016/j.energy.2015.11.015>

Patnode, A. M. (2006). *Simulation and performance evaluation of parabolic trough solar power plants* [University of Wisconsin-Madison].

<http://www.minds.wisconsin.edu/handle/1793/7590>

Payaro, A., Naik, A. A., Guedez, R., & Laumert, B. (2018). Identification of required cost reductions for CSP to retain its competitive advantage as most economically viable solar-dispatchable technology. *AIP Conference Proceedings*, *2033*.

<https://doi.org/10.1063/1.5067064>

Perez, R., Rábago, K. R., Trahan, M., Rawlings, L., Norris, B., Hoff, T., Putnam, M., & Perez, M. (2016). Achieving very high PV penetration - The need for an effective electricity remuneration framework and a central role for grid operators. *Energy Policy*, *96*, 27–35. <https://doi.org/10.1016/j.enpol.2016.05.016>

Petrollese, M., & Cocco, D. (2016). Optimal design of a hybrid CSP-PV plant for achieving the full dispatchability of solar energy power plants. *Solar Energy*, *137*, 477–489. <https://doi.org/10.1016/j.solener.2016.08.027>

Pfahl, A., Coventry, J., Röger, M., Wolfertstetter, F., Vásquez-Arango, J. F., Gross, F., Arjomandi, M., Schwarzbözl, P., Geiger, M., & Liedke, P. (2017). Progress in heliostat development. *Solar Energy*, *152*, 3–37.

<https://doi.org/10.1016/j.solener.2017.03.029>

Pfahl, A., Coventry, J., Röger, M., Wolfertstetter, F., Vásquez-Arango, J. F., Gross, F., Arjomandi, M., Schwarzbözl, P., Geiger, M., Liedke, P., Dieckmann, S., Dersch, J., Giuliano, S., Puppe, M., Lüpfert, E., Hennecke, K., Pitz-Paal, R., Taylor, M., Ralon, P., ... Pitz-Paal, R. (2017). Techno-economic analysis of concentrated solar power plants in terms of levelized cost of electricity. *AIP Conference Proceedings*, *1850*(June), 17–21. <https://doi.org/10.1063/1.4984535>

Platzer, W. (2014). PV-enhanced solar thermal power. *Energy Procedia*, *57*, 477–486.

<https://doi.org/10.1016/j.egypro.2014.10.201>

- Polo, J., Antonanzas-Torres, F., Vindel, J. M., & Ramirez, L. (2014). Sensitivity of satellite-based methods for deriving solar radiation to different choice of aerosol input and models. *Renewable Energy*, *68*, 785–792.
<https://doi.org/10.1016/j.renene.2014.03.022>
- PV Info Link. (2018). *Spot prices*. <https://en.pvinfoLink.com/>
- PVInsights. (2020). *PVinsights Grid the world*. Solar PV Module Weekly Spot Price.
<http://pvinsights.com/index.php>
- REN21. (2019). *2019 Global Status Report* (F. S. Fabiani Appavou, Adam Brown, Bärbel Epp, Duncan Gibb, Bozhil Kondev, Angus McCrone, Hannah E. Murdock, Evan Musolino, Lea Ranalder, Janet L. Sawin, Kristin Seyboth, Jonathan Skeen (ed.)).
https://www.ren21.net/wp-content/uploads/2019/05/gsr_2019_full_report_en.pdf
- REN21. (2020). *Renewables 2020 Global Status Report*. https://www.ren21.net/wp-content/uploads/2019/05/gsr_2020_full_report_en.pdf
- Rojas, R. G., Alvarado, N., Boland, J., Escobar, R., & Castillejo-Cuberos, A. (2019). Diffuse fraction estimation using the BRL model and relationship of predictors under Chilean, Costa Rican and Australian climatic conditions. *Renewable Energy*, *136*, 1091–1106. <https://doi.org/10.1016/j.renene.2018.09.079>
- Schwarzbözl, P., Eiden, U., Pitz-Paal, R., Zentrum, D., & Scott, J. (2006). A TRNSYS Model Library for Solar Thermal Electric Components (STEC) Reference Manual. In *DLR, Germany* (Issue November).
- SEA. (2014). *Declaración de Impacto Ambiental: Planta de Concentración Solar de Potencia Copiapó Solar*.
<http://seia.sea.gob.cl/documentos/documento.php?idDocumento=2129864122>
- Sharma, C., Sharma, A. K., Mullick, S. C., & Kandpal, T. C. (2017). Cost reduction potential of parabolic trough based concentrating solar power plants in India. *Sundaray and Kandpal, IRENA*. <https://doi.org/10.1016/j.esd.2017.10.003>
- Solar Energy Laboratory. (2017). *TRNSYS 18 Mathematical Reference* (Vol. 4).
<http://web.mit.edu/parmstr/Public/Documentation/05-MathematicalReference.pdf>
- SolarGis. (2017). *SolarGis*. <http://solargis.com/>
- Starke, A. R., Cardemil, J. M., & Colle, S. (2018). Multi-objective optimization of a solar-assisted heat pump for swimming pool heating using genetic algorithm. *Applied*

- Thermal Engineering*, 142(September 2017), 118–126.
<https://doi.org/10.1016/j.applthermaleng.2018.06.067>
- Starke, A. R., Cardemil, J. M., Escobar, R. A., & Colle, S. (2016). Assessing the performance of hybrid CSP + PV plants in northern Chile. *Solar Energy*, 138, 88–97.
<https://doi.org/10.1016/j.solener.2016.09.006>
- Starke, A. R., Cardemil, J. M., Escobar, R., & Colle, S. (2018). Multi-objective optimization of hybrid CSP+PV system using genetic algorithm. *Energy*, 147, 490–503. <https://doi.org/10.1016/j.energy.2017.12.116>
- SunEdison. (2015). *MEMC Silvantis M330 Module*. <http://fmscopk.com/wp-content/uploads/2015/08/SunEdison.pdf>
- TRNSYS. (2020). *TRNSYS Transient System Simulation Tool*. <http://www.trnsys.com/>
- Turchi, C. S., Boyd, M., Kesseli, D., Kurup, P., Mehos, M., Neises, T., Sharan, P., Wagner, M. J., & Wendelin, T. (2019). *CSP Systems Analysis - Final Project Report* (Issue May). <https://www.nrel.gov/docs/fy19osti/72856.pdf>
- Turchi, C. S., & Heath, G. a. (2013). *Molten Salt Power Tower Cost Model for the System Advisor Model (SAM)* (Issue February). <https://doi.org/10.2172/1067902>
- University of Wisconsin-Madison. (2005). *TRNSYS A Transient System Simulation Program*.
- Valenzuela, C., Mata-Torres, C., Cardemil, J. M., & Escobar, R. A. (2017). CSP + PV hybrid solar plants for power and water cogeneration in northern Chile. *Solar Energy*, 157(January), 713–726. <https://doi.org/10.1016/j.solener.2017.08.081>
- Wagner, M. J. (2008). *Simulation and Predictive Performance Modeling of Utility-Scale Central Receiver System Power Plants*. University of Wisconsin-Madison.
- Zakeri, B., & Syri, S. (2015). Electrical energy storage systems: A comparative life cycle cost analysis. *Renewable and Sustainable Energy Reviews*, 42, 569–596.
<https://doi.org/10.1016/j.rser.2014.10.011>
- Zhai, R., Chen, Y., Liu, H., Wu, H., Yang, Y., & Hamdan, M. O. (2018). Optimal Design Method of a Hybrid CSP-PV Plant Based on Genetic Algorithm Considering the Operation Strategy. *International Journal of Photoenergy*, 2018.
<https://doi.org/10.1155/2018/8380276>
- Zhai, R., Liu, H., Chen, Y., Wu, H., & Yang, Y. (2017). The daily and annual technical-

economic analysis of the thermal storage PV-CSP system in two dispatch strategies.

Energy Conversion and Management, 154(June), 56–67.

<https://doi.org/10.1016/j.enconman.2017.10.040>

Zurita, A., Castillejo-Cuberos, A., García, M., Mata-Torres, C., Simsek, Y., García, R., Antonanzas-Torres, F., & Escobar, R. A. (2018). State of the art and future prospects for solar PV development in Chile. *Renewable & Sustainable Energy Reviews*,

92(September), 701–727. <https://doi.org/10.1016/j.rser.2018.04.096>

Zurita, A., Mata-Torres, C., Cardemil, J. M., & Escobar, R. A. (2020). Assessment of time resolution impact on the modeling of a hybrid CSP-PV plant: A case of study in Chile. *Solar Energy*, 202, 553–570. <https://doi.org/10.1016/j.solener.2020.03.100>

Zurita, A., Mata-Torres, C., Valenzuela, C., Felbol, C., Cardemil, J. M., Guzmán, A. M., & Escobar, R. A. (2018). Techno-Economic Evaluation of a Hybrid CSP+PV Plant Integrated with Thermal Energy Storage and a Large-Scale Battery Energy Storage System for Base Generation. *Solar Energy*, 173(ISSN 0038-092X), 1262–1277.

<https://doi.org/10.1016/j.solener.2018.08.061>

APPENDICES

APPENDIX A: APPENDIX FOR CHAPTER 2

Cost functions implemented in Chapter 2 for the CAPEX and OPEX calculations of the CSP plant are described below.

$$CAPEX_{CSP} = C_{d,CSP} + C_{id,CSP} \quad (A.1)$$

$$C_{d,CSP} = [C_{HF} + C_{pb} + C_{TES} + C_{tow} + C_{rec}] \cdot (1 + \%Cont_{CSP}) \quad (A.2)$$

$$C_{HF} = (c_{si} + c_{HF})A_{HF} \quad (A.3)$$

$$C_{pb} = (c_{BoP} + c_{pb})P_{gross,turb}^e \quad (A.4)$$

$$C_{TES} = c_{TES}P_{TES}^{th} \quad (A.5)$$

$$C_{tow} = c_{tow} \cdot \exp\left(\tau_{tow} \cdot \left(h_{tow} - \frac{h_{rec}}{2} + \frac{h_{hel}}{2}\right)\right) \quad (A.6)$$

$$C_{rec} = c_{rec} \left(\frac{A_{rec}}{A_{rec,ref}}\right)^{\tau_{rec}} \quad (A.7)$$

$$C_{id,CSP,t} = C_{d,CSP} \cdot \%EPC_{CSP} \quad (A.8)$$

$$OPEX_{CSP} = c_{f,O\&M,CSP} \cdot P_{net,CSP}^e + c_{v,O\&M,CSP} \cdot E_{annual,CSP} \quad (A.9)$$

APPENDIX B: APPENDIX FOR CHAPTER 3

Appendix B1: Supplementary Data

Supplementary data to this article can be found online at <https://doi.org/10.1016/j.solener.2020.03.100>. Supplementary data represents the coefficients of the power block regression model described in the following equations:

$$W_{net} = a_1 \cdot T_{amb} + a_2 \cdot T_{inHTF} + a_3 \cdot T_{inHTF} \cdot T_{amb} + a_4 \cdot \dot{m}_{inHTF} + a_5 \cdot \dot{m}_{inHTF} \cdot T_{amb} + a_6 \cdot \dot{m}_{inHTF} \cdot T_{inHTF} + a_7 + a_8 \cdot \dot{m}_{inHTF}^2 + a_9 \cdot T_{inHTF}^2 + a_{10} \cdot T_{amb}^2 \quad (B.1)$$

$$m_{cond} = b_1 \cdot T_{amb} + b_2 \cdot T_{inHTF} + b_3 \cdot T_{inHTF} \cdot T_{amb} + b_4 \cdot \dot{m}_{inHTF} + b_5 \cdot \dot{m}_{inHTF} \cdot T_{amb} + b_6 \cdot \dot{m}_{inHTF} \cdot T_{inHTF} + b_7 + b_8 \cdot \dot{m}_{inHTF}^2 + b_9 \cdot T_{inHTF}^2 + b_{10} \cdot T_{amb}^2 \quad (B.2)$$

$$h_{cond} = c_1 \cdot T_{amb} + c_2 \cdot T_{inHTF} + c_3 \cdot T_{inHTF} \cdot T_{amb} + c_4 \cdot \dot{m}_{inHTF} + c_5 \cdot \dot{m}_{inHTF} \cdot T_{amb} + c_6 \cdot \dot{m}_{inHTF} \cdot T_{inHTF} + c_7 + c_8 \cdot \dot{m}_{inHTF}^2 + c_9 \cdot T_{inHTF}^2 + c_{10} \cdot T_{amb}^2 \quad (B.3)$$

$$T_{outHTF} = d_1 \cdot T_{amb} + d_2 \cdot T_{inHTF} + d_3 \cdot T_{inHTF} \cdot T_{amb} + d_4 \cdot \dot{m}_{inHTF} + d_5 \cdot \dot{m}_{inHTF} \cdot T_{amb} + d_6 \cdot \dot{m}_{inHTF} \cdot T_{inHTF} + d_7 + d_8 \cdot \dot{m}_{inHTF}^2 + d_9 \cdot T_{inHTF}^2 + d_{10} \cdot T_{amb}^2 \quad (B.4)$$

Appendix B2: Cost Data

Cost data implemented in Chapter 3 for the CAPEX and OPEX calculations of the PV, CSP and BESS sections is presented below.

Table B2.1. Economic parameters considered for the CSP plant.

Description	Unit	Value
<i>Direct capital cost</i>		
Heliostat field	USD/m ²	160
Power block	USD/kW _e	1100
Storage	USD/kWh _t	29
Tower cost	USD/m	95,000

Receiver cost	USD/kW _t	140
Contingency and other costs	-	10%
<i>Indirect capital cost</i>		
EPC profit rate	% of direct cost	10%
Sales tax	%	0
<i>Operation and Maintenance</i>		
Fixed cost by capacity	USD/kW-yr	48
Variable cost by generation	USD/MWh	3.7

Table B2.2. Economic parameters considered for the PV plant and BESS.

Description	Unit	Value
<i>PV plant</i>		
<i>Direct capital cost</i>		
Module cost	USD/W _{dc}	0.30
Inverter cost	USD/W _{ac}	0.05
Electrical BoS	USD/W _{dc}	0.08
Mechanical BoS	USD/W _{dc}	0.09
Installation labor	USD/W _{dc}	0.10
Installer margin and overhead	USD/W _{dc}	0.05
Contingency	%	3
<i>Indirect capital cost</i>		
EPC profit rate	USD/W _{dc}	0.08
Sales tax	%	0
<i>O&M costs</i>		
O&M cost for fixed tilt	USD/kW-yr	9
<i>BESS</i>		
<i>Capital cost</i>		
Cost of storage section	USD/kWh	209
Power conversion system cost	USD/kW	70
Structural BoS	USD/kW	10
Electrical BoS	USD/kW	70
<i>Operation and Maintenance</i>		
Fixed O&M cost	USD/kW-yr	6.9
Variable O&M cost	USD/MWh	2.1
<i>Replacement</i>		

Replacement cost	USD/kWh	2/3 of the cost of storage section
------------------	---------	------------------------------------

Appendix B3: Cost Functions

Cost functions implemented in Chapter 3 for the CAPEX and OPEX calculations of the PV, CSP and BESS sections are described below.

$$A_f = \frac{r}{1 - \frac{1}{(1+r)^L}} \quad (\text{B3.1})$$

$$CAPEX = CAPEX_{PV} + CAPEX_{CSP} + CAPEX_{BESS} \quad (\text{B3.2})$$

$$OPEX = OPEX_{PV} + OPEX_{CSP} + OPEX_{BESS} \quad (\text{B3.3})$$

$$CAPEX_{PV} = C_{d,PV} + C_{id,PV} \quad (\text{B3.4})$$

$$C_{d,PV} = \left[(c_{mod} + c_{BoS,PV} + c_{inst} + c_{overh}) P_{PV}^{DC} + c_{inv} \cdot P_{inv}^{AC} \right] \cdot (1 + \%Cont_{PV}) \quad (\text{B3.5})$$

$$C_{id,PV} = C_{d,PV} \cdot \%EPC_{PV} \quad (\text{B3.6})$$

$$CAPEX_{CSP} = C_{d,CSP} + C_{id,CSP} \quad (\text{B3.7})$$

$$C_{d,CSP} = [C_{HF} + C_{pb} + C_{TES} + C_{tow} + C_{rec} + C_{other}] \cdot (1 + \%Cont_{CSP}) \quad (\text{B3.8})$$

$$C_{HF} = c_{HF} A_{HF} \quad (\text{B3.9})$$

$$C_{pb} = c_{pb} P_{gross,turb}^e \quad (\text{B3.10})$$

$$C_{TES} = c_{TES} P_{TES}^{th} \quad (\text{B3.11})$$

$$C_{tow} = c_{tow} \cdot (h_{tow} - h_{rec}) \quad (\text{B3.12})$$

$$C_{rec} = c_{rec} P_{rec}^{th} \quad (\text{B3.13})$$

$$C_{id,CSP,t} = C_{d,CSP} \cdot \%EPC_{CSP} \quad (\text{B3.14})$$

$$CAPEX_{BESS} = (c_{PCS,BESS} + c_{BoS,BESS}) P_{BESS}^{inv} + c_{stor} \cdot S_{BESS} \quad (\text{B3.15})$$

$$OPEX_{PV} = c_{O\&M,PV} \cdot P_{PV}^{AC} \quad (B3.16)$$

$$OPEX_{CSP} = c_{f,O\&M,CSP} \cdot P_{net,CSP}^e + c_{v,O\&M,CSP} \cdot E_{annual,CSP} \quad (B3.17)$$

$$OPEX_{BESS} = c_{f,O\&M,BESS} \cdot P_{BESS}^{inv} + c_{v,O\&M,BESS} \cdot E_{annual,BESS} \quad (B3.18)$$

$$C_{rep,BESS} = \sum_{j=1}^k \frac{1}{(1+r)^{jt}} c_{rep} \cdot S_{BESS} \quad (B3.19)$$

$$z = E_{disch,BESS} / S_{BESS} \quad (B3.20)$$

$$t = n/z \quad (B3.21)$$

APPENDIX C: APPENDIX FOR CHAPTER 4

Cost functions implemented in Chapter 4 for the CAPEX and OPEX calculations of the PV, CSP and BESS sections are described below.

$$CAPEX = CAPEX_{PV} + CAPEX_{CSP} + CAPEX_{BESS} \quad (C.1)$$

$$CAPEX_{PV} = C_{d,PV} + C_{id,PV} \quad (C.2)$$

$$C_{d,PV} = (c_{mod} + c_{BoS,PV} + c_{inst} + c_{EPC} + c_{overh})P_{PV}^{DC} + c_{inv} \cdot P_{inv}^{AC} \quad (C.3)$$

$$C_{id,PV} = C_{d,PV} \cdot \%EPC_{PV} \quad (C.4)$$

$$c_{PV} = c_{ref} \left(\frac{P_{PV}}{P_{PV,ref}} \right)^{exp,ref} \quad (C.5)$$

$$CAPEX_{CSP} = C_{d,CSP} + C_{id,CSP} \quad (C.6)$$

$$C_{d,CSP} = [C_{HF} + C_{pb} + C_{TES} + C_{tow} + C_{rec}] \cdot (1 + \%Cont_{CSP}) \quad (C.7)$$

$$C_{HF} = c_{HF}A_{HF} \quad (C.8)$$

$$C_{pb} = c_{pb}P_{gross,turb}^e \quad (C.9)$$

$$C_{TES} = c_{TES}P_{TES}^{th} \quad (C.10)$$

$$C_{tow} = c_{tow} \cdot (h_{tow} - h_{rec}) \cdot \left(\frac{h_{tow} - h_{rec}}{h_{rec,ref}} \right)^{exp,tow} \quad (C.11)$$

$$C_{rec} = c_{rec} \cdot P_{rec}^{th} \cdot \left(\frac{P_{rec}^{th}}{P_{rec,ref}^{th}} \right)^{exp,rec} \quad (C.12)$$

$$C_{id,CSP,t} = C_{d,CSP} \cdot \%EPC_{CSP} \quad (C.13)$$

$$CAPEX_{BESS} = (c_{PCS,BESS} + c_{BoS,BESS})P_{BESS}^{inv} + c_{stor} \cdot S_{BESS} \quad (C.14)$$

$$c_{BESS} = c_{ref} \left(\frac{S_{BESS}}{P_{BESS}^{inv}} \right)^{exp,ref} \quad (C.15)$$

$$OPEX_{(i)} = OPEX_{PV(i)} + OPEX_{CSP(i)} + OPEX_{BESS(i)} \quad (C.16)$$

$$OPEX_{PV(i)} = c_{f,O\&M,PV} \cdot P_{PV}^{AC} \quad (C.17)$$

$$OPEX_{CSP(i)} = c_{f,O\&M,CSP} \cdot P_{net,CSP}^e + c_{v,O\&M,CSP} \cdot E_{annual,CSP} \quad (C.18)$$

$$OPEX_{BESS(i)} = c_{f,O\&M,BESS} \cdot P_{BESS}^{inv} + c_{v,O\&M,BESS} \cdot E_{annual,BESS} \quad (C.19)$$

$$C_{rep,BESS(i)} = \sum_{j=1}^k \frac{1}{(1+r)^{jt}} c_{rep} \cdot S_{BESS} \quad (C.20)$$

APPENDIX D: SIMULATION MODEL IN TRNSYS

This section introduces the simulation platform as well as a brief description of the mathematical models and the software used. Simulation models were developed and implemented in the TRNSYS simulation environment at a component level.

In general, TRNSYS presents a main visual interface name TRNSYS simulation studio. The workspace of the simulation studio allows creating the projects by connecting components together in a visual layout. The simulation studio saves the information in a TRNSYS project file (*.tpf), and it creates also an input file (*.dck) in which all the information about the information is saved. The workspace it is only used as a graphic interface to set the global simulation parameters, variables and outputs of the components. For instance, Figure D-1 illustrates the simplified scheme of the hybrid plant in the TRNSYS simulation studio.

In this interface, each component is connected to each other, establishing relationships between them related to inputs and outputs of transfer mass, energy, and control equations. Every component is also configured by a set of parameters and input values. Some parameters are defined through input files that contain specific information to follow.

The actual transient simulation is solved by the simulation engine, also called kernel, that is programmed in Fortran. This engine is compiled into a Windows Dynamic Link Library (DLL), TRNDdll. In this way, the TRNSYS kernel reads the TRNSYS input file (*.dck) and any additional data file required by the simulation and creates the output file. For instance, it is also necessary to provide the file with the meteorological and solar data associated to a location with a specific time resolution. Then, the kernel is called by an executable program of TRNSYS (*.exe) to run the simulation.

For the purpose of this dissertation, a Matlab script was developed by the author to call TRNSYS's executable program and kernel. The coupling between Matlab and TRNSYS allows to automatize the process to perform parametric analyses that consider the execution of numerous simulations, and to integrate the multi-objective optimization algorithm of Matlab with the TRNSYS simulation.

Input files required to run the simulation of the hybrid plant in TRNSYS were:

- Input file with the design variables of the plant (*.txt) including:
 - Nominal PV size.

- Number of heliostats in representation of the CSP plant's Solar Multiple.
- TES capacity in terms of thermal energy.
- BESS energy capacity.
- BESS inverter power.
- Meteorological and solar input data (*.txt or *.csv) given by a location and a time resolution.
- Dispatch profile data (*.txt) given by a dispatch strategy. Electric market prices data can also be provided in this file.
- Inverter efficiency data (*.txt).
- Heliostats efficiency matrix data (*.txt).
- The coefficients for the power block's component (*.txt).

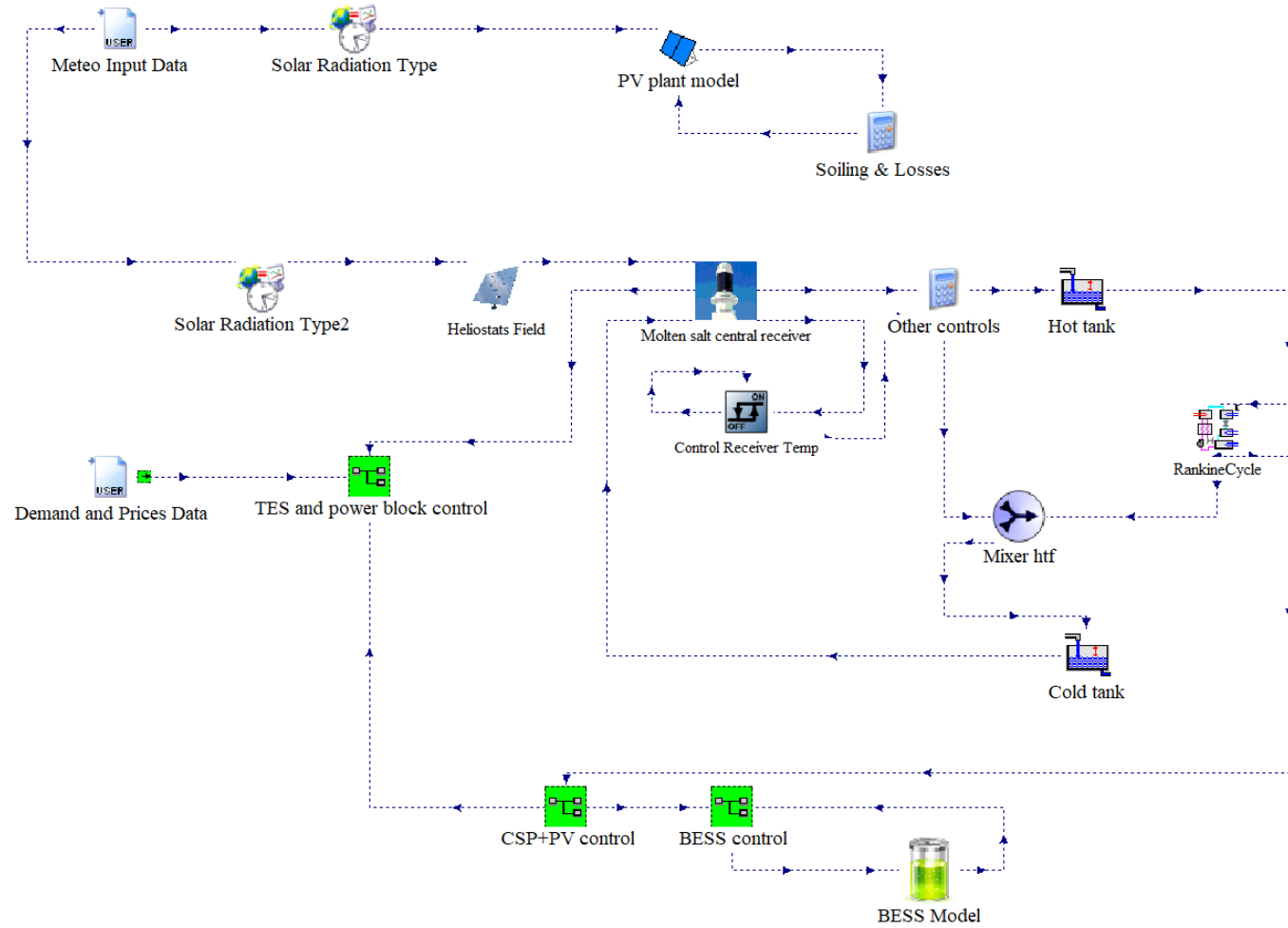


Figure D-1: Simplified and illustrative scheme of the hybrid plant model in TRNSYS simulation studio.

APPENDIX D1. PV plant model

Figure D-2 illustrates a scheme of the PV plant model in TRNSYS simulation studio. This model was developed using the following components:

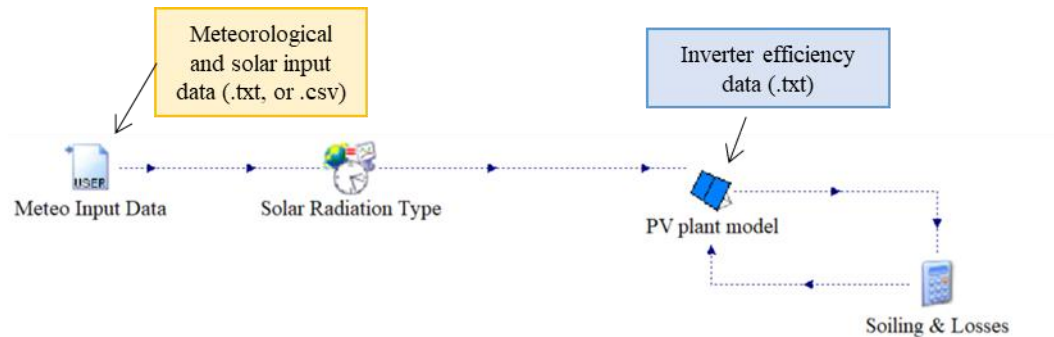


Figure D-2: Illustrative scheme of the PV plant model in TRNSYS.

- Type 9e-Data Reader for Generic Data Files - Expert Mode (Free format).
- Type 2804-Solar radiation model on tilted surfaces (*developed by the author*).
This component calculates the solar geometry on horizontal or tilted surfaces introducing an input file with the weather and solar data. Calculation can be made considering different time resolution of the weather data. Solar radiation on tilted surfaces is computed based on the Perez's model (1990).
- Type 190d – Photovoltaic array with MPPT and inverter.
This component is based on the model presented by DeSoto et al (2005) to determine the electrical performance of a photovoltaic array with a Maximum Power Point Tracker (MPPT). The model allows specifying an inverter coupled to the PV array. It requires of an external file to include the inverter efficiency effects. More information about the mathematical model can be found in (Solar Energy Laboratory, 2017).

The PV array was modeled considering a solar cell technology of silicon monocrystalline based on the MEMC-330 Sun Edison modules (SunEdison, 2015) with a nominal power of 330 W_{dc}. The inverter is an ULTRA-TL-1100 of ABB with a maximum AC power of 1 MW_{ac} (ABB, 2017). Then, the nominal PV plant size was

scaled in terms of the number of inverters to reach the design capacity specified in the input file.

APPENDIX D2. CSP plant based on central receiver technology

Figure D-3 illustrates a scheme of the CSP plant model in TRNSYS simulation studio. The model includes the heliostat field section, the central receiver model, the power block of the CSP plant, and the molten salt tanks.

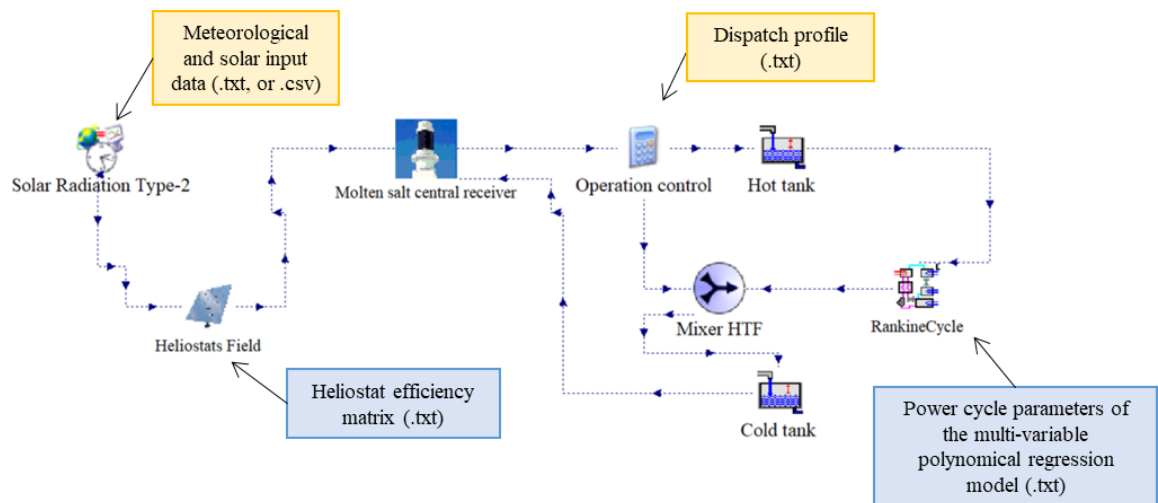


Figure D-3: Illustrative scheme of the CSP plant model in TRNSYS.

This model was developed using the following components:

- Type 9e-Data Reader for Generic Data Files - Expert Mode (Free format).
- Type 2804-Solar radiation model on tilted surfaces (*developed by the author*).
- Type 4601: Heliostat field (*in-house development in Grupo Solar UC*).

This component is based on Type 394 of the Solar Thermal Electric Components (STEC) library (Schwarzbözl et al., 2006), which provides the incident power on the receiver surface, including a daily soiling rate and cleaning period. This type uses as input a matrix indicating the field efficiency at different solar azimuth and zenith angles, which interpolates during the simulation to obtain the heliostats field

efficiency in terms of solar position. A soiling rate of 0.5% and a cleaning frequency of 15 days were considered.

- Type 4606: Molten salts central receiver (*developed by the author and integration of in-house development in Grupo Solar UC*).

The developed model calculates in a simplified manner the thermal power absorbed by the HTF in the receiver based on the work developed by (Wagner, 2008) introducing as inputs the receiver and tower dimensions, which are optimized in terms of the SM using SolarPILOT from NREL. The model formulation considers an equations system of energy balances on a receiver tube element, including the incident radiation and thermal losses, which are constituted by radiation, natural and forced convection losses. Thus, the outlet HTF mass flow rate and temperature are calculated in terms of the absorbed thermal power, while the receiver surface temperature is calculated considering the heat transfer across the receiver tube wall from the HTF fluid running through the tube to the receiver surface. Since there are many relationships in the equation system, the receiver model comprises an iterative process that is computed until the receiver surface temperature, the HTF outlet temperature, and the HTF mass flow rate in the receiver converge.

The electric power consumption of the HTF tower pumps is also considered. Besides, the receiver includes the simple modeling of a thermal capacitance to represent the thermal inertia of the receiver. With this purpose, an adiabatic capacitance was added after the receiver calculation, in which the inlet stream is the HTF outlet mass flow rate of the receiver, and the outlet stream is the HTF mass flow rate that goes to the hot TES tank with the capacitance temperature. This approach allows adding the thermal inertia to the receiver performance without penalizing the computational time.

- Type 5050: Rankine cycle (*developed by the author*).

The power block is composed by a steam train generator which includes a reheating stage, two Closed Feed-Water Heaters (CFWH), a deaerator, two feed-water pumps, an Air-Cooled Condenser (ACC), and a turbine with a high-pressure stage and three mass flow rate extractions in the low-pressure stages. The layout of the Rankine cycle is illustrated in Figure D-4.

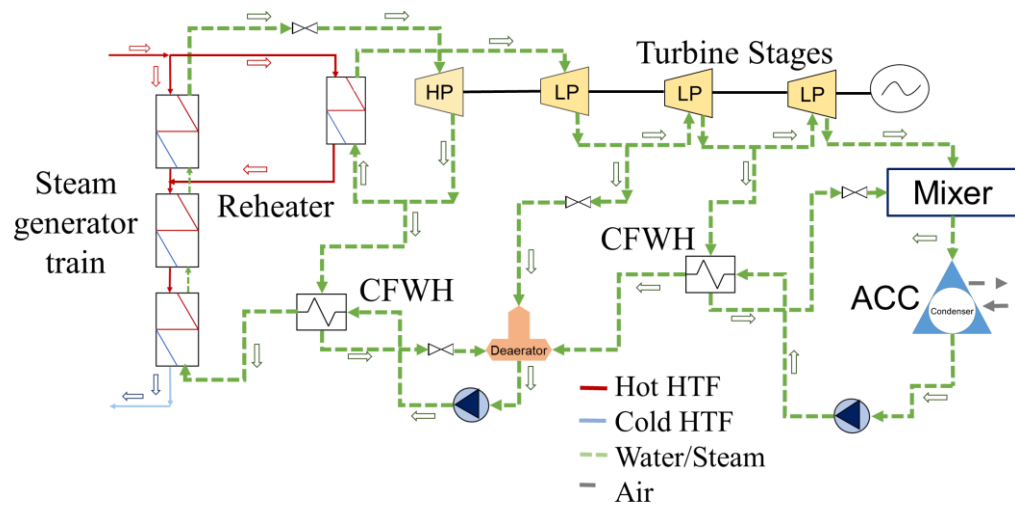


Figure D-4: Layout of the power cycle.

The power block's model in TRNSYS consists of multi-variable polynomial regressions that represent the performance under nominal and off-design conditions of the power cycle. This model allows evaluating the power block operation in a significantly low computational time. The TRNSYS's component is based on a model developed in the Equation Engineering Solver (EES), that is comprised of mass, energy, and heat transfer balances at every component of the Rankine Cycle. The EES model was used to create a performance map of the power block through a parametric analysis varying three operational conditions: the inlet hot HTF temperature, the HTF mass flow rate, and the ambient temperature. Then, a polynomial multi-variable regression model was developed, employing the data coming from the parametric analysis.

Output variables of the regression model (and the TRNSYS component) are the net power output from the turbine-generator, the exhaust mass flow rate of the turbine, and temperature of the HTF returning to the solar field. The equations and coefficients of the multi-variable polynomial regression model are provided in detail in Appendix B1: Supplementary Data.

- Type 39: Variable volume tank.

This component models a fully mixed tank with a constant cross-sectional area that contains a variable quantity of fluid. In its simplest form, a single flow enters from a

hot source and a single flow stream exits to a load. Since the incoming and outgoing flows need not be equal, the level of fluid in the tank can vary. The level is allowed to vary between user specified high and low level limits (Solar Energy Laboratory, 2017).

APPENDIX D3. BESS model



Figure D-5: Illustrated scheme of the BESS model in TRNSYS simulation studio.

- Type 6300: Battery bank (*developed by the author*).
This component calculates the State of Charge (SOC) of the battery through a balance of the energy charged and discharged from the previous to the next time step. The model uses as inputs the battery energy size, the power rate, and the charging and discharging efficiency.